

SKBF
KBS

TEKNISK
RAPPORT

83-16

**Stability of deep-sited smectite
minerals in crystalline rock –
chemical aspects**

Roland Pusch

Division of Soil Mechanics, University of Luleå
1983-03-30

STABILITY OF DEEP-SITED SMECTITE MINERALS IN
CRYSTALLINE ROCK - CHEMICAL ASPECTS

Roland Pusch

Division of Soil Mechanics, University of Luleå
1983-03-30

This report concerns a study which was conducted for SKBF/KBS. The conclusions and viewpoints presented in the report are those of the author(s) and do not necessarily coincide with those of the client.

A list of other reports published in this series during 1983 is attached at the end of this report. Information on KBS technical reports from 1977-1978 (TR 121), 1979 (TR 79-28), 1980 (TR 80-26), 1981 (TR 81-17) and 1982 (TR 82-28) is available through SKBF/KBS.

STABILITY OF DEEP-SITED SMECTITE MINERALS
IN CRYSTALLINE ROCK - CHEMICAL ASPECTS

LULEÅ MARCH 30 1983
DIV. OF SOIL MECHANICS
UNIVERSITY OF LULEÅ

ROLAND PUSCH

	<u>Page</u>
<u>CONTENTS</u>	
<u>SUMMARY</u>	
<u>INTRODUCTION</u>	1
1. <u>MONTMORILLONITE AND OTHER SMECTITES</u>	5
1.1 <u>Crystal structures</u>	5
1.2 <u>Lattice stability</u>	8
1.3 <u>Cementation</u>	14
1.4 <u>Conclusions, scope of study</u>	15
2. <u>KINNEKULLE BENTONITES</u>	16
2.1 <u>General</u>	16
2.2 <u>Geology</u>	16
2.3 <u>Current concept of mineral origin</u>	17
2.3.1 <u>Smectite/illite</u>	17
2.3.2 <u>Kaolinite</u>	20
2.3.3 <u>Biotite and chlorite</u>	20
2.3.4 <u>Feldspar</u>	20
2.3.5 <u>Quartz</u>	20
2.4 <u>Stress conditions</u>	
2.5 <u>Temperature conditions</u>	
2.5.1 <u>Heat flow calculation</u>	22
2.5.2 <u>Conodont analyses</u>	24
2.5.3 <u>Additional</u>	24
2.5.4 <u>Conclusion</u>	25
2.6 <u>Recent study</u>	
2.6.1 <u>Purpose</u>	25
2.6.2 <u>Element analyses</u>	26
2.6.3 <u>Mineral analyses (XRD)</u>	30
2.6.4 <u>Microstructural investigations</u>	33
2.6.5 <u>Physical condition</u>	38

3.	<u>MARGRETEBERG SMECTITIC CLAYS</u>	<u>Page</u>
	3.1 <u>General</u>	40
	3.2 <u>Geology</u>	40
	3.3 <u>Stress conditions</u>	42
	3.4 <u>Temperature conditions</u>	42
	3.5 <u>Recent study</u>	42
	3.5.1 <u>Purpose</u>	42
	3.5.2 <u>Element analyses</u>	43
	3.5.3 <u>Mineral analyses</u>	48
	3.5.4 <u>Microstructural investigations</u>	50
	3.5.5 <u>Physical condition</u>	56
4.	<u>DISCUSSION</u>	60
	4.1 <u>General conclusions</u>	60
	4.2 <u>Hypohetical mechanism of the <u>charge change</u></u>	61
5.	<u>ACKNOWLEDGEMENTS</u>	66
6.	<u>REFERENCES</u>	67
	<u>APPENDICES</u>	

STABILITY OF DEEP-SITED SMECTITE IN CRYSTALLINE ROCK-
- CHEMICAL ASPECTS

SUMMARY

A recent survey of possible conditions and mechanisms of smectite alteration, with special respect to the Swedish concept of radioactive waste disposal, has shown that the charge change by replacement of tetrahedral Si by Al is the key mechanism of the only practically important alteration, namely that of smectite/illite conversion. If K is available in sufficient quantities it will be fixed and permanent conversion to the unwanted illite-type minerals is a fact; if not, the smectite will be beidellite-like with practically unchanged physico/mechanical properties. Heating to more than about 100°C is thought to be the cause of the charge change.

One other process may be critical and that is cementation of various substances. A possible cementation mechanism, i.e. that of quartz precipitation, is very probably associated with the smectite/illite conversion.

Practical examples of smectite alteration and survival under reasonably well documented geological conditions with respect to temperature and pressure are available, one being that of the Kinnekulle bentonites, another one, although less well known, being the smectitic clay beds in the Höganäs depression. Rather comprehensive core sampling was made at both sites and elemental and mineral analyses were conducted as well as microstructural studies. They support the hypothesis that practically important charge change through Si/Al replacement requires a temperature of more than 100°C, and that such replacement does not yield permanent lattice collapse unless K is available in

sufficient quantities. The Höganäs case also serves as an example of drastic loss in plasticity and swelling potential by cementation of other precipitates than quartz, namely iron compounds.

INTRODUCTION

The Swedish KBS multibarrier concept for the disposition of highly radioactive, unreprocessed reactor wastes implies that copper canisters containing radioactive material be surrounded by dense Na bentonite clay (Fig.1). Repositories consisting of tunnel systems with deposition holes for the canisters will be located at a depth of about 500 m in crystalline rock, the tunnels being backfilled with in situ-compacted sand/bentonite mixtures.

The physical and mechanical properties of bentonite make it an ideal sealing substance, but it is required that they are preserved during the operative lifetime of such repositories, which is about 10^6 years. This implies that the crystal structure of the main mineral constituent, montmorillonite, be maintained, in principle. Thus, mineral lattice stability of this mineral in repository environment is a key question which is the topic of this report. Influence of radiation from waste products will not be considered here, while the effect of temperature will be a major point.

Precompacted Na bentonite in the form of blocks or of a tightly fitting envelope is applied in the space between the rock and the canister. The geometry of the deposition hole and the thickness of the bentonite annulus may differ from the appearance in Fig.1.

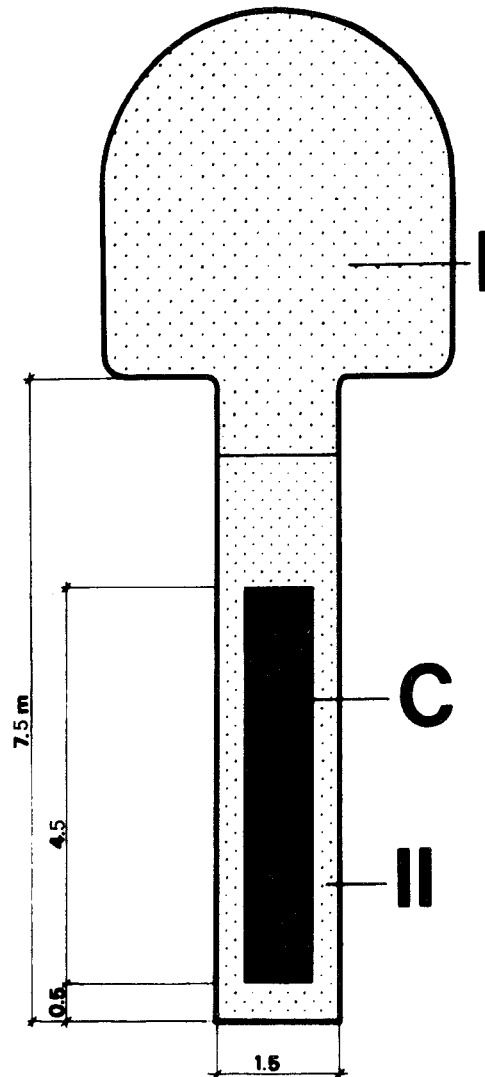


Fig. 1. Cross section of tunnel with deposition hole. Canister (C) containing highly radioactive wastes is embedded in highly compacted bentonite (II). The tunnel backfill consists of sand and bentonite (I). All dimensions are in metres.

The bentonite has a degree of water saturation of about 60% at the application and it will absorb water from the rock by which its bulk density increases to 2.0 - 2.1 t/m³. The ultimate water content will be 25-30%. Water enters the bentonite through fine fissures and pores in the rock crystal matrix but the main water source is the system of joints and fractures which traverse the holes. In rock with very few joints, several hundred years may actually be required to reach saturation.

The heat production of the radioactive waste yields a surface temperature of the canister of less than 90°C in the KBS concepts, the temperature gradient initially being about 1°C per centimeter.

In the course of the water uptake, the gradient and the temperature drop in the bentonite but the latter may be higher than 60°C for several thousand years.

Through the water uptake, which is due to the high affinity of montmorillonite to water, the bentonite expands and fills the space between the rock and the canister and exerts a swelling pressure of about 10 MPa on the confinement.

The rather extreme specific surface area (600-800 m²/g dry clay) means that the larger part of the pore water will be adsorbed and strongly held in inter-layer positions, but a certain small fraction of the pore water will be located in more or less continuous passages ("voids") between clay particle aggregates. It will behave as free, bulk water and its pressure will be equal to the piezometric head in the repository; i.e. the pressure will depend on the groundwater level. It will reach a maximum value of about 5 MPa.

The fact that water migrates towards the canister and that this process is associated with an expansion of the clay, means that water will in principle not be present in free form at the copper/clay interface; the canister will be contacted by a clay mass which strongly retains its pore water. The contact may be established between the clay and metallic copper or copper compounds like oxide or hydroxide.

Under the expected conditions, ionic migration of copper will be very limited in the pH-range of Na bentonite. It will tend to produce ion exchange by which sodium is released and copper ions occupy exchange sites (2). It is a true ion exchange process which only affects the electrical intra-aggregate force fields and it has but one important bearing on the physical properties of the bentonite: the permeability will probably be increased by 2-5 times. Lattice alterations with concomitant loss in expansibility will not take place. Such alteration is associated with temperature and ground water chemistry effects on which the present study is focused.

1. MONTMORILLONITE AND OTHER SMECTITES

1.1 Crystal structures

Smectites have an octahedral sheet coordinated with two tetrahedral sheets in which oxygens are shared. Cationic substitution occurs in octahedral as well as tetrahedral sheets which yields different properties and forms the basis of classification:

montmorillonite with Si in tetrahedral positions and Al and Mg in octahedral positions, beidellite with Si and Al in tetrahedral positions and Al in octahedral positions, and nontronite with Si and Al in tetrahedral positions and Fe in octahedral positions (Fig.2). In practice, most natural smectites have compositions differing from the idealized versions.

Expansion and shrinkage of the smectite lattice are affected by the nature of absorbed ions and it is usually assumed that the amount of adsorbed interlayer water depends on the exchangeable cations.

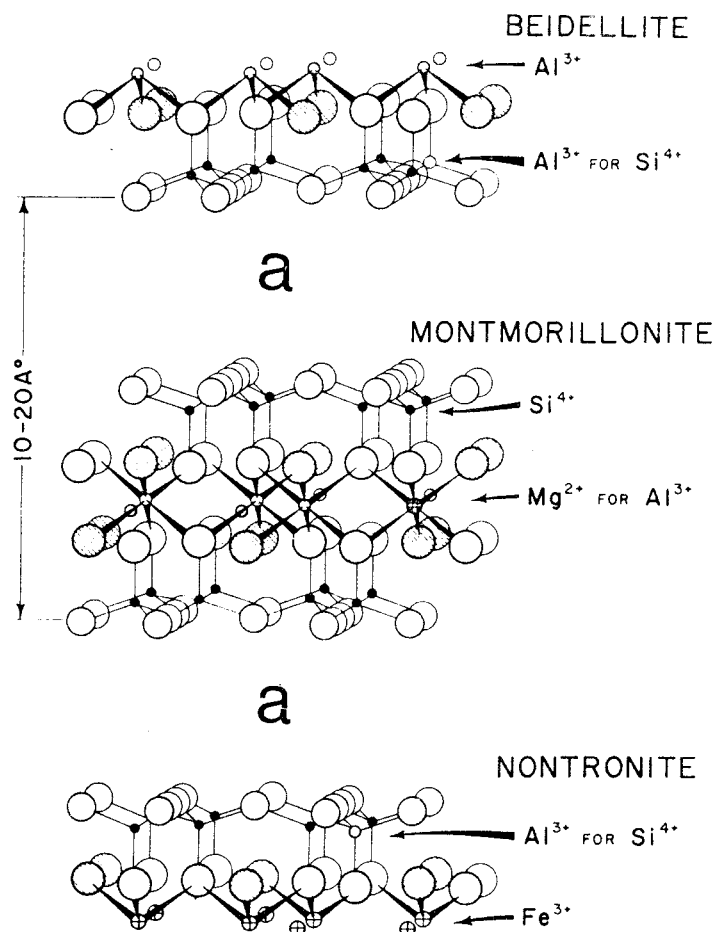


Fig. 2 Crystal structures of the main smectite types. (a) represents interlamellar space with water and cations.

NMR and dielectric measurements (3) as well as systematic determinations of the swelling pressure of smectites (4) indicate, however, that the coupling of water molecules, mutually and to intercrystalline surfaces of smectites, leads to a structural organization of adsorbed water which does not primarily depend on the presence of exchangeable cations. Such ions only seem to give rise to well-defined structural modifications of the adsorbed water lattice.

These observations support the idea of a smectite structure with primary water molecule adsorption sites and exchangeable cationic lattice components.

Such an alternative version, often referred to, is the montmorillonite structure suggested by EDELMAN & FAVEJEE. It is illustrated in Fig. 3 together with the earlier, traditional model, both being projected in a slightly different manner than in Fig. 2.

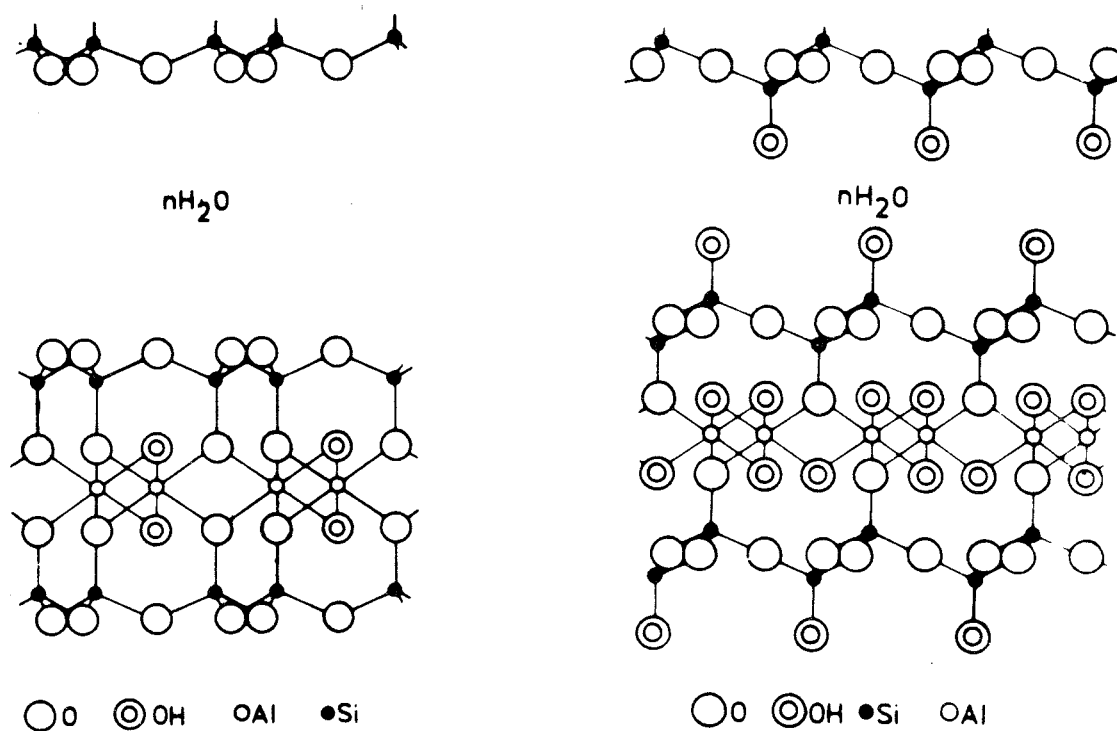


Fig. 3 Possible montmorillonite crystal structures. Left: Traditional version (HOFMANN, ENDELL & WILM). Right: Alternative version (EDELMAN & FAVEJEE), $n(\text{H}_2\text{O})$ represents intercrystalline water.

EDELMAN & FAVEJEE's model deviates from the previously shown structure with respect to the type of coordination of the tetrahedra. We see that every second tetrahedron of the silicious sheets is inverted, thus exposing apical OH:s, which adsorb water through hydrogen bonding and which can also exchange the proton. We will see later that this structure model offers an explanation of certain temperature-induced structural transformations.

Thermogravimetric measurements show that intercrystalline water is largely removed at about 100°C, eventually including some surface hydroxyls, while differential thermal analyses indicate additional lattice reorganization with respect to surface hydroxyls extending into the temperature interval 150-200°C (3). Not until the temperature exceeds 300-400°C partial dehydroxylation of the octahedral sheet takes place. It is actually highly probable that the surface reorganization ultimately involves a conversion from the EDELMAN & FAVEJEE structure to that of HOFMANN et al, beginning at much less than 100°C and being completed at about 150°C, cf (3).

1.2 Lattice stability

While the physical and mechanical properties of smectites can be somewhat and even substantially affected by exchange of adsorbed cations (Ca for Na, for example) caused by possible changes in groundwater chemistry in the considered 10^6 years time, they can be drastically altered by crystal lattice transformations. Such lattice alterations, which result from elevated temperature and changes in the chemical environment, may lead to a substantial contraction of the clay elements and a dramatic loss in homogeneity and plasticity. All these negative effects are caused by partial or complete loss in swelling ability which, in turn, results from a firm coupling between the individual lattice sheets or by their fixation through precipitated substances.

pH effects

Extreme pH conditions, i.e. pH lower than about 6 or higher than about 10, may cause lattice breakdown but such deviations from the normal pH

range at 500 m level in Swedish crystalline rock are not expected. Local and temporary pH extremes will probably be buffered by exchange reactions. If the EDELMAN & FAVEJEE model is applicable, such reactions are readily explained by considering the reactivity of the apical OH-groups (5).

Smectite/illite alteration, current hypothesis

The establishment of firm sheet-to-sheet coupling is essentially that of smectite → illite (S/I) alteration through potassium uptake in interlayer positions, although one alternative mechanism is possible, namely heating in combination with high pressure. S/I-conversion (cf. Fig.4) requires considerable layer charge increase, while "inactivation" through heating under pressure may take place also in low charge smectite (~0.1 equiv./unit cell). The entire problem complex has been dealt with in detail in a recent study under the guidance of prof. DUWAYNE M.ANDERSON (6). It specified the following main questions concerning S/I conversion in the KBS case:

- 1 What is the prerequisite for and the nature of the mechanism by which smectite clays are altered to illite?
- 2 Which are the likely sources of potassium with respect to the KBS concept?
- 3 Is it probable that the conversion of smectite to illite will be of importance in a 10^6 years' time frame?

The investigators concluded that S/I conversion involves three fundamental steps:

- a) The creation of a high lattice charge by the removal of silicons and their concomitant replacement in the lattice by aluminum, locally available from the dissolution of accessory minerals, or the exchangeable ion complex, etc.

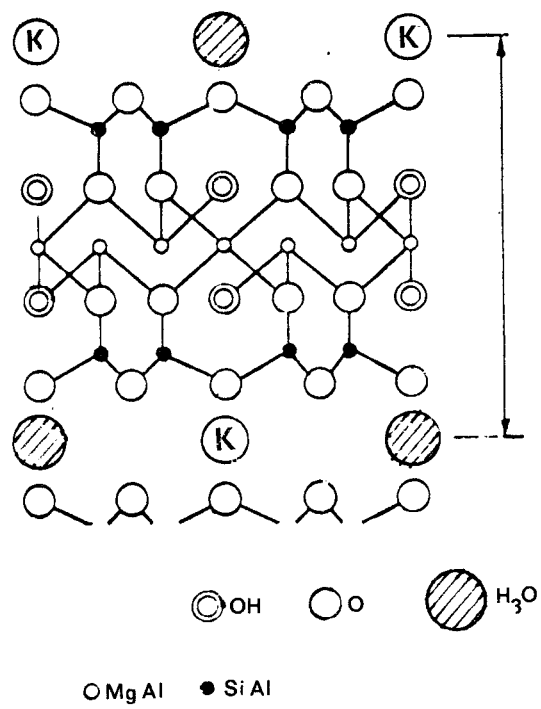


Fig.4. Idealized illite crystal structure.

- b) Influx of potassium ions derived from local dissolution of potassium-bearing minerals, percolating groundwater etc, to saturate the exchange capacity of the now highly charged smectite intermediate.
- c) Irreversible collapse of the high lattice charge smectite intermediate to the typical non-expanding illite lattice.

They stated that the most critical, rate-limiting step is the production of a highly charged smectite lattice by the progressive substitution of aluminum for the silica in the tetrahedral layers. This requires an environmental temperature sufficiently high to allow passage of these ions out of and into the lattice, and there is both laboratory and field evidence to substantiate the conclusion that the exchange of silicon and aluminum is relatively rapid at temperatures above about 100°C.

The investigators considered it to be likely that the process begins when temperature exceeds about 60°C, while other investigators have suggested that the exchange may take place even at 40°C, thus indicating that it is an Arrhenius-type process with a rather wide activation energy spectrum. However, as will be shown later in the present report, there are reasons to believe that 100°C or thereabout may actually be a threshold value. The investigators also hold that the aluminum required for the substitution for silica is sufficiently ubiquitous, available for instance at the corner edges of the smectite sheets, that its availability cannot be regarded as a rate-limiting step. At temperatures approaching the 100°C range, the rate of charge change is sufficiently rapid that the supply of potassium ions regulates the rate at which individual lattice sheets collapse to the illite configuration and become nonexpanding.

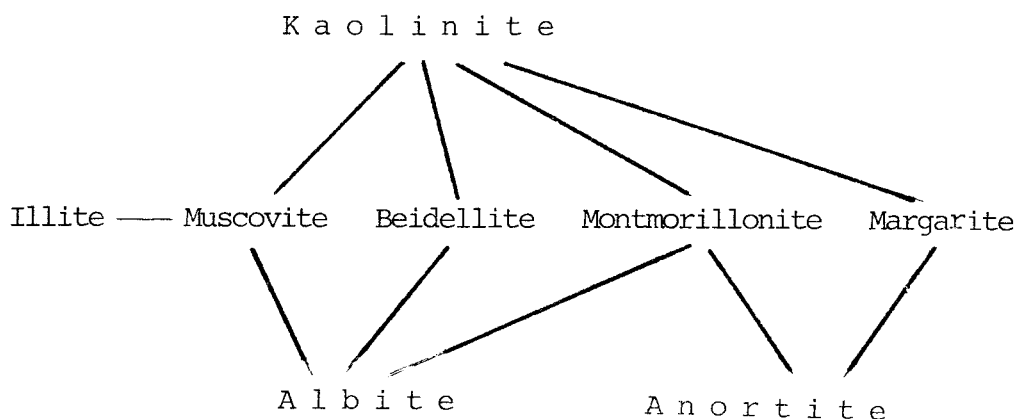
As to the KBS concept, it was assumed that potassium is furnished by groundwater which percolates through the confining rock and the bentonite around the waste canisters. By assuming a conservative permeability coefficient ($k=5 \cdot 10^{-12}$ m/s) a hydraulic gradient of 10^{-2} , a potassium concentration in the groundwater of 10 ppm, and a cation exchange capacity of 70 meq/100 g clay, the investigators found that complete K-saturation of the bentonite annulus would require much more than 10^6 years. Even more important was their conclusion that the expected 60-90°C temperature will not be sufficient for the formation of a high lattice charge in the smectite to render it vulnerable to collapse, and that an influx of potassium ions merely converts the smectite to its potassium form. Thus, it was firmly stated that under the projected conditions of the KBS storage facility, smectite clays are expected to function effectively as a buffer material over times greatly in excess of the 10^6 years required.

A further conclusion would be that the smectite components of bentonite/sand mixtures should also be stable even if the sand contains K-bearing minerals as long as the temperature is well below 100°C. Once the temperature approaches a level where charge change and potassium liberation and migration become substantial, S/I conversion is expected to be very rapid.

Smectite conversion, alternative approach

It is obvious that if the critical temperature that is required to alter the lattice charge should be very low, the conversion of smectites to nonexpanding forms may take place in the long run in any smectitic clay mass in nature.

In fact, this seems to be evidenced by the very scarce supply of bentonites older than about $4 \cdot 10^8$ years. Low-temperature conversion may be in accordance with the general transformation scheme below. It concerns possible feldspar weathering sequences based on stoichiometric analyses and does not allow for direct smectite/muscovite/illite transformation. It would require oxidizing conditions and a considerably increased pH, as well as a net loss in SiO_2 to form firstly kaolinite - not necessarily crystalline matter - and secondarily mica-type compounds, which implies that potassium is supplied from external sources.



Main transformation sequences in the course of feldspar weathering (A.Gustafsson) *.

As to the KBS concept this approach yields the same conclusion as the previous one which presupposes higher critical temperatures, i.e. that the highly compacted Na bentonite will not be altered to nonexpanding forms in less than 10^6 years. This is because reducing conditions will prevail and because the potassium uptake will require much more than 10^6 years.

* Chief, mineral department,
Höganäs AB
(priv. comm.)

This suggests that temperature is a determinant. The detailed processes are very incompletely understood, however. The matter is further dealt with in the final chapter of this report.

1.3 Cementation

Precipitation of crystalline or amorphous matter that welds together the edges of stack-wise arranged smectite lattice sheets inhibits spontaneous swelling if the bonds are sufficiently strong to resist the expanding forces associated with hydration. A sufficiently comprehensive precipitation also prevents water molecules from entering intercrystalline space. It is a wellknown fact that many bentonite beds are slightly or even substantially affected by cementation such that rather intense mechanical agitation is required to break up the aggregates. This is easily achieved in laboratory preparation for X-ray diffraction analyses, for instance, which suggests that the bentonite is smectite-rich while it is largely inactive as concluded from swelling pressure tests. Thus, industrial processing usually must involve mechanical activation processes such as grinding, heating, or freezing, to activate the clay.

Cementation may not be critical per se as concerns the function of the clay materials in a repository. Thus, if it takes place after the initial period of swelling and equilibration of the clay, it would actually reduce its permeability. It is required, however, that the cement bonds are sufficiently weak to be broken if slight rock displacements occur so that the original swelling and self-healing properties are regained, i.e. the clay

becomes activated . As to natural bentonites, slight drying usually sets up sufficiently high thermal stresses to break the majority of weak cementation bonds - this is generally the case with the Wyoming Na bentonite and with many of the Sardinian Ca bentonites - but there are also many examples of ancient smectite-rich clays which swell spontaneously when contacted with free water. This is in fact the usual behavior of clay-weathered zones in crystalline rock which present much difficulty in rock excavation operations in Scandinavia and elsewhere.

There are many indications that cementation is associated with smectite/illite alteration. If it is due to thermal effects it is associated with the replacement of tetrahedral Si by Al which leads to liberation and precipitation of Si. If it is a low-temperature process it must be associated with long-term percolation of solutions characterized by a pH exceeding 8-10. Both processes may represent the alternative mechanism leading to firm sheet-to-sheet coupling (cf p.9).

1.4 Conclusions, scope of study

The general pattern of chemical changes that may alter the montmorillonite to an unwanted form is fairly well understood but there are only few examples of natural clay strata which can be taken as integral examples of a long term alteration scenario. The Kinnekulle bentonite beds in Sweden represent an exception, since they have been described in detail with respect to mineralogy and fossil contents, and it was assumed that rather limited additional analyses might offer a rather complete picture of chemical alterations of the presently discussed minerals as well as of the involved kinetics.

Such a study, sponsored by SKBF/KBS, was therefore conducted in late 1982 and it is reported in the following chapter. Parallel to this investigation, a similar study was made of another smectite-rich clay sequence in Margreteberg, northwestern Skåne and it is reported here as well. Both studies turned out to offer much information and form the basis of the final discussion.

2. KINNEKULLE BENTONITES

2.1 General

The mineralogy of the bentonite beds at Kinnekulle, Sweden, exhibits variations which illustrate chemical alterations of primary silicate minerals due to temperature effects and dissolution kinetics, and it offers, therefore, an opportunity to test the validity of the previously cited model of the chemical stability of smectite minerals. The text comprises a short geological description of the beds with particular reference to their origin, and of the mechanical stress and temperature histories as well as of recently conducted studies concerning the chemical composition and physical properties of borehole samples.

2.2 Geology

Considerable effort has been put to the evaluation and explanation of the origin and chemical history of the Kinnekulle bentonites (7, 8, 9). They represent a number of strata with a thickness varying from less than one centimeter to about two meters. They are of Middle Ordovician (Viruan) age. The beds were deposited in the form of volcanic ash which sedimented in sea water. The identified and

1) We refer here to the Mossen area just below the peak of Högekullen

analyzed larger crystals (phenocrysts) that are contained in the clay matrix indicate that the parent lava had a rhyolite or dacite composition. The devitrified glass components now consist of a clay material which is composed of mixed layers of montmorillonite and illite in a random interstratification and with a proportion of montmorillonite layers, that is high in the central part of a thick, major bed, (Fig. 5), but lower in adjacent thinner layers (8). It has not been clear from earlier studies whether the recorded variations in the concentration of various minerals and elements, such as potassium, results from chemical alteration caused by sea water percolation, or by circulating groundwater, or through diffusion from external sources. This matter will be thoroughly dealt with in the present study.

2.3 Current concept of mineral origin

2.3.1 Smectite/illite

The smectite/illite minerals entirely originate from devitrification of the glassy components of volcanic ash. In principle, the major part of the clay fraction forms aggregates of phyllosilicates intermediate to that of montmorillonite and illite of the dioctahedral type (8). The thick bed primarily consists of a clay with a K_2O -content of 2.7%, and a base-exchange capacity of about 70 meq/100 g. The minerals are "mixed layer" composites of illite and montmorillonite, the proportions being determined by the potassium content. As to their origin, analyses show that the central thick bed contains large amounts of phenocrysts, while the thin adjacent bentonite layers exhibit a smaller amount of specimens of this sort (8). This may be due to somewhat different magma compositions, the latter hypothesis being supported by an observed markedly higher

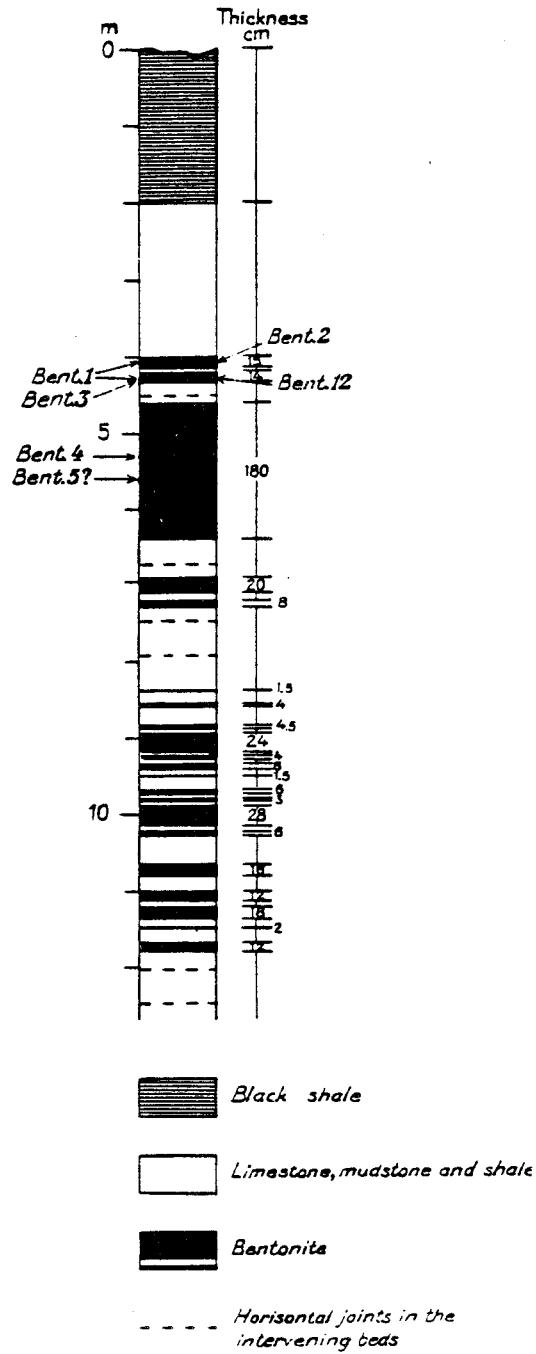


Fig. 5. Stratigraphic diagram at Mossen, Kinnekulle (8).

titanium content in the upper thin layers than in the thick bed. BYSTRÖM showed that the central thick bed contains less potassium than the adjacent thin beds, and later found that there is actually a gradient in potassium concentration from the upper boundary of the thick bed, where it is high, to its central parts, where it is low. This variation, which has been reported by VELDE & BRUSEWITZ (9), is associated with a variation in aluminum concentration - a most important fact, since it actually verifies that a charge change is required for illitization. The thick bed shows the drop in K and increase in Al from the top and downwards that are specified in Table 1, which supports the hypothesis that temperature-induced tetrahedral replacement of Si by Al is the first stage in smectite-illite conversion.

Table 1. K and Al concentrations in the thick Kinnekulle bed according to VELDE & BRUSEWITZ (9). Percentages refer to atom percent of total amount of cations.

Distance from upper boundary, cm ¹⁾	K %	Al %	Remarks
Upper boundary	5.1	24	
0 - 5	4.8	23	
9 - 30 (finer)	4.2	23	
9 - 30 (coarser)	4.3	23	
30 - 37	4.1	21	
45 - 60	3.3	20	
60 - 70	3.2	20	
75 - 80	3.2	20	
~ 110	3.1	21	Center of bed

¹⁾ levels kindly provided by A.M. Brusewitz

2.3.2 Kaolinite

The presence of kaolinite, which amounts to a few percent of the total mineral mass, has been ascribed to the weathering of plagioclase forming about 5-10% of the total mass (8). The weathering has taken place after the deposition in Ordovician time, and it seems to have led to in situ recombination of the feldspar constituents to form kaolinite (9).

2.3.3 Biotite and chlorite

Although the biotite content is low, i.e. 2-3% of the total mass (7), this Fe-bearing mineral actually gives the Kinnekulle bentonites their characteristic appearance, particularly with respect to their color, which is brownish. The second most important Fe-containing mineral is chlorite, which is approximately as abundant as biotite. The biotite crystals have been subjected to weathering which has yielded some of the chlorite and some silica which probably crystallized as quartz, except for a slight quantity of amorphous silica amounting to less than 0.5% of the total mass (8).

2.3.4 Feldspar

While the plagioclase has almost completely changed to kaolinite, the alkali feldspars, mainly sanidine, seem to be quite stable in the surrounding clay matrix (8). This suggests that K-bearing feldspars were not a major K-source for the smectite/illite transformation. Sanidine forms approximately 5% of the total mineral mass.

2.3.5 Quartz

BYSTRÖM reported that quartz, mainly in the form of thin wavy, or wedge-shaped microscopic plates, is the most frequent phenocryst species in the bentonite (8). These quartz grains, which seem to be most abundant in the 2-6 μm size interval and which form up to 40% of the total mineral mass locally,

were probably deposited as such.

This investigator observed a peculiar feature which was ascribed to precipitated, finely divided quartz. Thus, slight or moderate resistance to dispersion of the clay was observed and microscopic studies suggest that finely divided quartz crystallites act as spot weldings which hold the smectite flakes together. It is generally assumed, however, that the larger part of the silica released in the smectite illite transformation has been transported away from the bentonite to contribute to the formation of adjoining cherty beds.

2.4 Stress conditions

Pressure values deduced from the weight of the present overlying strata and estimated glacier loads in Quaternary time are the only fairly safe measures of the stress history, although Devonian sediments, later eroded, may have been determinants of the maximum preconsolidation pressure (10). The ice pressures suggest that the maximum vertical stress was of the order of 20 MPa, which is not sufficient to produce noticeable pressure solution phenomena in smectitic clay.

2.5 Temperature conditions

The maximum temperature experienced by the bentonite beds was caused by the intrusion of magma which forms the present basalt cover on the top of the mountain. The heating can be estimated in three ways: through heat flow calculation based on the actual stratigraphy, through conodont analyses, and through argon dating.

2.5.1 Heat_flow_calculation

The general stratigraphy of the Kinnekulle mountain is as follows:

- 30 m top layer of basalt
- 55 m graptolite-bearing shale and slate
- 35 m trilobite-bearing shale
- 5-10 m limestone/shale
- 7 m bentonite/limestone/shale

The absence of scoria and glassy components indicates that the basalt bed was formed by magma intrusion into a sediment sequence, which suggests that Silurian and possibly Devonian sediments were present when the intrusion occurred in early Permian time (11). If so, these sediments must have been lifted and separated from the graptolite-bearing shales by the penetrating magma flow. The structure of the top part of the basalt is more coarse-grained than that of its basal part, which indicates that the present upper surface once formed the central part of the basalt bed (11). It is therefore assumed that its original thickness was much greater than 30 m; 60 m being a reasonable estimate. Assuming, further, that the temperature of the magma was 1100°C , and that its lateral extension was sufficiently large to have yielded almost uniaxial heat flow, the temperature in the bentonite layers can be calculated. Such an analysis was conducted by Roland Blomquist, Studsvik Energiteknik AB, the calculation being based on the assumption that the initial bentonite temperature was 15°C , and that the heat capacity of all materials was $2.16 \times 10^6 \text{ J/m}^3 \text{ K}$. Also, "symmetric" conditions were assumed in the sense that the heat produced by the lower 30 m magma bed was transferred downwards. Two heat conductivity sets were

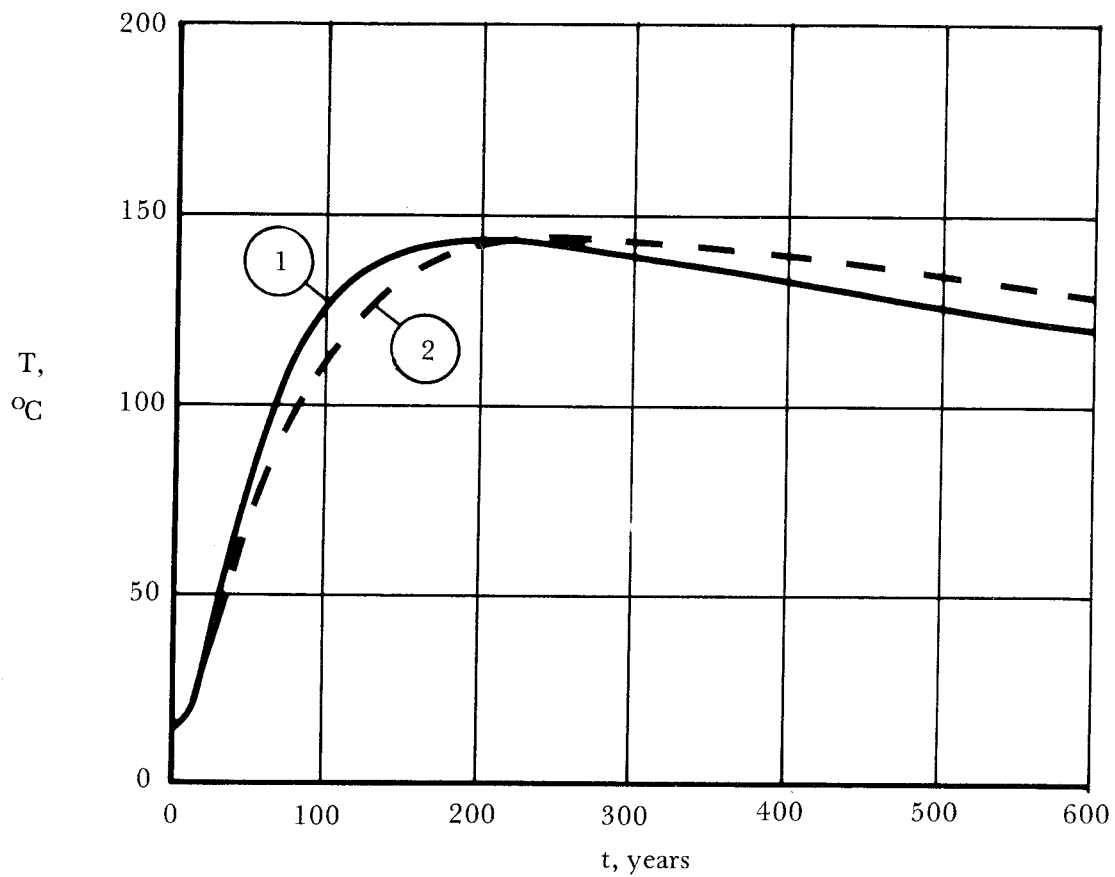


Fig. 6. Hypothetic temperature history of the Kinnekulle bentonite beds
(Calculation made by Roland Blomquist, Studsvik Energiteknik AB.)

assumed:

- (1) 2.5 W/m, K for the rock and
1.5 W/m, K for the bentonite clay
- (2) 1.5 W/m, K for the rock and
0.5 W/m, K for the bentonite clay

These two sets are referred to as (1) and (2) in Fig. 6, which shows the outcome of the calculation. It indicates that heat parameter variations are fairly unimportant and that the bentonite beds were exposed to 100-140°C for about 1000 years.

2.5.2 Conodont analyses

Conodonts, a group of widely distributed phosphatic microfossils, turn out to be useful as a semiquantitative index of thermal metamorphism (12). The color changes exhibited by conodont specimens during gradually increased heating are quite obvious and experience shows that they permit temperature assessments within the interval from 80°C up to 500°C. Such analyses of the limestone, located less than 10 m above the bentonite in the Mossen area, have yielded temperatures in the range of 110-200°C¹⁾, which is thus in good agreement with the heat calculation.

2.5.3 Additional

Argon dating actually also offers an indication of the temperature history and it has yielded an approximate value of 160°C for the Mossen bentonites²⁾. Furthermore, recent excavation of large block samples in the former Mossen bentonite quarry has shown that the main bed is traversed by steeply oriented, several millimeter wide fractures filled with calcite.

1) Prof. Stig M. Bergström, Dept of Geology and Mineralogy, Ohio State University (Pers. comm.)

2) Dr Ann Mari Brusewitz (Pers. comm.)

These features are probably desiccation fractures which were later filled with precipitated matter originating from hydrothermal solutions. The formation of open fractures of this width in a clay bed covered by almost 100 m of limestone and shales requires considerable heating, the magma intrusion in Permian time offering the most logical explanation.

2.5.4 Conclusion

The various temperature indications referred to here suggest that the bentonites in the Mossen area have been heated to at least 110°C by the Permian magma intrusion, and that their temperature has been at least 100°C for several hundred years. Probably, however, the temperature dropped to considerably less than 100°C in one or a few thousand years after this event.

2.6 Recent study

2.6.1 Purpose

It was considered that the very valuable mineralogical investigations conducted by previous investigators (8,9) could favorably be extended to give a more comprehensive picture of the potassium distribution for possible evaluation of its source, and for possible identification of cementing agents, as well as for determination of certain soil physical data. For this purpose four 10 m long Ø52 mm cores were taken in the fall 1982. The drilling was made by the TGB¹⁾ company and the cores were transported to the Division of Soil Mechanics, University of Luleå, for extraction of samples for analysis. Element and mineral analyses as well as microstructural investigations were made by the EMV Associates Inc²⁾, while water contents and liquid limits were determined by the Division of Soil Mechanics, University of Luleå.

1) Tung Geoteknisk Borrning AB, Gråbo, Gothenburg

2) EMV Associates Inc Microanalysis Laboratory,
15825 Shady Grove Road, Rockville, Maryland 20850,
USA

The drilling operation took place about 50 m north-east of the old Mossen bentonite quarry, and gave cores that covered approximately the same profile as that shown in Figure 5. A stratigraphic columnar section of the presently investigated core is shown in Figure 7.

2.6.2 Element analyses

The main purpose of the analyses was to:

- 1 Investigate whether the K-concentration profile shows the same pattern in the lower as in the upper part of the thick bed, i.e. exhibiting increasing concentration of this species towards both outer boundaries. This would evidence that K has migrated through diffusion from over- and underlying, outer K-rich sources and not from phenocrysts in the bentonite.
- 2 Investigate whether there is a concentration gradient in boron which should indicate leaching of fresh groundwater in Quaternary time.
- 3 Investigate whether the Al-concentration profile shows the same pattern as the K-profile. This would exclude internal transfer of Al from smectite edges to tetrahedral lattice sites as the only aluminum migration mechanism, and instead indicate diffusion of Al from outer sources.
- 4 Investigate whether Fe- and Ca-profiles indicate diffusion into the bentonite from outer sources rich in the respective species.

Three separate types of analyses were run:

- 1 Atomic Absorption Spectrometry (AAS) was performed to determine absolute concentrations of potassium and boron in the samples.

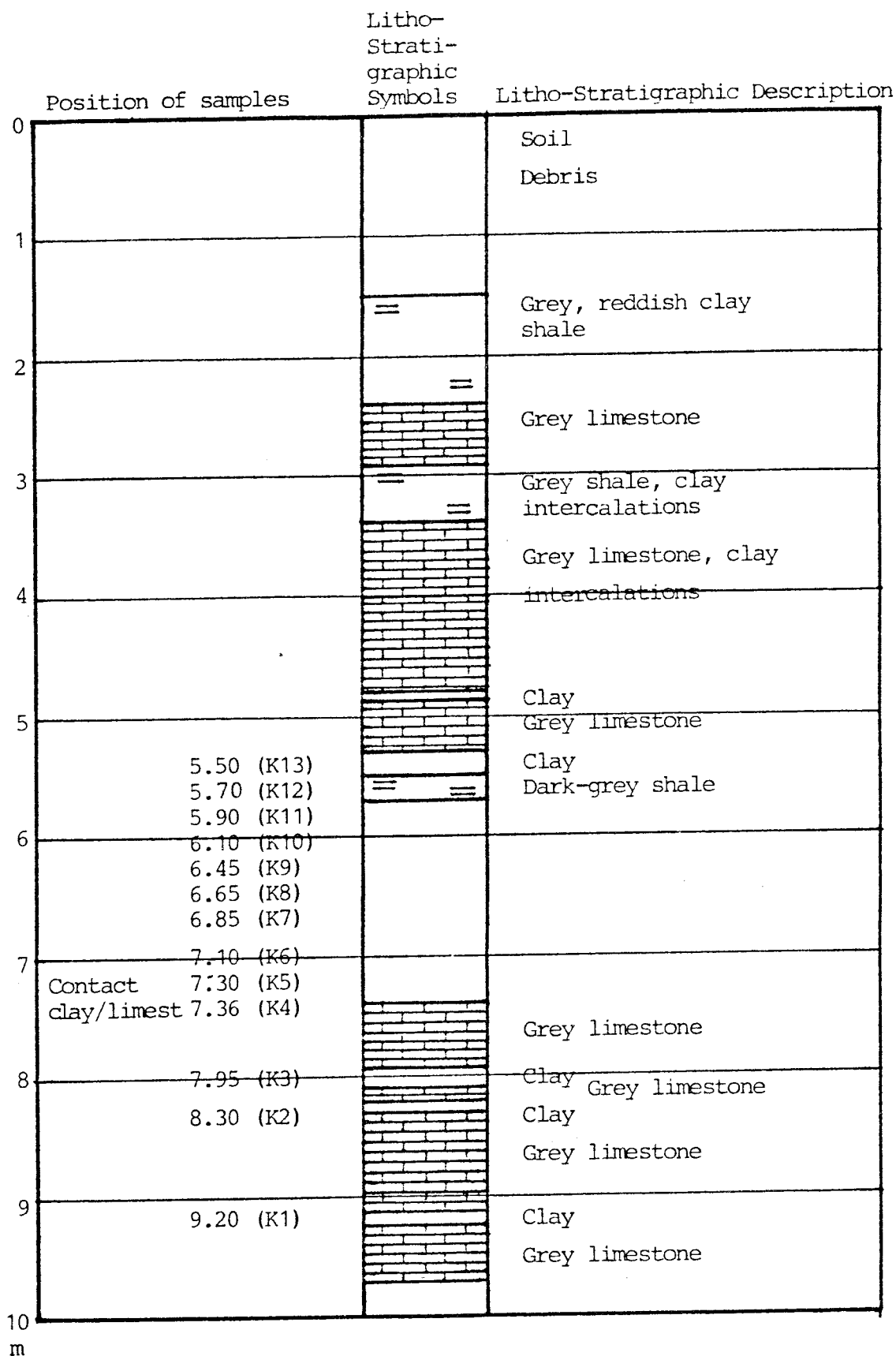


Fig. 7. Stratigraphic Columnar Section, RP 1 (standard Legend Royal Dutch Shell group of companies). Figures in front of sample code denote depth in meter below ground surface.

- 2 Energy Dispersive (X-ray) Spectrometry (EDS) was performed to qualitatively determine the overall elemental composition of the samples within the detectability limits of this method.
- 3 X-ray Line Scans and Mapping were performed on freeze-fracture surfaces to determine distribution characteristics of potassium in the samples.

The AAS analysis had a detection limit for potassium of 6 ppm, the repeatability being approximately $\pm 15\%$. The detection limit for boron could not be reduced below 25-50 ppm and since the uncertainty in this limit is approximately $\pm 50\%$ it means that in a sample showing a 50 ppm concentration, the actual boron content could be as high as 75 ppm. The boron test turned out to be of very limited value, and is left out in this report since most of the actual boron contents were found to be lower than 70 ppm.

The EDS analyses involved preparation through grinding into a fine powder and packing it into a 2 mm diameter recess in a SEM specimen stub, which was subsequently carbon-coated through evaporation. A Hitachi HHS-2R SEM microscope and a Kevex 5000 X-ray energy spectrometer were used by the EMV company for the EDS as well as for the potassium line scans and mapping, for which purpose an Ortec 550 single channel analyzer was attached. Line scans and maps were produced at 100 x magnification on identical sample fields over a linear sample distance of at least 2 mm. A description of the preparation will be found in the report on microstructural analyses.

The main results of the AAS and EDS runs are listed in Table 2. The concentrations refer to the dry weight of the material.

Table 2. Elemental analyses of Kinnekulle samples

Sample	AAS	EDS				Location
	ppm	relative concentrations ¹⁾				
	K	K	Fe	Al	Ca	Upper
K 1	3120	3.5	1.5	4.0	1.2	Lowest thin layer
K 2	10400	3.8	2.0	4.1	1.1	Lower thin layer
K 3	3620	3.8	1.9	4.0	1.2	Lower thin layer
K 4	4130	1.7	1.9	2.9	1.3	Lower bound. of thick bed
K 5	2450	1.8	1.8	3.0	1.6	
K 6	1870	1.5	1.5	3.1	1.2	
K 7	1540	1.6	1.5	2.9	1.2	
K 8	2100	1.7	1.7	3.0	1.2	} Central part of thick bed
K 9	1860	1.4	1.5	2.5	1.0	
K10	1190	1.4	1.3	3.7	1.0	
K11	1380	1.5	1.5	2.5	1.1	
K12	3530	3.1	1.9	3.8	1.1	Upper bound. of thick bed
K13	5500	3.1	1.9	3.9	1.1	Thin layer

1) Observed counts/500 for specified elements, the value 10 representing the reference intensity of Si for all the samples

Table 2 shows that there is a tendency of the K, Fe, and Al-concentrations to be higher in the outer parts of the thick bentonite bed and highest in the separate upper and lower layers. This confirms, in principle, the conclusions of VELDE & BRUSEWITZ that K and Al are correlated in the conversion of smectite to illite (Table 1), but the approximate symmetry of the concentration profiles also suggests that not only K and Fe but also Al have migrated into the bentonite series from outer sources. This may well have been initiated by the temperature rise which was caused by the magma intrusion, but it is admitted that Al migration is difficult to explain. Possibly, therefore, variations in Al and also Fe may at least

partly be explained by different parent ash compositions. It is obvious that the Ca concentration varies less than that of the other investigated cations. Possibly, the higher value found for K5 than for K4, K3 etc indicates Ca diffusion from the underlying limestone. It cannot be excluded that calcite fillings in closely located traversing fractures have had an influence as well.

The line scans and maps for the investigation of the distribution of K have been interpreted as follows (cf. Appendix 1). The relative K-concentration is clearly lower in the central part of the thick bed (Samples K5-K10) than in its outer parts and in the adjacent thin layers. As to the occurrence of potassium it is obvious that this element is fairly uniformly distributed through the clay (see maps) with occasional random microagglomerations. Areas relatively devoid of potassium probably represent phenocrysts which are not K-bearing. All these observations suggest that potassium did not emerge from minerals contained in the clay but that this element has migrated from external sources as stated by VELDE AND BRUSEWITZ.

2.6.3 Mineral analyses (XRD)

The main purpose of the mineral analyses was merely to get a picture of the uniformity of the mineral composition and not to conduct a very detailed investigation of the clay mineral constitution, which has been the subject of previous, carefully conducted studies (8).

The investigation, which was made through the EMV laboratories, involved preparation of the samples by light grinding in an agate mortar and pestle. The samples were set on a glass slide with acetone and analyzed after slow air-drying. The air-dried specimens showed both random and oriented characteristics and because they were not fully oriented - this would have masked a number of non-smectite reflections - the changes normally occurring as a result of glycolation were not as marked as they could be. Following

this analysis, the slides were placed in a desiccator containing ethylene glycol for 48 hours. These glycolated samples were then subjected to a renewed analysis.

The equipment used was a Philips Automated Powder Diffractometer with a Cu long, fine focus tube with maximum loading of 1.8 kW; normal run conditions were 40 kV, 30 mA. A theta-compensating slit permitted good resolution to $4^{\circ}2\theta$ and fair resolution to $2^{\circ}2\theta$. The computer used was a NOVA 4/S with 32K word capacity; Philips software was used.

One outcome of the analyses is that the general mineral compositions deduced for a limited number of samples by earlier investigators of this profile turn out to be representative of the entire sequence. Thus, smectite/illite combinations, micas, chlorite/kaolinite, quartz and feldspars are the main constituents throughout the bentonite series. However, the present study clearly shows that the thick central bed has a clay mineral composition that differs from that of the adjacent thinner layers (cf. Table 3). While the upper and lower thin beds show a particularly high background/wide-peak pattern in the interval 7-14Å, indicating substantial biotite/chlorite/mixed-layer representation, as well as a diffuse swelling pattern with very moderate expansion only, all the samples in the central thick bed exhibit a largely uniform composition characterized by phyllosilicates with $d = 14.7-15.5\text{Å}$, as well as 10Å when air-dry and with $d = 17.1-17.9\text{Å}$ when glycolated. The highest intensities of the $d \sim 15\text{Å}$ reflections, which suggest that Ca is the dominant adsorbed cation, are exhibited by samples K7 and K8, i.e. the ones situated in the center of the thick bed. This shows that the central part has the largest portion of swelling constituents of the entire bentonite series. The conclusion from the element analysis that the investigated bentonite layers are affected by dissolved agents, primarily potassium, which have entered from external sources situated above as well as below the series, is certainly supported by the present mineral study.

Table 3. Main reflections of Kinnekulle samples evaluated from X-ray diffraction plottings ¹⁾

Sample	Reflections ¹⁾	Remarks
K1	Air-dry 11.80/54 7.23/7 5.60/9 5.02/25 4.74/13 4.51/100 3.35/61	} Lower thin layers Boundary layer } Central, thick bed } Upper thin layer
	Eth.gl. 35.03/43 12.48/16 9.33/14 5.28/17 4.49/92	
K2	Air-dry 12.13/10 10.22/7 7.16/2 5.02/5 4.52/12 4.32/13 3.36/100	
	Eth.gl. 29.82/32 13.07/18 10.11/29 9.18/14	
K3	Air-dry 14.35/14 12.16/38 10.14/51 7.17/23 5.03/55 4.51/79 3.36/100	
	Eth.gl. 30.60/31 13.07/20 10.16/25 9.39/18	
K4	Air-dry 15.33/28 10.60/12 7.41/13 5.12/9 4.59/22 4.34/21 3.39/100	
	Eth.gl. 17.13/28 10.17/14 7.21/9	
K5	Air-dry 15.52/27 10.52/4 7.38/7 5.13/11 4.58/26 4.34/21 3.39/100	
	Eth.gl. 17.89/24 10.39/5 7.33/7	
K6	Air-dry 14.75/25 10.05/9 7.19/6 5.02/6 4.50/16 4.27/22 3.35/100	
	Eth.gl. 17.47/20 10.15/5 7.18/7	
K7	Air-dry 15.23/35 10.32/5 7.27/9 5.06/8 4.54/18 4.30/17 3.37/75	
	Eth.gl. 17.25/17 10.17/4 7.21/6	
K8	Air-dry 15.31/36 10.25/8 7.23/8 5.07/7 4.53/20 4.30/20 3.35/100	
	Eth.gl. 17.20/29 10.20/5 7.21/5	
K9	Air-dry 14.79/17 10.38/3 7.23/3 5.07/5 4.53/9 4.29/21 3.36/100	
	Eth.gl. 17.10/10 10.18/2 7.19/3	
K10	Air-dry 15.09/8 7.26/5 5.06/5 4.53/10 4.30/20 3.37/100	
	Eth.gl. 17.98/11 9.81/2 7.34/4	
K11	Air-dry 14.70/8 (13.41/6) 7.22/4 5.05/3 4.53/9 4.29/19 3.36/100	
	Eth.fl. 17.57/8 10.26/1 7.26/3	
K12	Air-dry (16.00/16) 12.31/43 10.41/42 7.33/13 5.51/17 5.05/19 4.57/83 4.30/48	
	Eth.gl. 32.64/16 13.41/11 10.23/33 9.33/10 7.23/7	
K13	Air-dry 12.73/47 12.03/50 10.01/79 7.15./6 5.01/20 4.49/62 4.27/18 3.34/100	
	Eth.gl. 35.42/5 13.62/12 10.14/29 9.29/7 7.32/3.6	

1) A/B-values represent d-spacing and relative intensity of major peaks, respectively.
For the ethylene glycol treated samples only low $2\theta^{\circ}$ -values are cited.

2.6.4 Microstructural investigations

Experience shows that smectitic clays present difficulties in the preparation of specimens for adequate electron microscopy. However, instant freezing followed by sublimation under low air pressure yields clay particle networks with reasonably well preserved geometrical arrangements for SEM investigation. The preparation involved gradual shaving to form sticks of the clay approximately 10 mm long x x 2.5 diameter. The specimens were then frozen in liquid freon and fractured with a chilled knife. Immediately thereafter they were placed in liquid nitrogen and then into "vacuum" to remove any internal (frozen) water. After sublimation, the stick was mounted to a SEM specimen stub with the fracture face upwards. Several tape pulls were performed to remove attached debris and the specimens were then evaporatively coated with gold. These coatings, having a combined thickness of a few hundred Ångström units, served to prevent beam charge accumulation in the SEM and to increase secondary electron emission, thereby improving image quality.

A Cambridge S180 scanning electron microscope with a resolution power of less than 100 Ångström units was used for the study, the most satisfactory results being obtained at an accelerating potential of 20 kV, using a tungsten filament. The specimens were scanned to ascertain valid fracture areas, and artifacts introduced by the knife were avoided. Three representative regions were selected for each sample. For each region micrographs were taken at 1000, 10 000, and 30 000 x.

All specimens exhibit the very characteristic microstructural pattern of Na montmorillonite particles, i.e. that of very thin but usually fairly large flakes, collected in an interwoven pattern and showing at least stack-wise alignment ("domains"), cf. (10). The interlamellar distance is so small that it cannot be distinguished, while the number of laminae in each domain usually ranges from less than 20 to more than 50. The larger domain units are separated by voids most of which appear to be in the size interval of 0.05 to 1 μm . Most larger domains are more or less oriented which gives the bentonite its slightly shaly macroscopic appearance.

The most important microstructural observation is the frequent occurrence of globular, very small precipitations along the edges of several domains in all the specimens as seen in the rather arbitrarily picked micrographs in Figs. 8-10. In most cases the precipitations seem to have grown to form discontinuous but rather long, cementitious bodies, which clearly must have a restraining effect on the swelling ability of the smectite. The fact that the precipitations are equally and very moderately abundant throughout the bentonite sequence indicates that it does not originate through diffusion from external sources. Instead, they appear to be identical with the finely divided cementitious quartz that was assumed to be responsible for the resistance to dispersion reported by BYSTRÖM. This suggests that the precipitations we observe in the micrographs emerge from liberation of Si in tetrahedral positions during the high-temperature period. Their uniform distribution logically results from the uniform temperature that once prevailed throughout the entire bentonite profile.

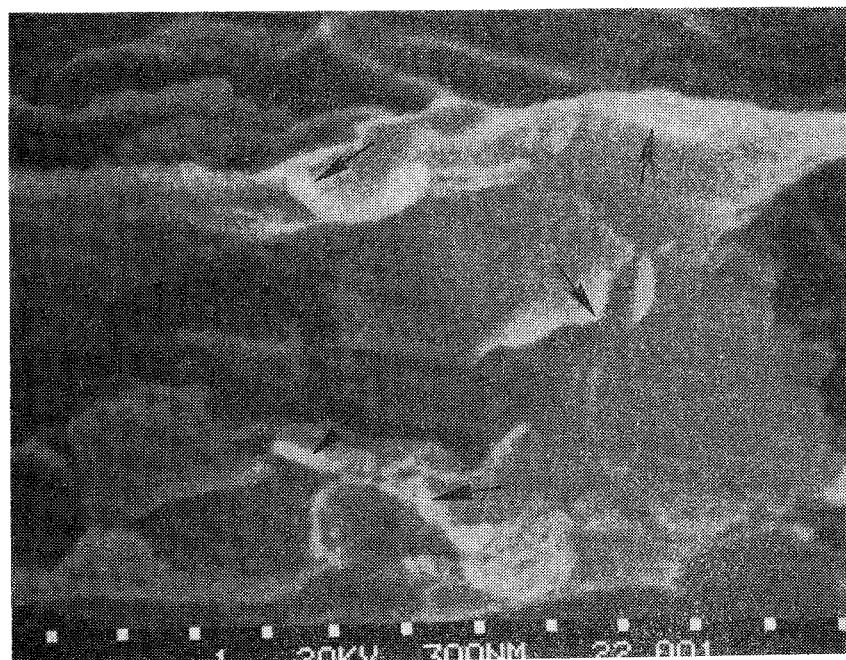
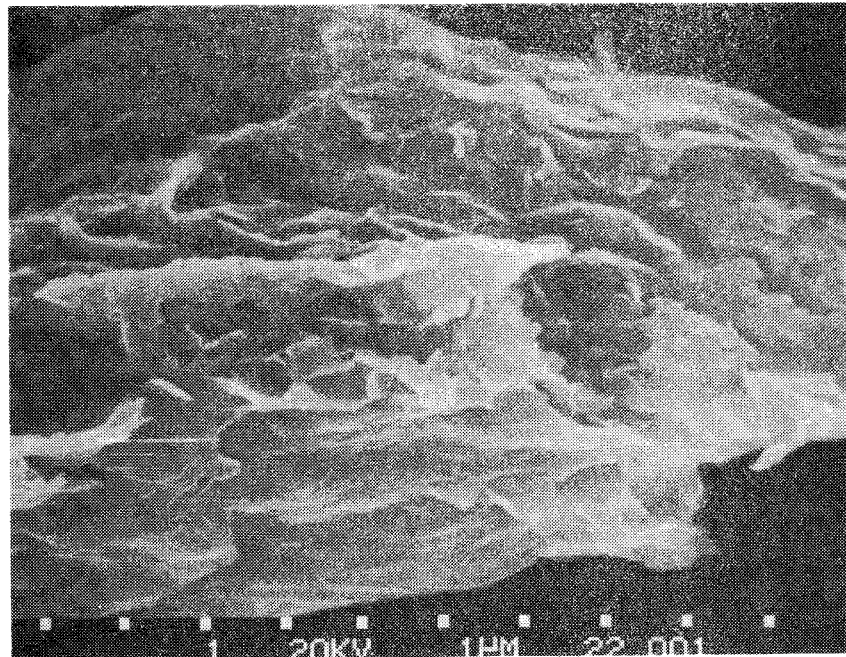


Fig. 8. SEM pictures of specimen from Sample K1 (lowest, thin bentonite layer). Magnification of upper picture is 10 000 x, and 30 000 x of lower picture. Notice the globular bodies on the edges of several domains.

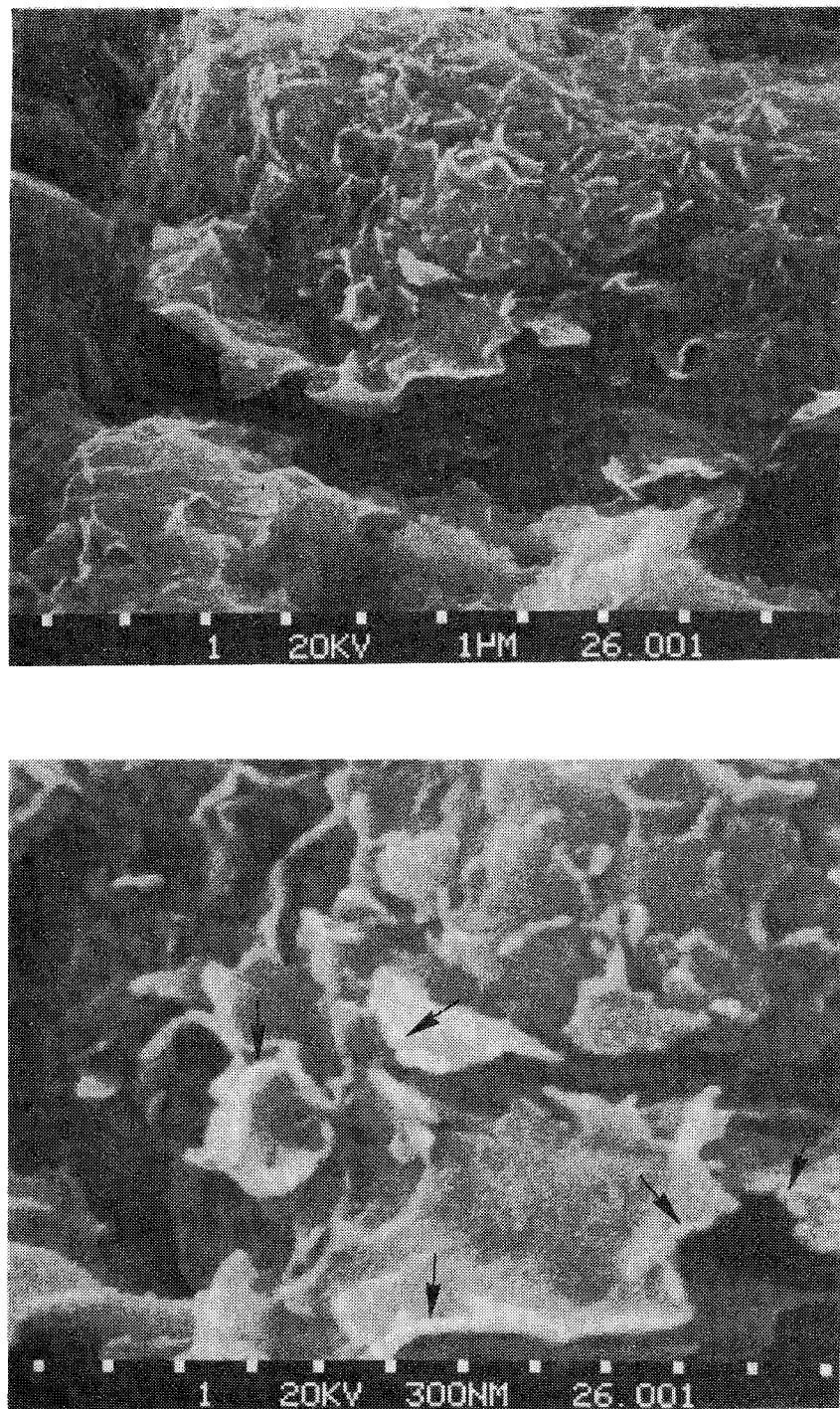


Fig. 9. SEM pictures of specimen from Sample K7 (central part of thick bed). Magnification of upper picture is 10 000 x, and 30 000 x of lower picture. The same features are seen as in Fig.8.

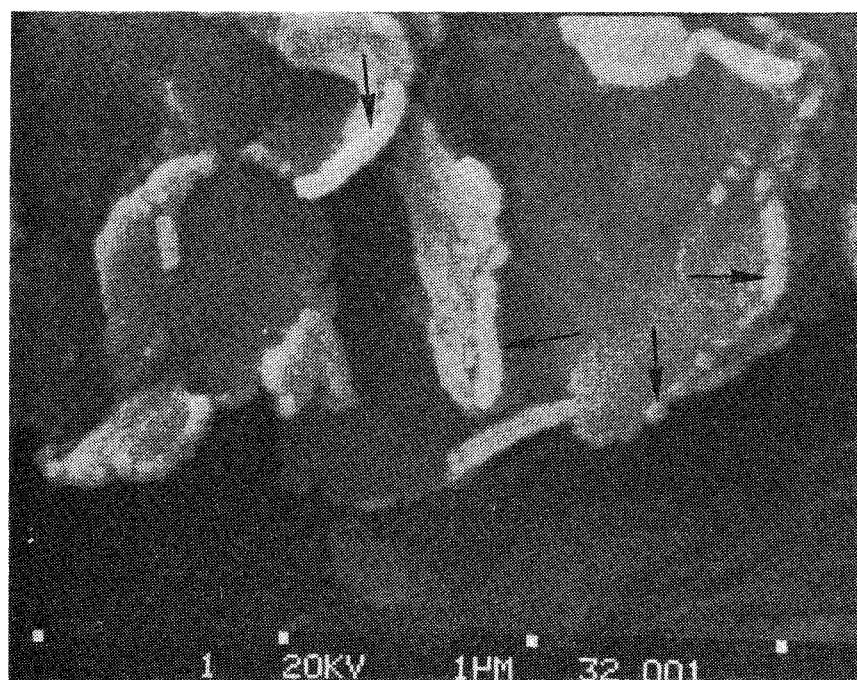
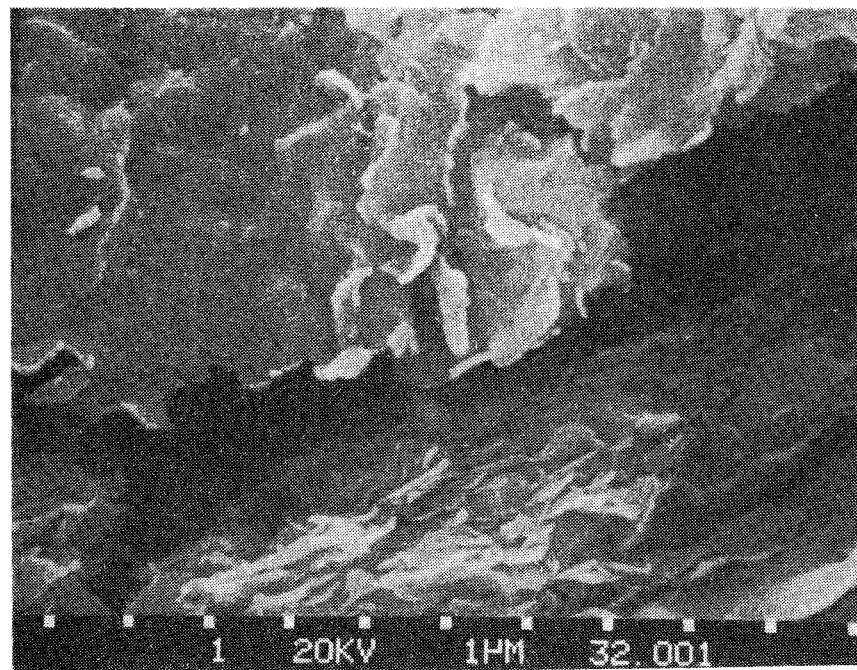


Fig. 10. SEM pictures of specimen from Sample K12. (Interface between upper part of thick bed and overlying shale). Magnification of upper picture is 10 000 x, and 30 000 x of lower picture. The same features are seen as in Figs. 8 and 9.

2.6.5 Physical condition

Despite the slight difficulty of dispersing certain Kinnekulle samples as reported by BYSTRÖM - the main reason for this being demonstrated in the preceding text - it is of great significance that a considerable fraction of cored samples swell spontaneously in water (7). A strong evidence of the very long time during which the swelling potential has been preserved is the present water content. Experience shows that a smectite-rich clay consolidated under a pressure to which the Kinnekulle series is likely to have been subjected, reaches equilibrium at a water content of 20% at maximum. The present content is, however, much higher as shown by Table 4, the maximum value being about 35% in the thick bed where the illitization is least developed and the swelling potential consequently the highest. This value corresponds to a bulk density of about 2 t/m^3 and a swelling pressure of less than 10 MPa. Clearly, the clay has adsorbed groundwater and swelled to the present state from a previous water content of about 20%. This took place at the unloading after the glaciations and the heaving is probably still going on since the present overburden is very moderate in the Mossen area.

Table 4. Natural water content, i.e. ratio of water to that of solid substance, dried at 105°C Kinnekulle samples.

Sample	Water content, %	Location, distance from ground surface, m
K1	27	9,20
K2	32	8,30
K3	27	7,95
K5	35	7,30
K6	27	7,10
K7	29	6,85
K8	28	6,65
K9	22	6,45
K11	23	5.90

A simple way of estimating the smectite content of commercial bentonite is to determine the liquid limit (i.e. the upper Atterberg consistency limit), since it is a function of the surface activity of the clay which, in turn, is determined by its clay mineral constituents and the adsorbed cations. This property is shown in Table 5. We can see that the liquid limit is rather constant, which seems to indicate that it is not the degree of illitization that determines the activity of this clay. The values are characteristic of Quaternary inorganic soils with a clay content (minus 2 micrometers) of about 60-80% and with illite and chlorite as main minerals, constituting about 75% of the clay fraction. The main bentonite bed in the Mossen area has a clay content of only 35-40% of which smectite/illite probably forms 75% at maximum. This would be in reasonable agreement with the recorded liquid limits and it actually suggests a high smectite/illite ratio considering the fact that pure Ca montmorillonite has a liquid limit of 100-150%.

Table 5. Liquid limit, Kinnekulle samples

Sample	w _L	Location
K1	75	Lowest thin layer
K5	69	} Central, thick bed
K6	63	
K9	75	
K11	70	
K13	77	Upper thin layer

3. MARGRETEBERG SMECTITIC CLAYS¹⁾

3.1 General

Smectitic Keuper clays in the Höganäs depression have been exploited commercially for many years by the Höganäs AB company and considerable information of their mineralogical and physical properties have long been available through a number of scientific and technical papers, cf.(13). As in the case of the Kinnekulle bentonites, analyses of a representative profile offer an opportunity to check the model of smectite stability. The text comprises a short geological description of the sediment sequence with particular reference to its origin, and of the mechanical stress and temperature histories, as well as of recently conducted studies concerning the chemical composition and physical properties of cored samples.

3.2 Geology

The approximately 15 m thick Keuper clay sediment layer in the Margreteberg area was deposited about 200 million years ago on top of the clastic Kågeröd Formation. The clay was probably formed in saline shallow coastal water, its very high degree of homogeneity indicating constant conditions of deposition. On top of it an approximately 5 m thick rather complex sand/kaolinite series, termed Upper Vallåkra, was then formed, and later the sequence was covered by organic-rich sediments which include coal seams.

1) Referred here to the Höganäs AB shallow quarry at Margreteberg

Is it possible that the origin of the Keuper clays is that of bentonite, but it is equally probable that it resulted from the weathering of feldspar-rich material from the nearby rocky area.

Subsequent complex tectonical processes yielded a 40° dip of the sediment sequence in the Margreteberg area, where three different horizons can be distinguished: the "yellow" (uppermost), the "grey" (intermediate), and the "red" (lowest) Keuper Clay, respectively. The "yellow" represents the approximately 2 m thick weathered shallow "dry crust" of the "grey" and of the "red". The last-mentioned bed, which is actually only slightly reddish, was considered to be of primary interest for possible practical use at the time when this study was initiated and the investigation was therefore focused on this particular bed and on the adjacent overlying yellow horizon. Numerous granulometrical and elemental analyses have been run on samples of these sediments; they are known to be very fine-grained and fairly rich in iron. Table 6 serves to illustrate the characteristic composition of the reddish and yellow Keuper clays.

Table 6. Chemical composition of Margreteberg Keuper clays

Compound	Reddish clay %	Yellow, weathered reddish clay %
SiO ₂	57.7	54.7
Al ₂ O ₃	19.3	23.4
Fe ₂ O ₃ 1)	8.8	5.5
MgO	1.2	1.2
CaO	0.6	0.8
Na ₂ O	1.5	0.6
K ₂ O	1.4	0.6
TiO ₂	1.0	1.5
H ₂ O	~9	~12

1) The figure refers to the total Fe content

We see that the iron concentration is lower in the yellow horizon than in its underlying source material, which suggests removal of iron from the upper horizon through groundwater percolation or simple diffusion in post-Triassic time. The silica and alkali contents are also clearly higher in the lower, unweathered clay which points to the same process. This has yielded a slight abundance of aluminum in the upper horizon, which may have produced some montmorillonite-beidellite transformation.

3.3 Stress conditions

As in the case of the Kinnekulle bentonites, pressures reduced from estimated Pleistocene ice loads give the only reasonably safe pre-stress level. It is assumed to have been of the order of 10 MPa (10).

3.4 Temperature conditions

The Keuper series in Margreteberg is not supposed to have been considerably heated. Thus, the closest post-deposition diabase outcrops appear several kilometers from the sampling site. However, rather intense post-Liassic faulting has taken place frequently in this area (13) and heating processes cannot be excluded. Fossil analyses have failed, unfortunately, because no suitable specimens could be identified in a preparative study.¹⁾

3.5 Recent study

3.5.1 Purpose

Preparatory tests on the swelling behavior of the Höganäs Keuper clays have shown that bulk samples do not swell readily.

1) The study was kindly made by Dr. Dorothy Guy-Ohlson, Swedish Museum of Natural History, Stockholm.

The rather "inactive" behavior of the reddish clay material in particular, is clearly contradictory to the richness in smectite that X-ray diffraction patterns of this clay indicate. This is supposedly explained by precipitated matter acting as cementation, the origin of which was considered to be of primary interest in this study. Element analyses, especially with respect to the concentration and distribution of iron, electron microscopy for the identification of cementing agents, as well as determination of certain soil physical data, were therefore scheduled and four 10 m long \varnothing 100 mm cores were drilled in August 1982. The drilling as well as the very careful packing of the sealed cores for transportation to the Division of Soil Mechanics, University of Luleå, was made by the Höganäs AB. Extraction of samples was made in Luleå, where the soil physics tests were run and from where specimens were sent to the EMV Ass. Inc. for elemental and mineral analyses as well as for microstructural investigations.

The borehole, which is termed BH 1976 by the Höganäs AB, is characterized by the columnar section in Fig. 11.

3.5.2 Element analyses

The main purpose of the analyses was to:

- 1 Investigate whether there is a Fe concentration profile that offers a way of identifying the Fe source and direction of Fe migration.
- 2 Investigate whether there is a concentration gradient in B which should indicate leaching of groundwater.

	Position of samples	Litho-Stratigraphic Symbols	Litho-Stratigraphic Description
0			Soil Debris
			Yellow plastic clay
1	1.15 (YK1)		
	1.65 (YK2)		
2	2.15 (RK3)		Reddish plastic clay
	2.65 (RK4)		
3	3.15 (RK5)		
	3.65 (RK6)		
4	4.15 (RK7)		Reddish stiff clay
	4.65 (RK8)		
5	5.15 (RK9)		
	5.65 (RK10)		
6	6.15 (RK11)		
	6.65 (RK12)		
7	7.15 (RK13)		
	7.65 (RK14)		
8	8.15 (RK15)		
	8.65 (RK16)		
9	9.15 (RK17)		
	9.65 (RK18)		
10 m			

Fig. 11 Stratigraphic Columnar Section, BH 1796 (Höganäs AB)
 (Standard Legend Royal Dutch/Shell group of companies)
 Figures in front of sample codes denote depth in meters
 below ground surface.

As in the Kinnekulle case the detection limit could not be sufficiently reduced to deduce meaningful results.

- 3 Investigate whether Al, K and Ca indicate leaching or diffusion processes. Together with the Fe profile this survey should indicate possible charge change associated with replacement of tetrahedral Si by Al, as well as illitization trends.

Three separate analyses were made:

- 1 Atomic Absorption Spectrometry (AAS) was performed to determine absolute concentrations of iron and boron in the samples.
- 2 Energy Dispersive (X-ray) Spectrometry (EDS) was performed to qualitatively determine the overall elemental composition of the samples.
- 3 X-ray Line Scans and Mapping were performed on freeze-fracture surfaces to determine distribution characteristics of iron in the samples.

The AAS analysis had a detection limit for iron of 10 ppm, the repeatability being approximately $\pm 15\%$. The EDS analyses, which also comprised line scans and mapping, were made in the same way as in the Kinnekulle case.

The main results of the AAS and EDS runs are listed in Table 6.

 The concentrations refer to dry weight of the material.

Table 7 reveals interesting elemental features of the profile. We see that there is no clear difference between the yellow and reddish plastic clays, except for slightly lower Al and Ca contents in the lowest part of the reddish plastic clay zone. Al is obviously present in concentrations that suggest beidellite-type smectites in the yellow horizon but the K-content is so low that no illitization has taken place.

The conclusion that Al-rich smectites dominate is actually in agreement with the outcome of earlier chemical and dehydration analyses (13).

The stiff reddish clay is not significantly different from the plastic materials with respect to Al and Ca but is slightly richer in K and Fe. The difference in concentration of the two last-mentioned species does not suggest large differences in physical properties, however.

Table 7. Elemental analyses of Margreteberg clays

Samle	AAS ppm Fe	EDS relative concentrations ¹⁾				Location
		Fe	K	Al	Ca	
YK1	16 100	2.6	1.0	3.4	1.0	Yellow plastic clay
YK2	65 000	5.0	0.8	3.4	1.0	
RK3	28 100	3.1	1.0	3.4	1.0	Reddish plastic clay
RK4	9 980	2.6	0.6	3.1	1.0	
RK5	17 900	2.6	1.0	2.7	0.7	
RK6	6 870	1.9	0.7	2.9	0.7	
RK7	34 000	2.7	1.2	2.8	0.7	Reddish stiff clay
RK8	23 300	4.2	1.8	3.4	1.0	
RK9	19 400	3.1	1.2	3.0	0.8	
RK10	23 000	2.4	1.2	3.0	0.7	
RK11	22 900	3.7	1.3	3.1	0.8	
RK12	38 700	5.4	1.5	3.1	1.0	
RK13	26 800	4.4	1.5	3.1	1.0	
RK14	33 800	4.0	1.3	3.0	0.9	
RK15	29 500	4.0	1.3	3.1	0.8	
RK16	34 000	3.6	1.2	3.7	0.8	
RK17	29 600	3.5	1.4	3.2	0.9	
RK18	27 100	3.2	1.2	3.3	0.8	

1) Observed counts/500 for specified elements, the value 10 representing the reference intensity for all samples. Counts do not give relative quantitation between different elements. However, for each element direct comparison can be made with the Kinnekulle core.

The K-content is actually less than that of minimum illitization of the thick Kinnekulle bed, which indicates that the observed inactivity with respect to spontaneous swelling is not due to K-fixation. This leaves the higher Fe-content of the stiffer clay as the most probable cementing agent.

It is worth noting that the Al content of the entire profile is of the same order as that of the boundary regions of the thick Kinnekulle bed, i.e. where increased lattice charge has taken place through replacement of tetrahedral Si by Al. In the Margreteberg case there is no Al concentration profile, which shows that aluminum did not have any external source.

If the beidellite-type structure has resulted from montmorillonite transformation, such that Al has occupied tetrahedral sites, thereby replacing Si, heating is a probable triggering mechanism as for the Kinnekulle bentonites. As suggested previously, the corner edges of the smectite sheets may then have served as an Al source so that aluminum was only locally redistributed over very short distances. However, it may also be that the beidellitic Keuper clays were formed directly from weathered albite feldspar in a suitably composed soft sediment (cf. p.13). This process requires oxidation and removal of some silica and potassium from the solution, and this may well have taken place under the conditions which prevailed in that area. If so, silica may actually have been precipitated through this process, thereby forming cementitious quartz between aggregates as well as brim quartz coatings of the kind observed in the Kinnekulle clays.

The line scans and mappings for the investigation of the distribution of Fe have been interpreted as follows (cf. Appendix 2). The "relative" Fe distribution illustrated by the line scans show the same distribution pattern as in Table 7, i.e. a substantially higher value for YK2 than for the other samples, which are not very different. As to the micro-regional distribution we see that the Fe element is fairly uniformly distributed in the clay (see maps) with occasional random microagglomerations which are rich in iron (YK2 and RK15 serve as examples). Areas relatively devoid of iron probably represent Fe-poor crystals.

3.5.3 Mineral analyses (XRD)

As in the case of the Kinnekulle samples the mineral analysis of the Margreteberg core served as a general survey rather than as a detailed study. The investigation, which was made through the EMV Ass., involved preparation and test runs as was specified for the Kinnekulle analyses.

Smectite, chlorite, kaolinite, quartz, and feldspars are the main constituents throughout the profile (cf. Table 8). There is an obvious difference between the plastic clays (YK1, YK2, RK3, RK5, and RK7¹⁾) and the stiff, underlying clay in the sense that the former are characterized by phyllosilicates with $d = 14.3 - 14.7 \text{ \AA}$ when air-dry and $d = 16.7 - 17.5 \text{ \AA}$ when glycolated, while the latter have $d = 12.2 - 12.5 \text{ \AA}$ when air-dry and $16.7 - 18.8 \text{ \AA}$ when glycolated. This suggests that Ca is the dominant adsorbed cation in the plastic clays, while Na occupies most exchange sites in the stiff clay. The entire profile is poor in 10 \AA minerals. The most important conclusion from the survey with respect to the initial question is that the stiff reddish clay is rich in readily swelling smectite when ground and air-dried on a laboratory scale.

1) RK7 is to be considered as an intermediate case of plastic and stiff reddish clay.

Table 8. Main reflections of Margreteberg samples evaluated from X-ray diffraction plottings

Sample	Reflections ¹⁾							Remarks
YK1	Air-dry	14.67/13	7.28/1	5.05/1	4.51/9	4.28/18	3.36/100	Yellow plastic clay
	Eth.gl.	17.05/14	(9.63/1)	7.21/2	4.50/8	4.26/23		
YK2	Air-dry	14.34/12	7.21/1	5.05/3	4.50/9	4.26/29	3.35/100	
	Eth.gl.	17.47/11	8.52/2	5.59/1	4.49/8			
RK3	Air-dry	14.72/11	7.20/1	4.96/1	4.50/16	4.27/23	3.35/100	Reddish plastic clay
	Eth.gl.	16.66/14	8.38/3	6.49/2	5.62/2	4.50/13	4.27/25	
RK5	Air-dry	14.28/2	4.52/9	4.28/26	3.36/100			
	Eth.gl.	16.69/8	4.52/8	4.27/24				
RK7	Air-dry	14.51/2	13.14/1	7.20/1	4.50/10	4.26/23	3.35/100	Reddish stiff clay
	Eth.gl.	16.79/9	(8.80/1)	7.13/1	4.86/1	4.51/7	4.27/22	
RK9	Air-dry	12.47/4	7.20/2	4.52/12	4.28/23	3.35/100		
	Eth.gl.	16.87/6	8.74/2	7.26/1	4.51/11	4.27/34		
RK11	Air-dry	(17.83/3)	12.18/6	7.20/1	4.50/14	4.26/25	3.35/100	
	Eth.gl.	18.79/7	16.89/7	(8.86/1)	7.26/1	4.52/8	4.28/16	
RK13	Air-dry	12.22/5	7.32/2	5.17/2	4.52/10	4.29/21	3.36/100	
	Eth.gl.	16.67/10	(8.87/2)	7.31/2	4.54/10	4.30/20		
RK15	Air-dry	12.40/9	7.25/2	4.52/13	4.47/10	4.28/20	3.36/100	
	Eth.gl.	17.70/6	(8.90/2)	7.31/2	4.54/7	4.29/19		
RK17	Air-dry	12.36/8	7.22/2	4.50/12	4.39/8	4.26/19	3.35/100	
	Eth.gl.	17.54/6	8.38/1	7.26/1	4.53/8	4.28/15		

1) A/B-values represent d-spacing and relative intensity of main peaks, respectively. For the ethylene glycol treated samples only low 2θ values are cited.

This is exceptionally clear considering the rather random orientation of the crystallites in the XRD analysis (Fig.12).

3.5.4 Microstructural investigations

The Margreteberg clays were investigated with respect to their microstructural features using the same technique as described previously. All specimens were found to exhibit the very characteristic pattern of bunches of interwoven smectite flakes (Fig. 13a). The "domain"-type stacking is frequently seen, the number of laminae in each stack being similar to that of the Kinnekulle bentonites. The larger domain units are separated by voids which appear to vary in size from 0.05 to a few micrometers.

An obvious microstructural feature is the presence of brim quartz coatings. They have the same appearance as in the Kinnekulle clays and are observed in all the samples throughout the core (Figs.13 b, 14 and 15). In addition to this we find a peculiar phenomenon in the stiff reddish clay, which is of great importance. It is the uniform coating of basal planes as well as domain edges by micro-nodules, which very probably consist of iron compounds, presumably goethite. The latter coating ¹⁾ affects the physico/mechanical properties of the clay in the sense that it strengthens the moderate cementation produced by the quartz precipitate, and also inactivates all basal planes that are exposed to voids in the clay. The latter effect means that the hydrophilic character becomes less obvious, which should manifest itself through a rather low Atterberg liquid limit.

1) Similar, but less obvious coating is seen also in the YK2 sample and occasionally in certain Kinnekulle samples as well. The fact that it does not appear at all in many samples despite the identical treatment certifies that it is not an artefact.

FILENAME: DPRK9.RD SAMPLE: DPRK9 10/14/82

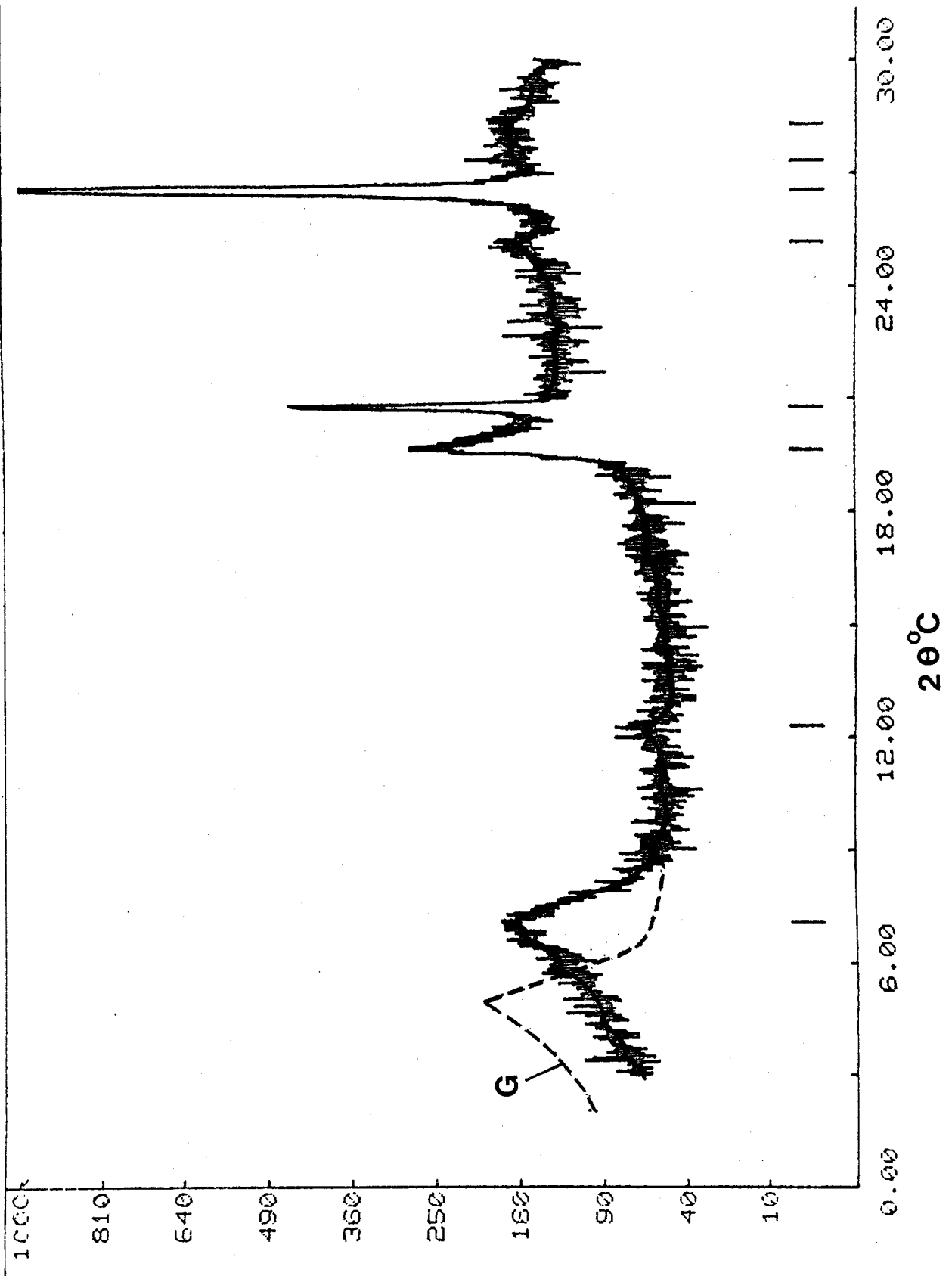


Fig. 12

Diffractogram of stiff, reddish clay from Margreteberg. G represents ethylene glycol treated, oriented sample.

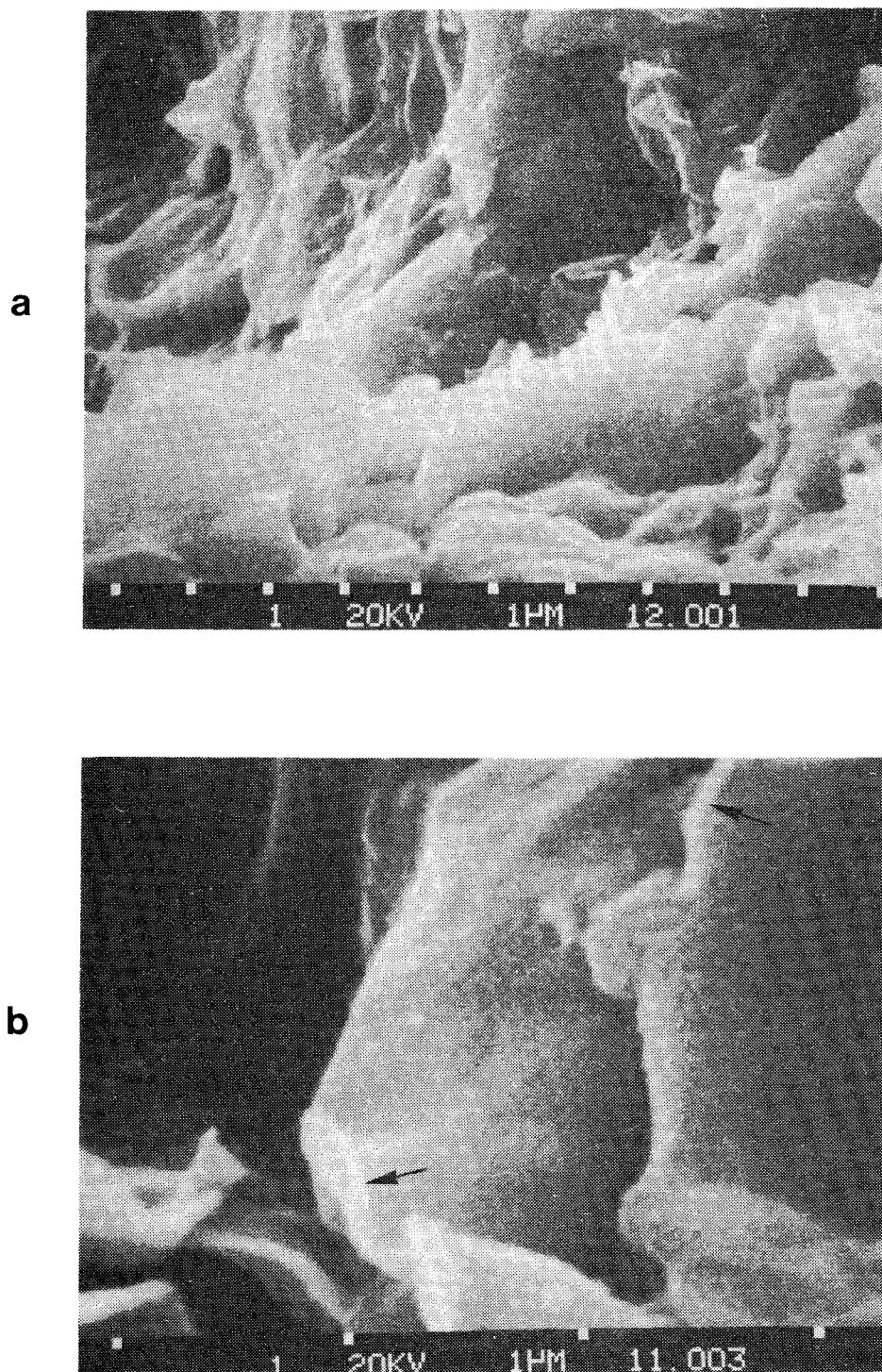


Fig. 13 SEM pictures of specimen from sample YK2 (yellow plastic clay). Magnification of upper picture is 10 000 x, and 30 000 x of lower picture. Lower picture shows quartz coating of domain brims.

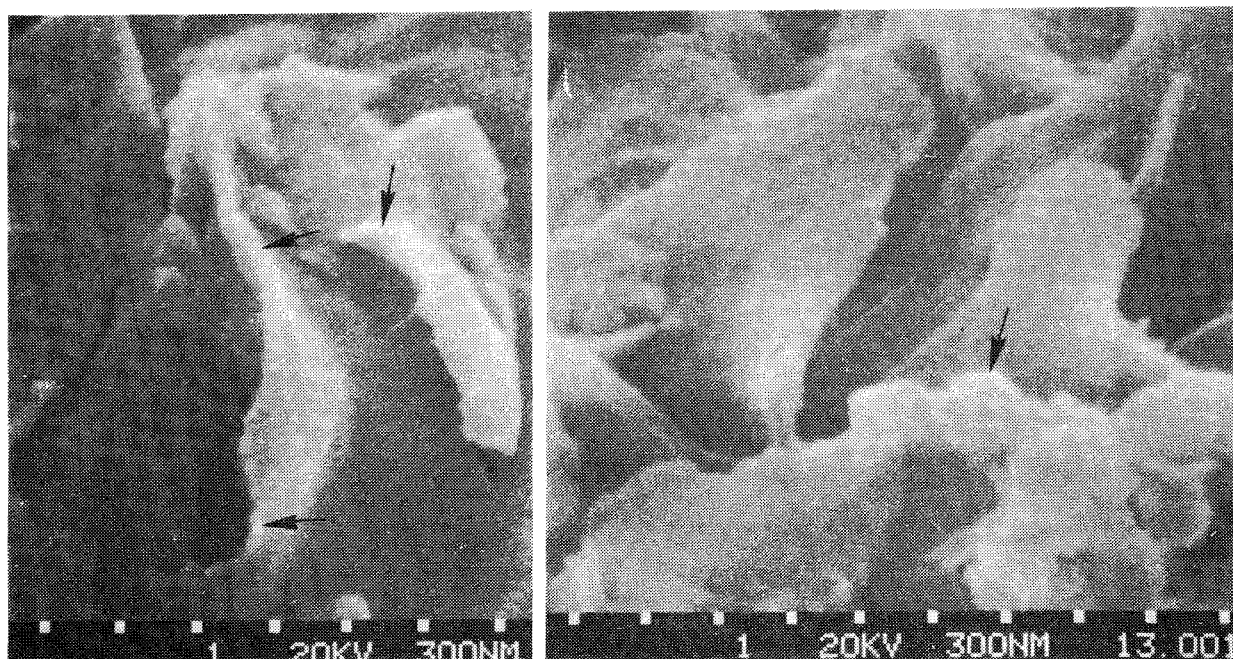
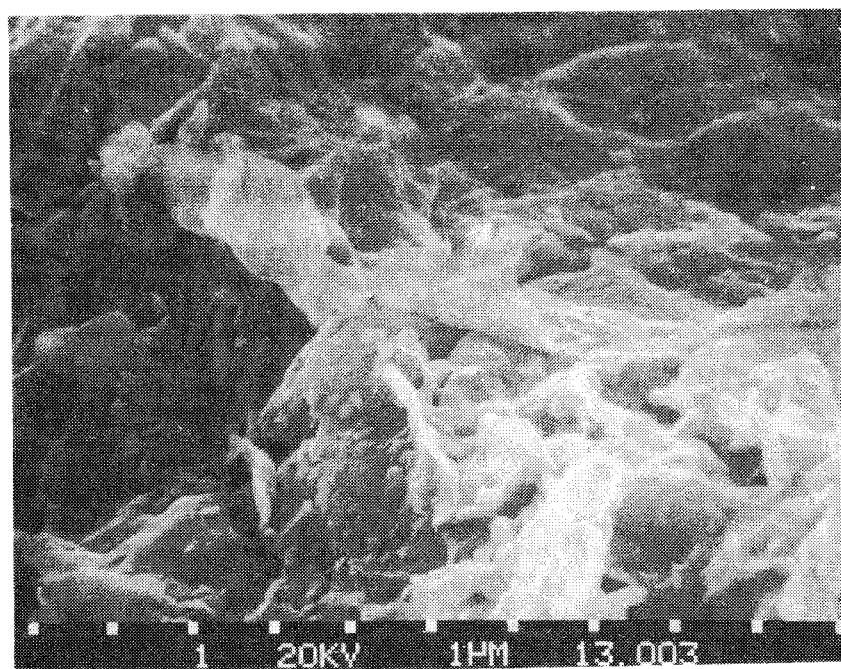


Fig. 14

SEM pictures of specimen from sample RK3 (reddish plastic clay). Magnification of upper picture is 10 000 x, and 30 000 x of lower picture. Lower picture shows quartz coating of domain brim.

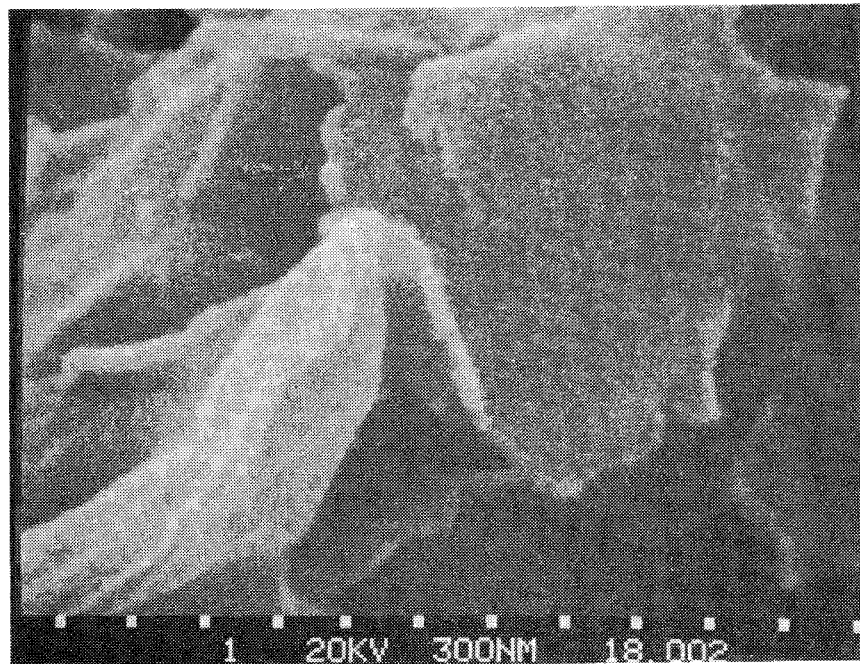
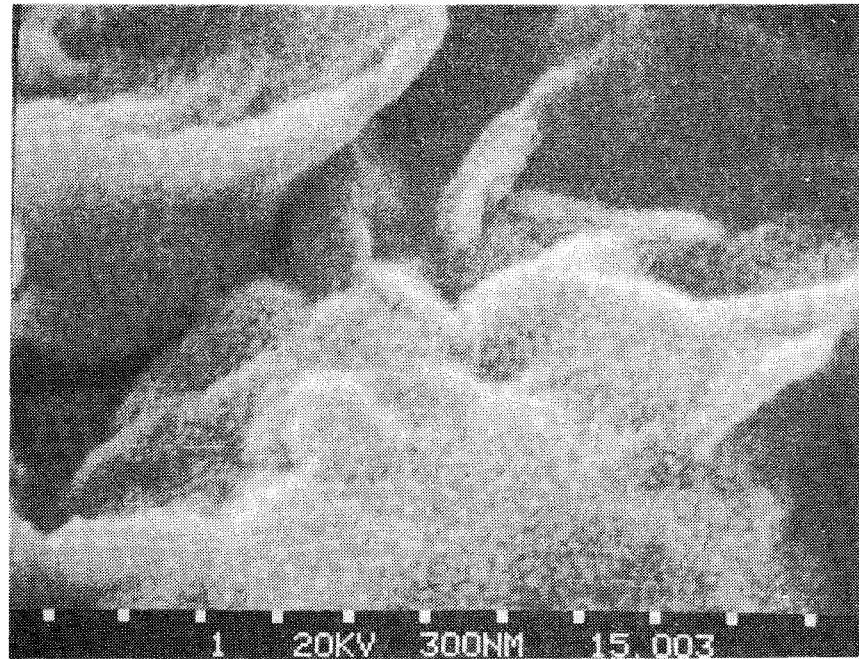


Fig. 15 SEM pictures of specimens from sample RK9 (upper) and sample RK13 (lower), both representing the stiff, reddish clay. Magnification 30 000 x. Both pictures show quartz brim coatings and micro-nodular iron compound coatings of all exposed surfaces.

It is concluded that only very intense mechanical agitation by grinding would cause sufficient exposure of internal surfaces to give the stiff reddish clay a plastic consistency. Chemical treatment is probably required to yield strong swelling and a high cation exchange capacity.

As to the chemical background of the two coatings - the iron compound seems to have been formed after the development of the quartz brim coatings - the quartz is indicative of heating and if its extension and frequency is taken to be proportional to the temperature, then, taking the Kinnekulle clays as a reference, the Margreteberg clays should have experienced an approximate temperature of 100°C. At present there is no geological evidence of such an event although it is not excluded that the heat source was magma intrusion in Jurassic, lower Cretaceous, or Tertiary time, the resulting basalt beds being eroded later.

The large number of Tertiary diabase necks in northeastern Skåne may actually suggest quite a large lateral extension of such beds although the distance to Margreteberg raises some doubt as to the connection between these Tertiary eruptions and the Margreteberg event. Alternatively, the previously mentioned intense post-Liassic faulting-leading to displacements of up to 160 m in the adjacent Höganäs area - may well have been associated with heating through penetrating thermal solutions. Faulting per se should be considered as a local heat source through the exerted friction (14), but neither the heat nor the duration of the heat production would be sufficient to raise the temperature in a large mass by many tens of centigrades.

If heating was not the cause of the quartz coating then direct feldspar-montmorillonite conversion according to the scheme on page 13 is a plausible mechanism, as mentioned previously. In the Author's opinion, however, the almost identical appearance of the brim globules of the Kinnekulle and Margreteberg smectite domains suggest that heating is responsible for their formation.

Turning now to the subsequent coating, it should be pointed out that the almost complete absence of iron compound micro-nodules in the yellow horizon, where they were probably numerous prior to the weathering, was probably caused by reduction through bacterial activity. The iron compounds were probably formed by the release of iron from silicates through a combined hydrolytic and oxidative reaction, presumably by the action of atmospheric oxygen. This may have been associated with desiccation in a dry and hot climate, possibly in connection with crustal uplift in Quaternary time. Actually, the last-mentioned effect is considered to be one main reason for the overconsolidation - in the soil mechanical sense - of certain Quaternary, sedimentary clays in southwestern Sweden.

3.5.5 Physical condition

The mechanical properties of the Margreteberg clay sequence are closely related to the stress history as well as to the chemical processes in terms of cementation. The four most important properties are:

Present water content. If the groundwater level is

 close to the ground level the water content should be highest in the shallow part of the profile. The bulk density should give an effective pressure equal to the swelling pressure. Deviations from these conditions indicate cementation.

2. The degree of water saturation. A degree a saturation substantially lower than 100% is an evidence of desiccation.
3. Swelling pressure. The swelling pressure is largely determined by the smectite content. Large deviations from the expected pressure point to cementation.
4. Liquid limit. (Atterberg consistency). This water content is a simple but valuable measure of the surface activity with respect to hydration ability.

Referring to the discussion of the Kinnekulle bentonites it can be stated that a smectite-rich clay consolidated under a pressure of 10 MPa, i e the probable maximum pressure to which the Margreteberg deposits were subjected, reaches equilibrium at a water content of about 25%. The present water content of the upper, plastic clays is considerably higher (see Table 9), which shows that these clays have swelled after the unloading that took place in postglacial time. The water content of the underlying stiff clays is considerably lower; it indicates a preconsolidation pressure of 30-50 MPa which is impossible.

Actually, it turns out that these lower clays are far from water saturated, the desiccation being associated either with heating or with a dry and hot climate. It should be pointed out that perfect sealing of the cores during the transportation certifies that evaporation did not take place. As concerns the swelling pressure, it can be concluded that the laboratory-derived values determined on air-dried, fine-ground and precompacted clay powder, which was then water-saturated in the swelling pressure oedometer (4), are much higher than the existing effective overburden pressures throughout the profile.

Table 9. Soil data of the Margreteberg clays

Depth below ground level, m	Bulk density ρ_s t/m ³	Natural water content W _n %	Liquid limit W _L %	Degree of water satura- tion 1) %	Existing effective pressure σ' MPa	Laboratory - determined swelling pressure P _s , MPa
1.9 (yellow plastic clay)	2.0	30-32	65-75	100	0.03	4.2 MPa ³⁾ for $\sigma = 2.2$ t/m ³
2.9 (reddish plastic clay)	1.8	35-36	-	100	0.04	-
3.9 (reddish stiff clay)	2.1	19	-	97	0.05	-
4.9 "	2.2	16	↑	100	0.06	↑
6.9 "	2.1	16-17	53-77 ²⁾	93	0.08	0.7 MPa for $\rho_s = 2.0$ t/m ³
8.7 "	2.1	17	↓	87	0.10	↓
9.7 "	2.2	11	↓	70	0.11	↓

1) Ratio of volume of pore water and total pore volume.
Calculated by assuming the mineral (compact) density to be
2.70 t/m³.

2) Lower value natural material; higher value after drying at 105°C.

3) Estimated swelling pressure for $\rho_s = 2.0$ t/m³ is 1 MPa.

This should have led to considerable swelling which was obviously resisted by intact cementation bonds in the undisturbed natural clay.

Finally, the liquid limit is 65-75% for the yellow plastic clay and 53-77% for the reddish stiff clay. The first-mentioned range corresponds to approximately half the liquid limit of Ca-saturated smectite. Since the smectite content of the Margreteberg clays is only slightly higher than 50% the recorded liquid limit of the yellow plastic clay is approximately equal to what is expected. The recorded liquid limit of the underlying Na-smectitic, stiff reddish clay is, however, only about one fifth of the expected value of Na smectite. This points to strong cementation and surface coating.

4. DISCUSSION

4.1 General conclusions

The two investigated smectitic sites, Kinnekulle and Margreteberg, serve to illustrate the major smectite alteration process predicted by the general lattice stability model (6), extended here to cover the associated quartz cementation effect. Both the investigated profiles indicate charge change through replacement of tetrahedral Si by Al ("beidellitization"), caused by temperatures which probably exceeded 100°C, although the Margreteberg clay may actually be an Al-rich smectite formed as such under normal temperature conditions. Assuming both clays to have undergone charge change through heating, the liberation of Si seems to be manifested through the precipitates at the edges of smectite flake domains, as well as through the increased Al content, which is particularly obvious in the Kinnekulle case. Here, K-uptake from surrounding layers also led to substantial illitization. It is of great importance, however, to notice that the illitization did not yield a very obvious loss in plasticity or in spontaneous expansibility on hydration, merely a fairly slight resistance to dispersion. As long as the temperature does not exceed 100°C it can therefore be assumed that when only heat-induced replacement of Si by Al takes place with concomitant precipitation of quartz; i.e. with K-uptake less than that in the Kinnekulle case, neither the plasticity nor the swelling properties will be severely altered. This definitely applies to the KBS concept.

A much more serious change in physico/mechanical behavior is caused by precipitation of other agents, such as the iron compounds in the reddish stiff Margreteberg clay.

Here, a drastic loss in plasticity and a considerable loss in swelling power have been accomplished by a fairly small amount of iron precipitates. It can be safely stated, however, that this sort of precipitation is not relevant to the KBS concept of bentonite surrounding the heat-producing canisters since the conditions will be reducing rather than oxidizing and the iron source will also be very sparse. Neither can it be expected to occur in deeply situated tunnel and shaft backfills containing mixtures of smectite-rich clay and rock-forming minerals since reducing conditions will prevail here as well.

Similarly, the possible conversion of montmorillonite and beidellite to muscovite/illite via kaolinite (cf. p.13) would be excluded in the KBS-case because of the reducing conditions.

4.2 Hypothetical mechanism of the charge change

From a scientific point of view it remains to demonstrate the exact nature of the mechanism by which tetrahedral Si is replaced by Al, this being the key mechanism of practically important lattice alterations. In this context the theory of lattice conversion is of particular interest since it involves a heat-induced loss of hydroxyls which is associated with liberation of Si as well. Further discussion requires a deeper understanding of the EDELMAN & FAVEJEE structural model (Fig.3) which is therefore first considered in some detail.

Objections were originally raised against the EDELMANN & FAVAJEE model since it yields a six times higher cation exchange capacity than the usually found experimental value if the apices carrying acidic hydroxyl groups are assumed to represent exchange sites with exchangeable protons.

This is because there are four unit charges per unit cell, while the average value observed is two-thirds of a charge unit per cell. The important statement has been raised that hydrophilic clays always become negatively charged in aqueous solutions, the reason being proton expulsion, and that this is independent of whether there are isomorphous substitutions and lattice vacancies or not. Actually, there are only fairly slight deviations from the average ion exchange capacity 80 mE/100 g clay despite the largely varying origin and chemical composition of investigated montmorillonites.

The discrepancy between the theoretical and actually observed cation exchange capacities has been explained by considering the coupling between the associated water lattice, which can be assumed to be of the ice lattice-type, and the basal planes of the montmorillonite crystallites (3). Fig 16 shows the protruding hydroxyls of the (001) plane with three unit cells marked, while Fig 17 shows the basal molecules of an ice lattice superimposed on these hydroxyls.

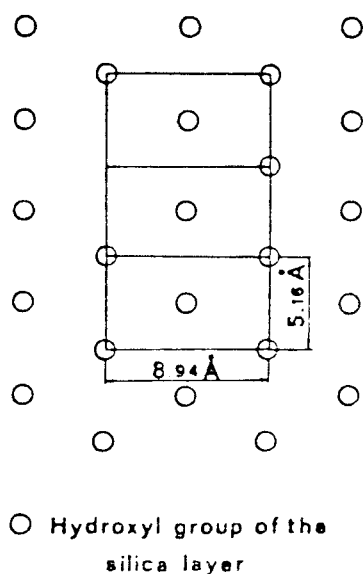


Fig. 16. Protruding hydroxyls of (001) plane. The dimensions of one unit cell are marked (3).

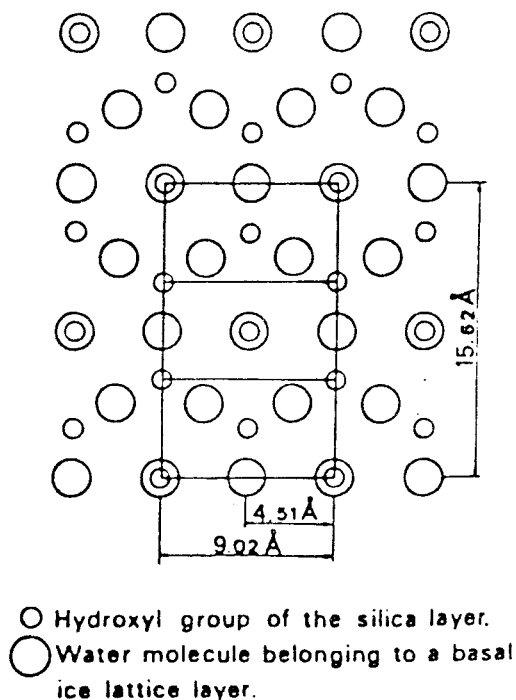


Fig. 17. Basal ice lattice molecules superimposed on the hydroxyls of the (001) plane (3).

It is immediately seen that there are only four hydrogen bonds formed between three unit cells and the associated water lattice. The charge of the crystallite will therefore attain a mean value of two-thirds of a charge unit per unit crystal cell, which is the experimentally observed mean value.

As stated earlier, heating liberates intercrystalline water which is practically removed at 105°C eventually including some surface dehydroxylation but leaving part of the surface hydroxyls intact even in the temperature interval $150\text{-}200^{\circ}\text{C}$. The liberated hydroxyls form free water that escapes, and silica, as well as hydrated silica, is then also free to move. Charge equilibrium then requires uptake or intralattice migration of other available ion species such as Al, and if K is present these ions sink into the silica layer as the lattice expands at rising temperature and tends to set up tensions and lattice distortions that

prevent surface rehydroxylation, [see also (3)].

For other common cations, dehydration of montmorillonite by heating below 200°C is, as a rule, reversible.

The liberated silica creates a concentration gradient which leads to lateral migration and precipitation in the form of quartz or silica compounds at the edges of the stacks of smectite flakes. The outward, interlamellar migration of water in connection with lattice collapse in the c-direction through heating, is probably the main Si-transporting mechanism, however.

Assuming this scenario to be true, the Si-releasing mechanism is largely that of hydroxyl liberation, which is largely governed by the hydrogen bond energy. This would enable us to state that, although some surface hydroxyl and Si loss takes place even at room temperature, major lattice conversion and practically important Si liberation is not obtained unless 100°C is exceeded.

One way of proving this would be to investigate, by applying high magnification SEM technique, natural bentonites which are known to have been exposed to high temperatures as well as bentonites which have not been heated. Such a study was recently conducted by the author (15), who used Silurian bentonite from about 300 m depth on northern Gotland, and Ordovician bentonite, exposed at the present ground surface near Lund (Fågelsång) in Skåne, as typical exponents of heavily precompressed, non-heated, and heated smectites, respectively.

The bentonite from Gotland, which cannot have been heated to much more than room temperature, showed no sign of globular brim coatings on the domains. The other bentonite is assumed to have experienced a temperature of 300°C according to conodont analyses¹⁾ and it exhibits a very irregular surface topography that indicates quartz "beads of perspiration". Representative micrographs are shown in Fig.18.

1) Pers.comm. Prof. Stig M. Bergström

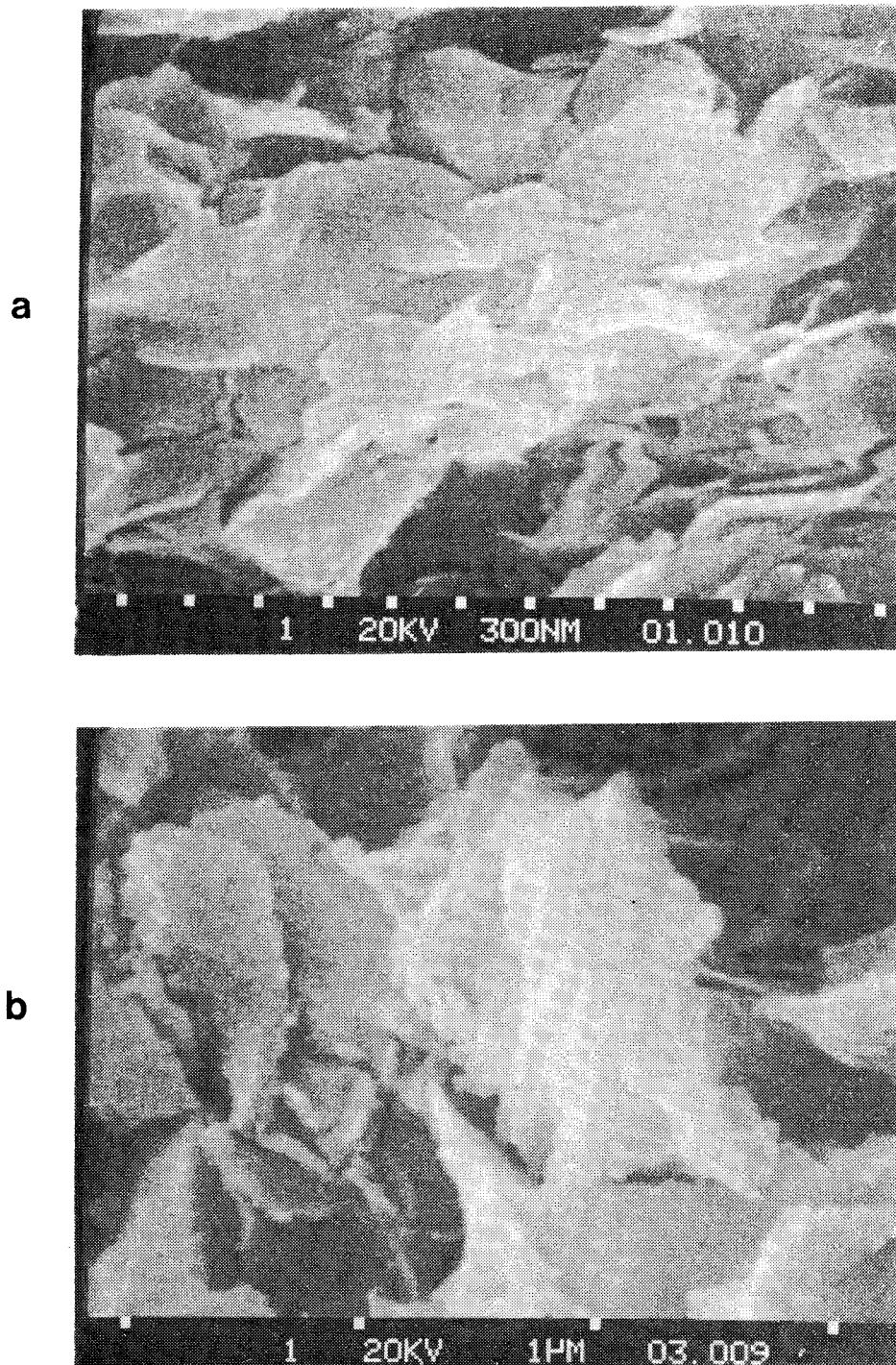


Fig. 18 SEM pictures of a) non-heated Silurian bentonite from Gotland, and b) Ordovician bentonite from Skåne, heated to about 300°C. Magnification 30000 X.

5. ACKNOWLEDGEMENTS

The author wishes to express his sincere gratitude to Dr. Ann Mari Brusewitz, who made very valuable comments on the manuscript, and whose research in this scientific field forms the basis of the present study.

Also, the author is very grateful to Prof. Ivar Hessland, former head of the Dept. of Geology, University of Stockholm, for his comments.

Thanks are extended to Dr. Poul Graff-Petersen, Geologisk Museum, Copenhagen; Prof. Stig M. Bergström, Dept. of Geology and Mineralogy, Ohio State University; Dr. James J. Howard, Schlumberger Doll Research, Ridgefield Connecticut, Prof. Valdar Jaanusson, Swedish Museum of Natural History, and Dr. Erik Saare, Dept. of Geology, Royal Technical Institute, Stockholm.

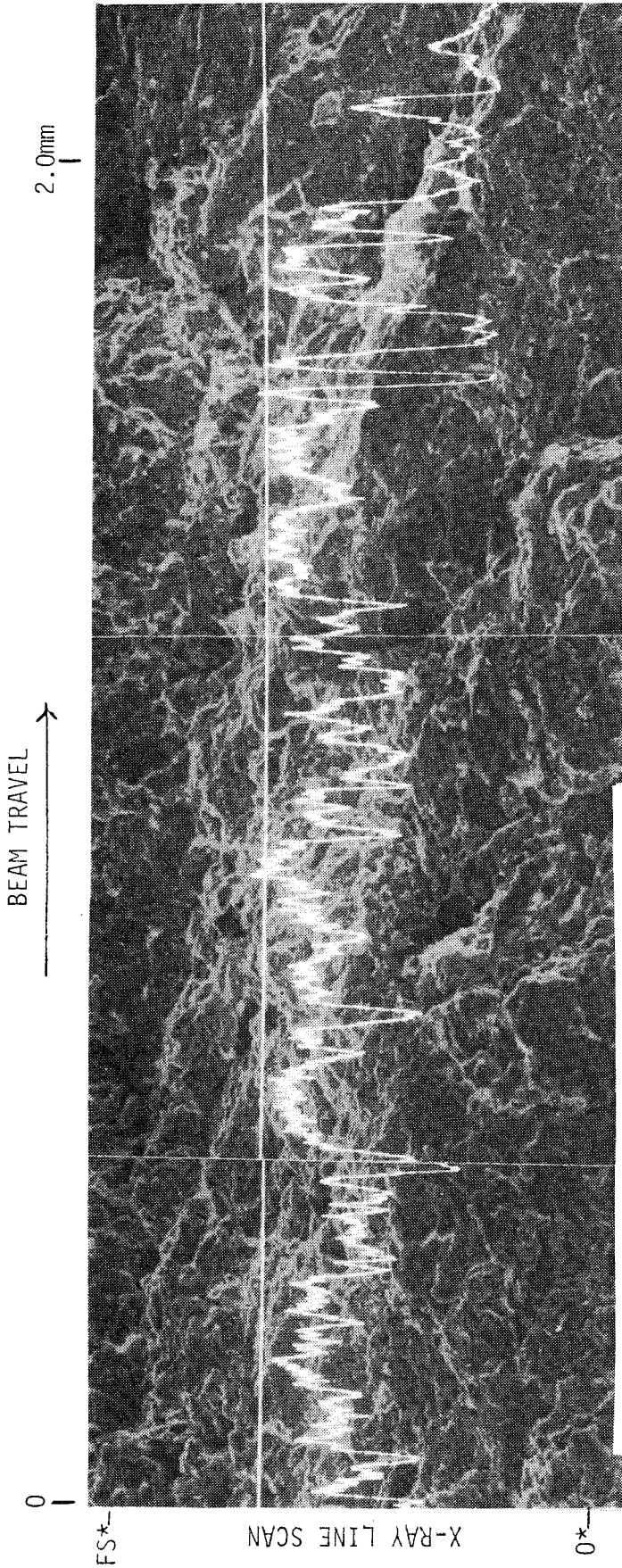
They all contributed in various ways, primarily by commenting on the manuscript, and by giving valuable suggestions.

Special thanks are due to Dr. Arne Gustafsson, Höganäs AB, whose expertise in stratigraphy and chemical mineralogy was very helpful in the preparation of the manuscript.

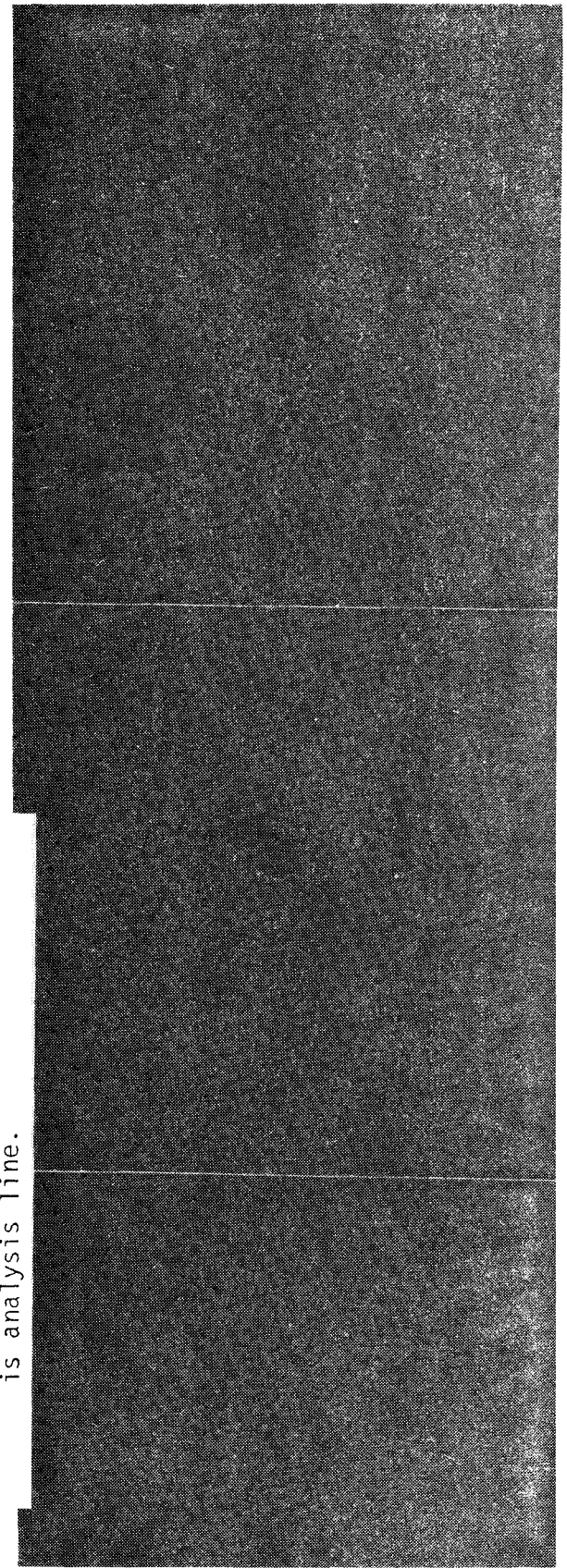
- 10 PUSCH, R. Microstructural features of pre-Quaternary clays. Acta Universitatis Stockholmiensis, Stockholm Contributions in Geology, Vol. XXIV:1, 1971.
- 11 JOHANSSON, S.,
SUNDIUS, N., &
WESTERGÅRD, A.H. Beskrivning till kartbladet Lidköping. SGU Ser. Aa 182, 1943.
- 12 BERGSTRÖM, S.M. Conodonts as paleotemperature tools in Ordovician rocks of the Caledonides and adjacent areas in Scandinavia and the British Isles. Geologiska Föreningens i Stockholm Förhandlingar, Vol.102, Pt.4, Stockholm ISSN 0016-786 X, 1980. (pp.377-392).
- 13 NORIN, R. Studier över den mineralogiska sammansättningen av några lertyper från NV. Skånes rät-lias-, Vallåkra- och Kågerödsbildningar. Geologiska Föreningens i Stockholm Förhandlingar, Bd 71, H.2, 1949 (pp.215-237).
- 14 OSTERMAN, J. Views on the stability of clay slopes. Swed. Geot. Institute. Reprints and preliminary reports, No.1, 1960.
- 15 PUSCH, R. Heat effects on natural, smectite-rich clays. (In preparation).

APPENDIX 1

KINNEKULLE BENTONITES
ELEMENT ANALYSES (EMV)



Note: *Approximate position. Straight line is analysis line.

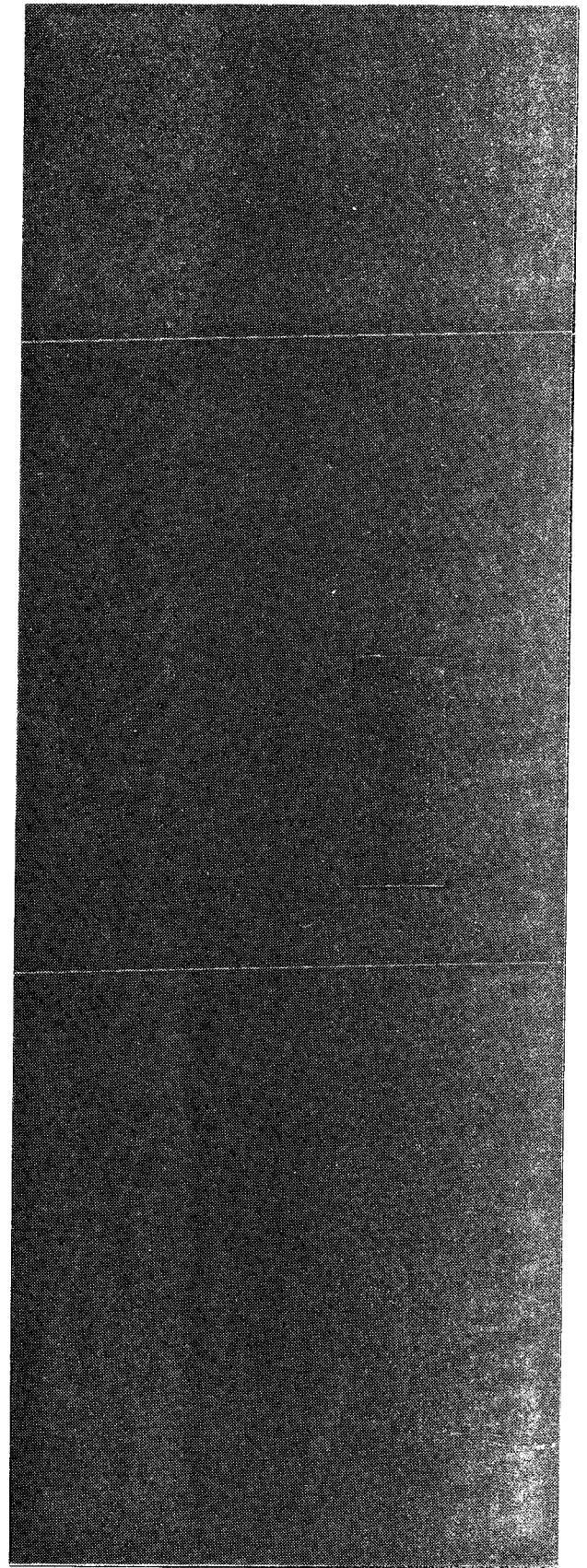
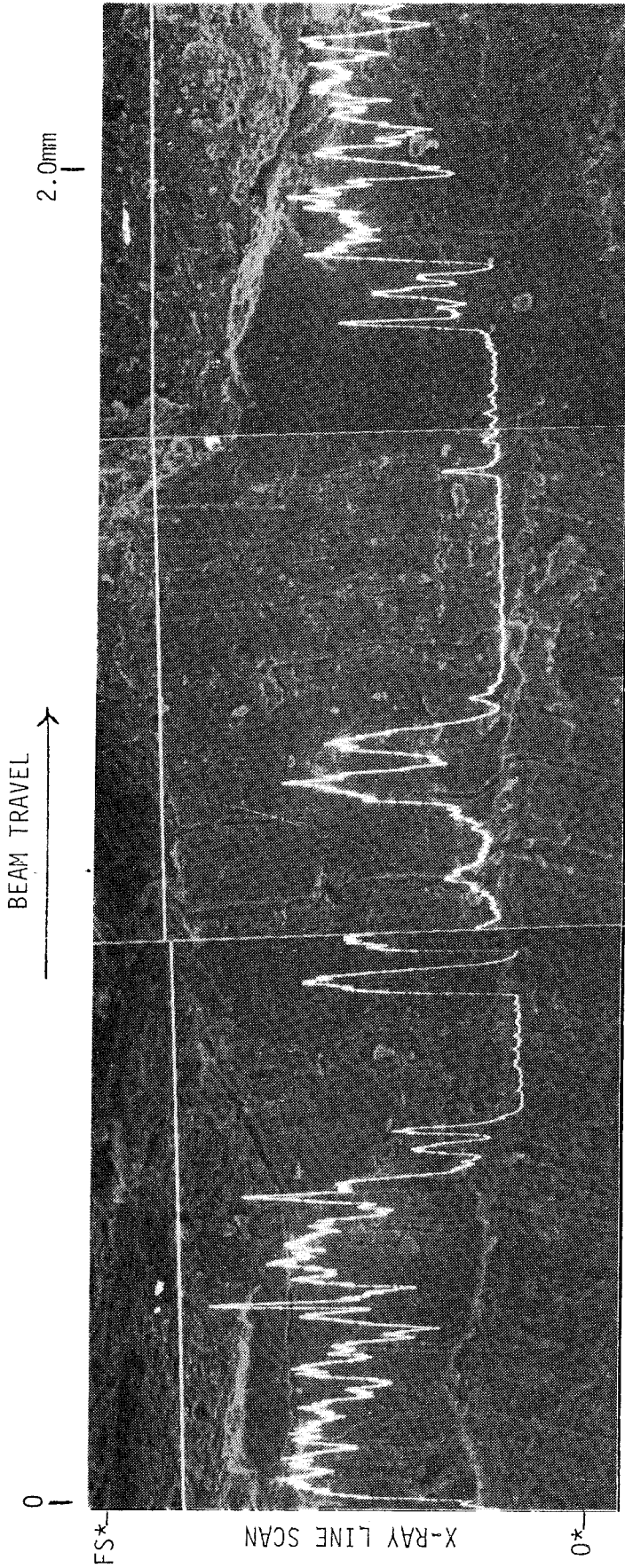


MACHINE SETTINGS

LINE - FULL SCALE SENSITIVITY: 1.0×10^3 cnts/sec.
 SCAN SETTING: 7
 MAP - SCAN SETTING: 11

SAMPLE K2

ELEMENT K



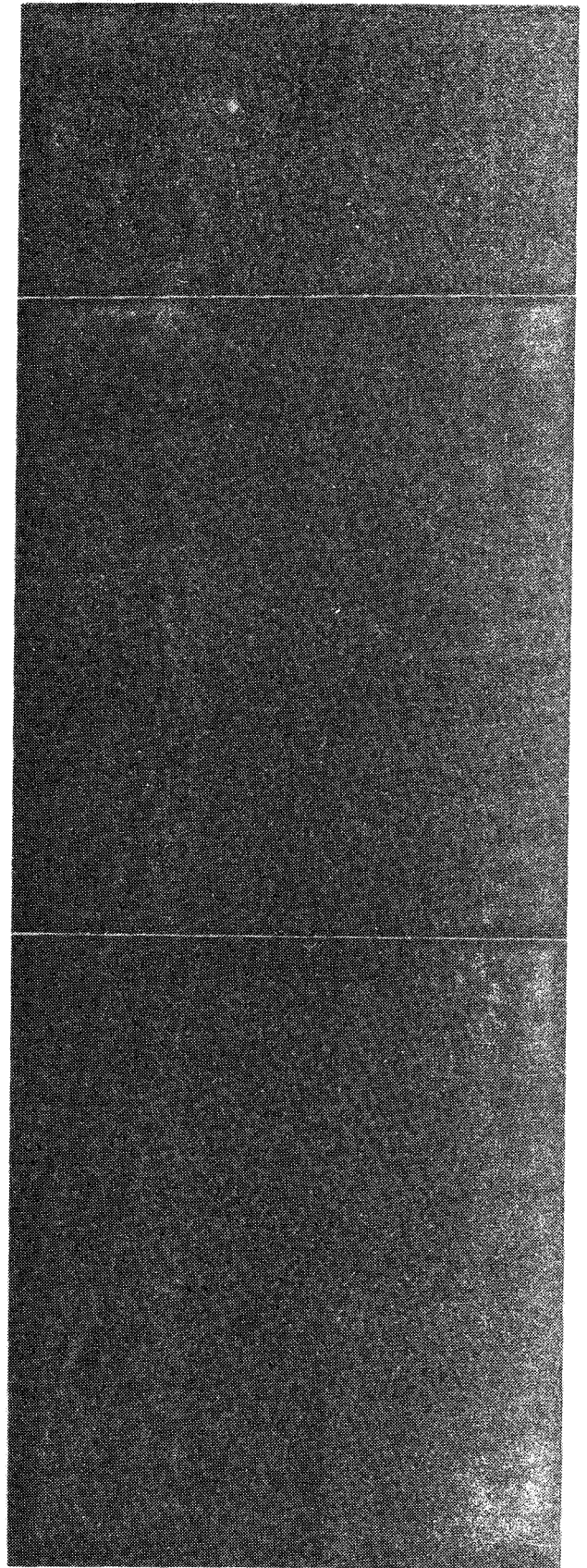
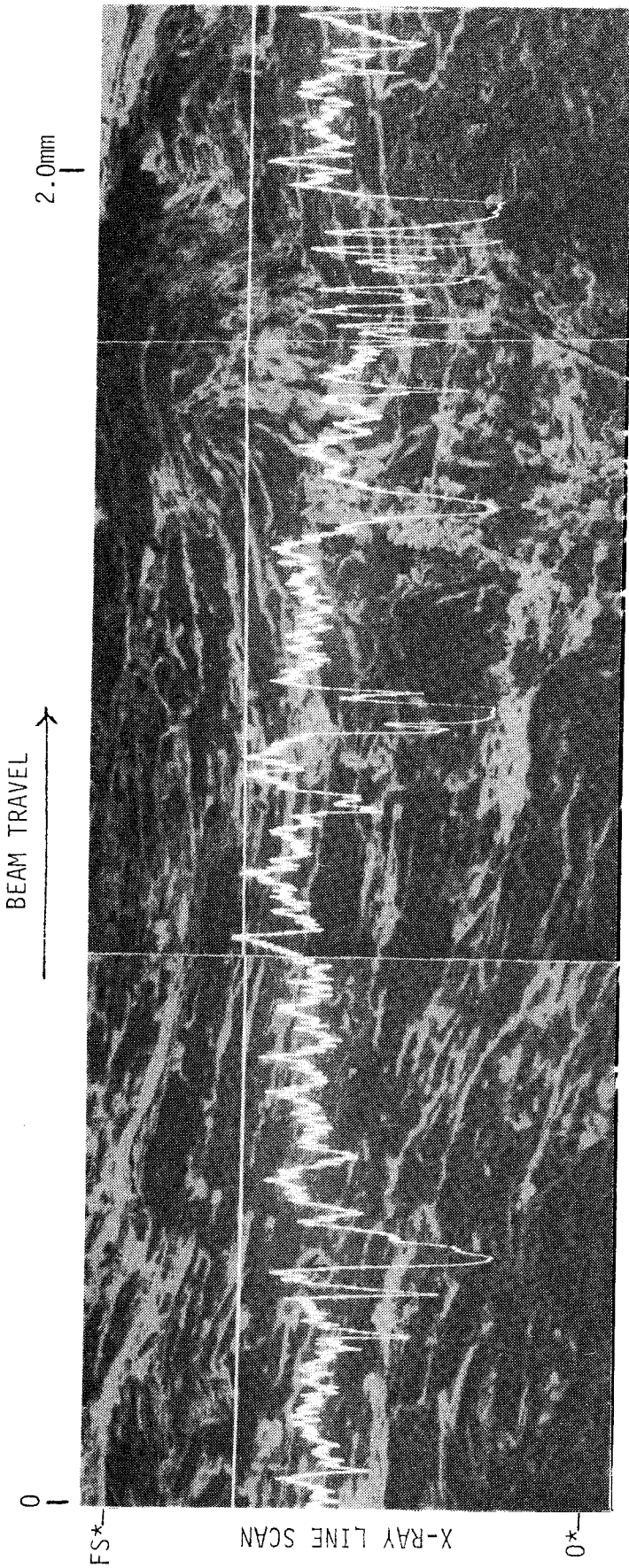
MACHINE SETTINGS

LINE — FULL SCALE SENSITIVITY: 1.0×10^3 cnts/sec.
SCAN SETTING: 7

MAP — SCAN SETTING: 11

SAMPLE K3

ELEMENT K



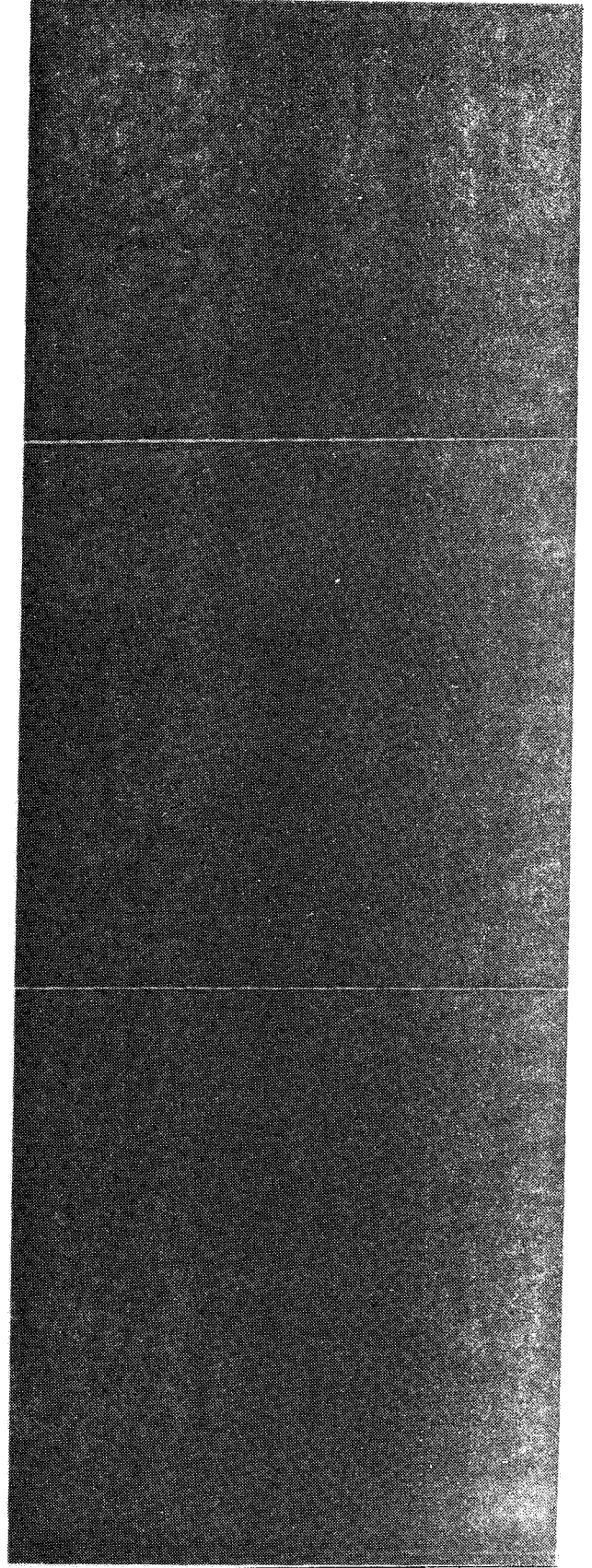
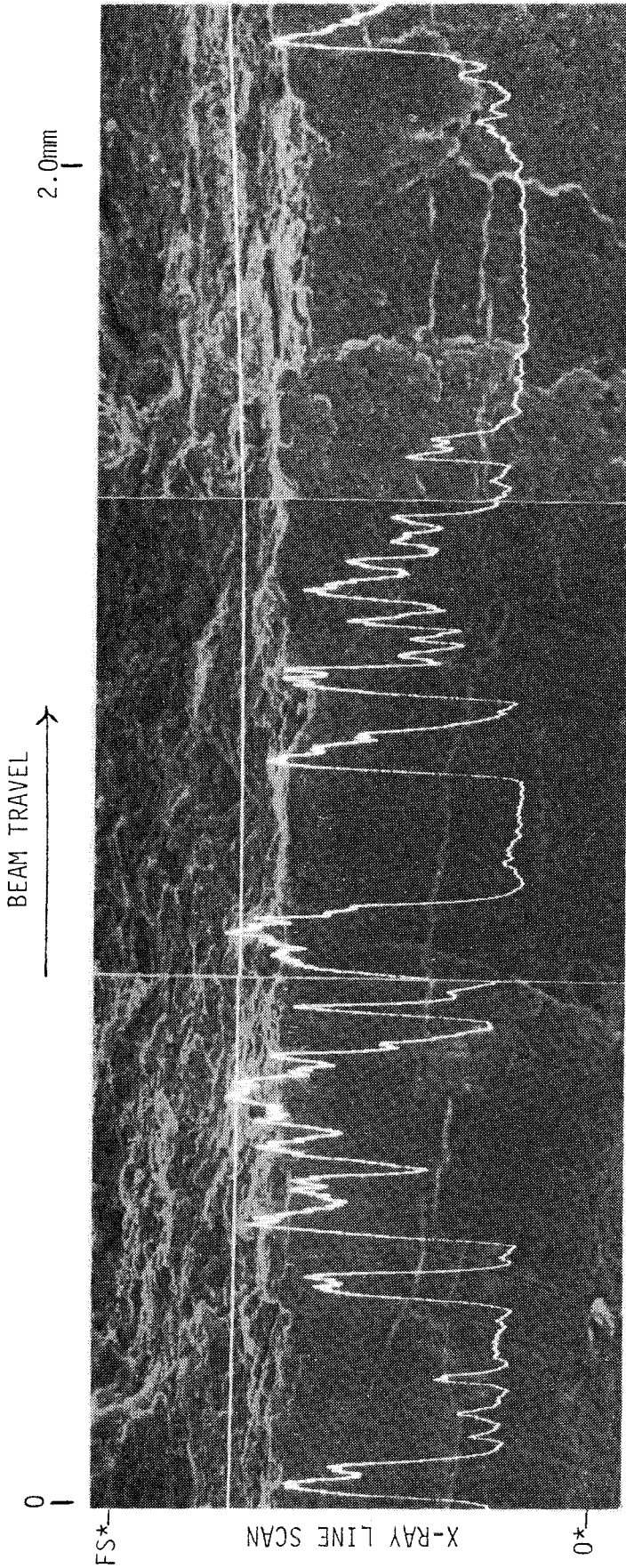
MACHINE SETTINGS

LINE -- FULL SCALE SENSITIVITY: 1.0×10^3 cnts/sec.
SCAN SETTING: 7

MAP -- SCAN SETTING: 11

SAMPLE K5

ELEMENT K



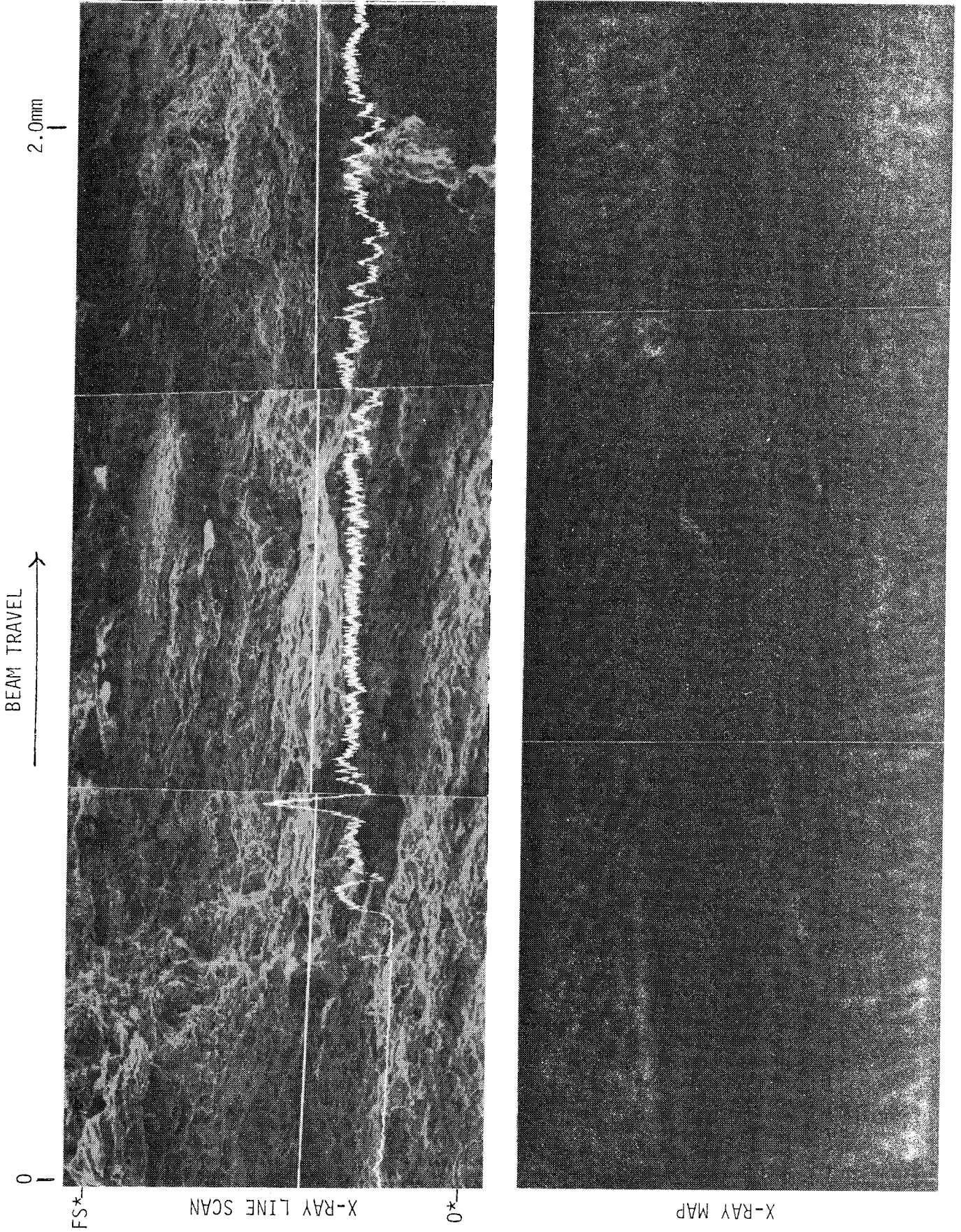
MACHINE SETTINGS

LINE - FULL SCALE SENSITIVITY: 0.5×10^3 cnts/sec.
SCAN SETTING: 7

MAP - SCAN SETTING: 11

SAMPLE K6

ELEMENT K



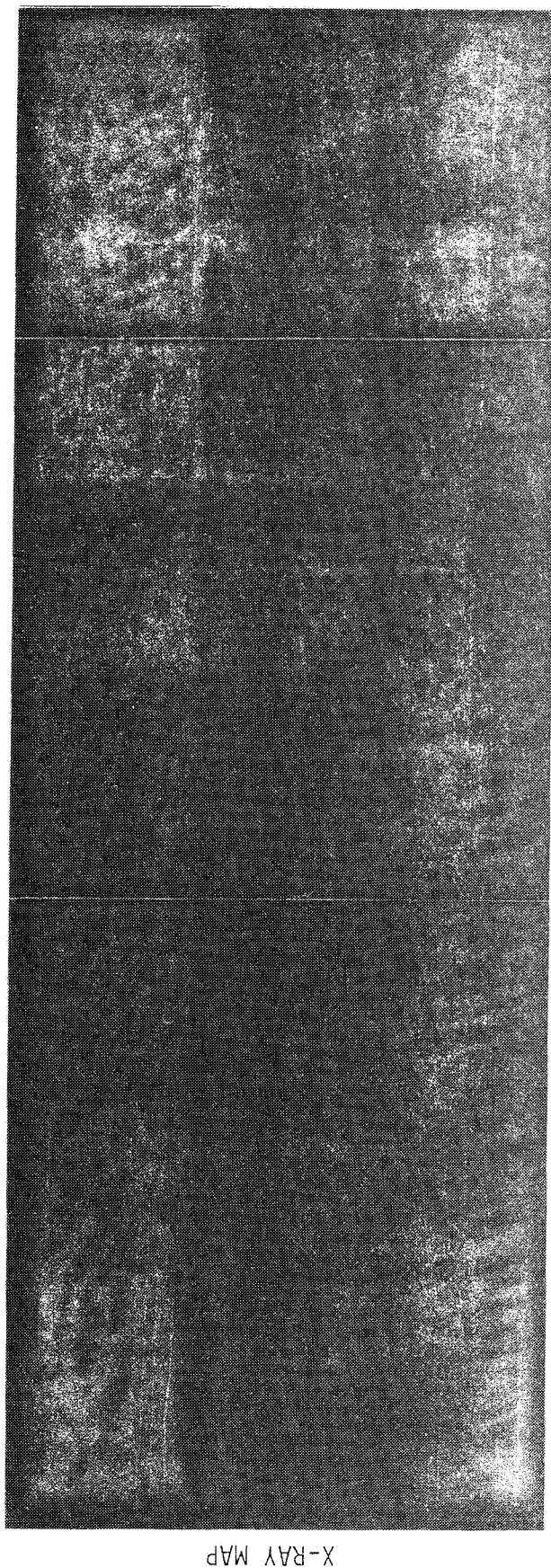
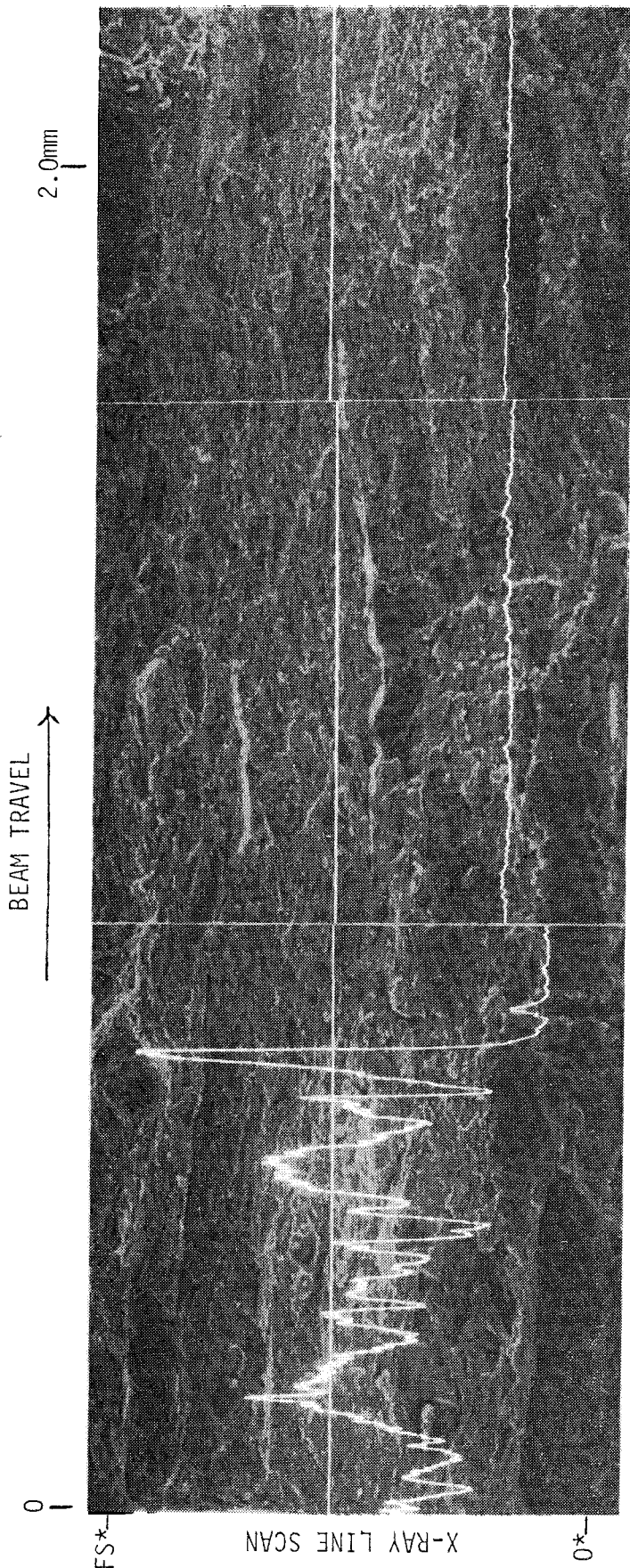
MACHINE SETTINGS

LINE -- FULL SCALE SENSITIVITY: 2.5×10^3 cnts/sec.
SCAN SETTING: 7

MAP -- SCAN SETTING: 11

SAMPLE K7

ELEMENT K



MACHINE SETTINGS

LINE - FULL SCALE SENSITIVITY: 0.5×10^3 cnts/sec.

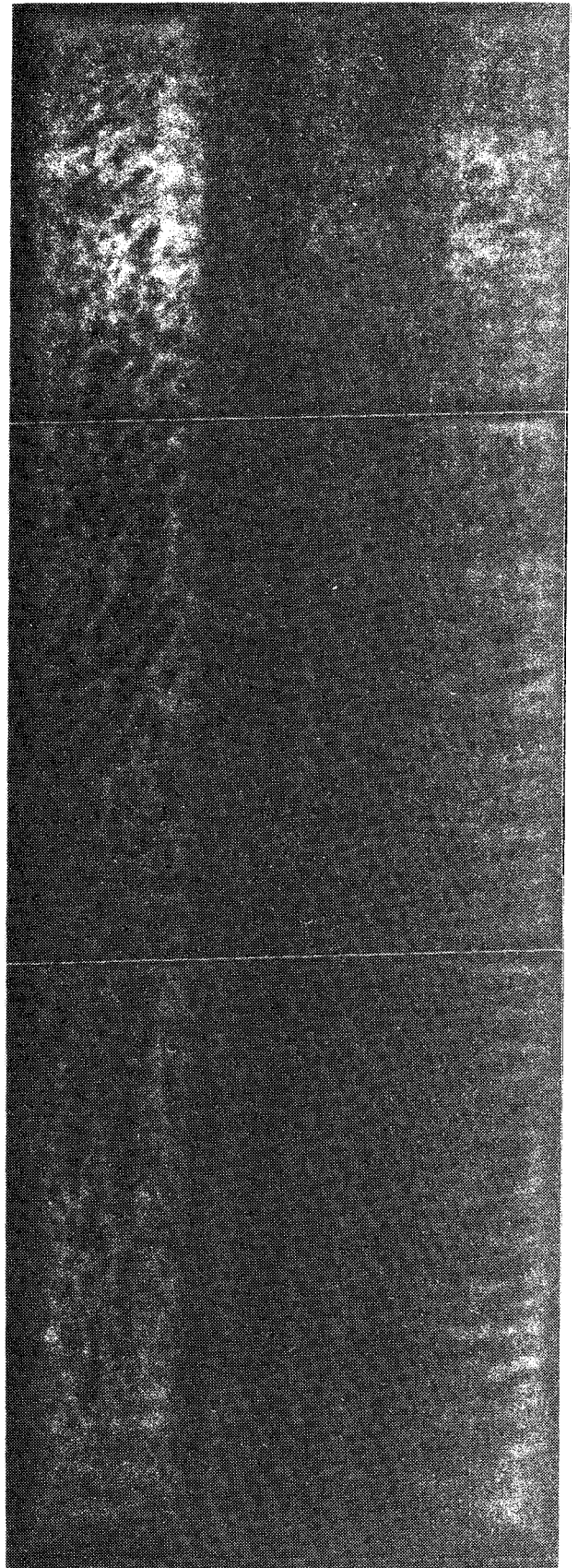
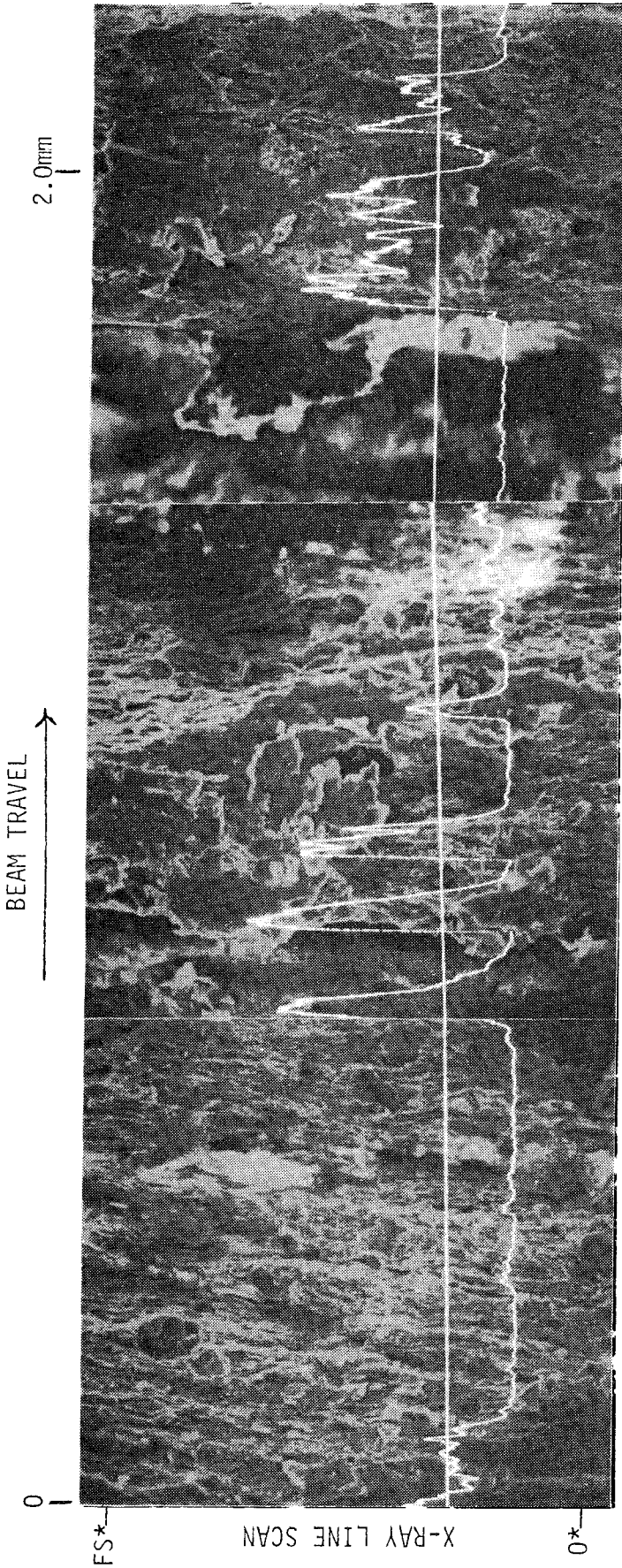
SCAN SETTING: 7

MAP -

SCAN SETTING: 11

SAMPLE K8

ELEMENT K



X-RAY MAP

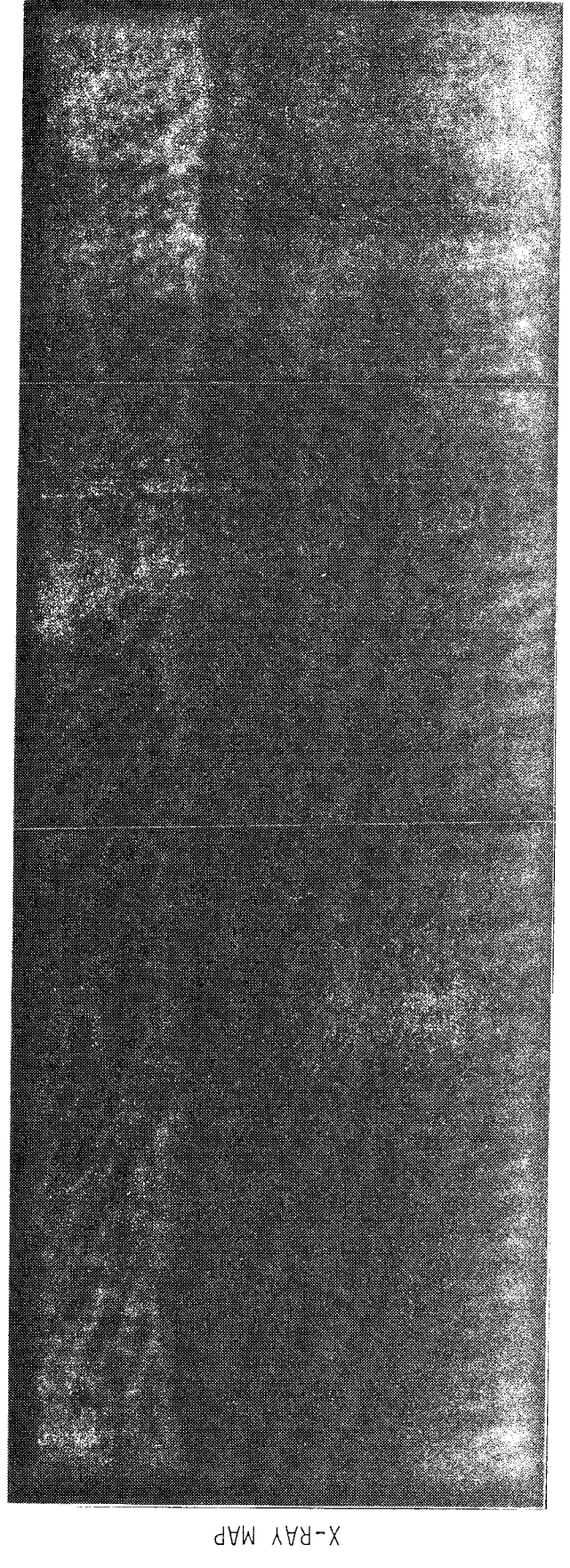
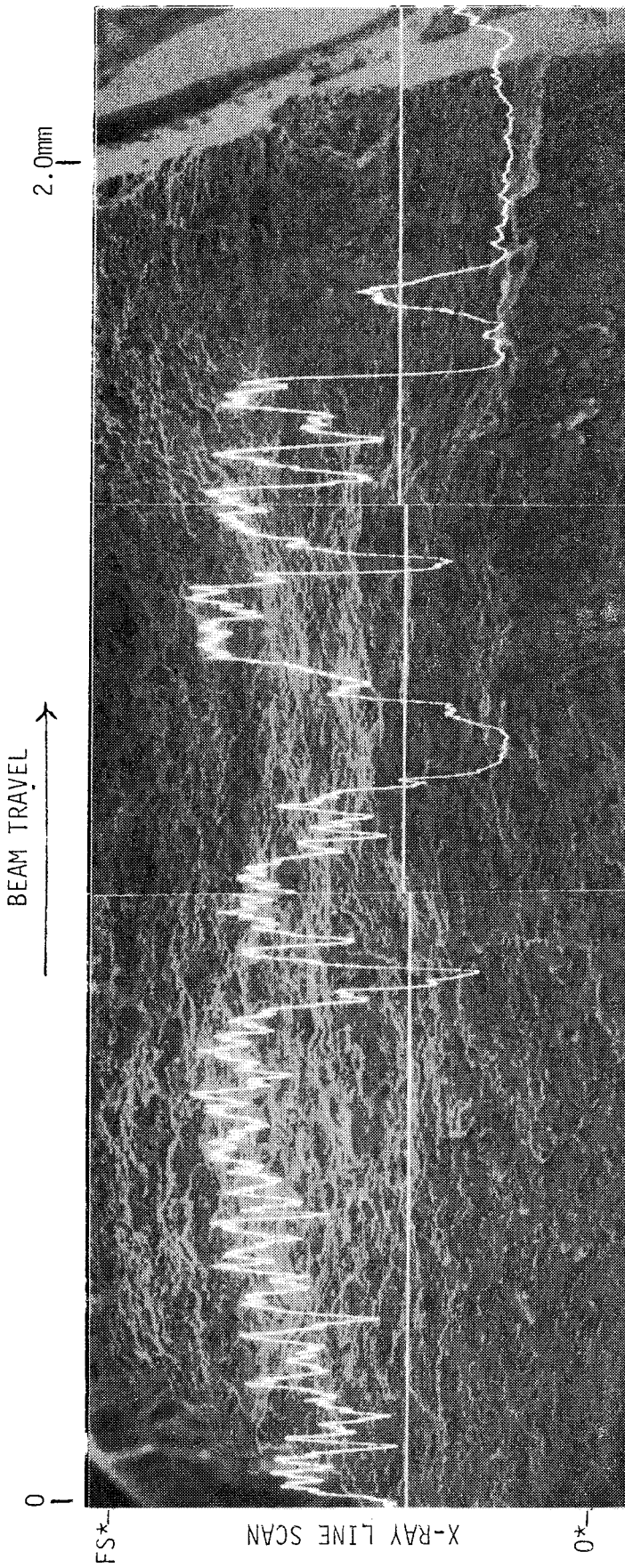
MACHINE SETTINGS

LINE - FULL SCALE SENSITIVITY: 0.5×10^3 cnts/sec.
SCAN SETTING: 7

MAP - SCAN SETTING: 11

SAMPLE K9

ELEMENT K



MACHINE SETTINGS

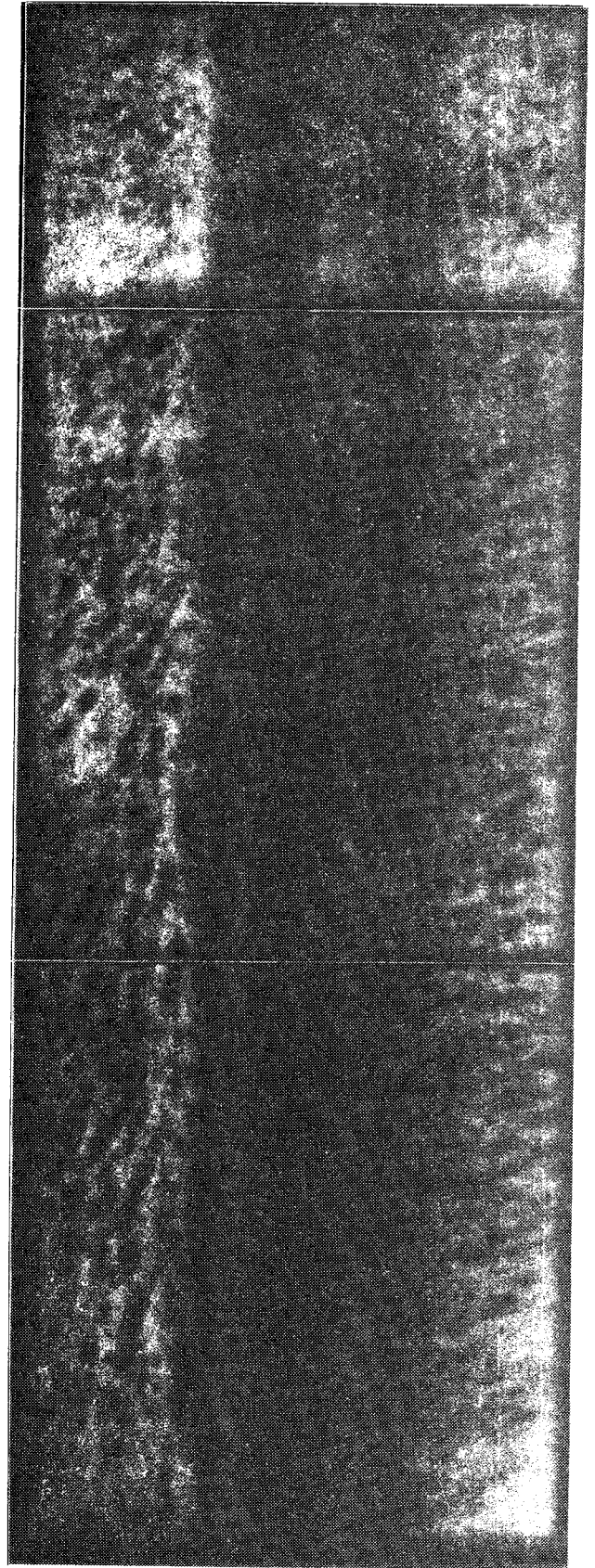
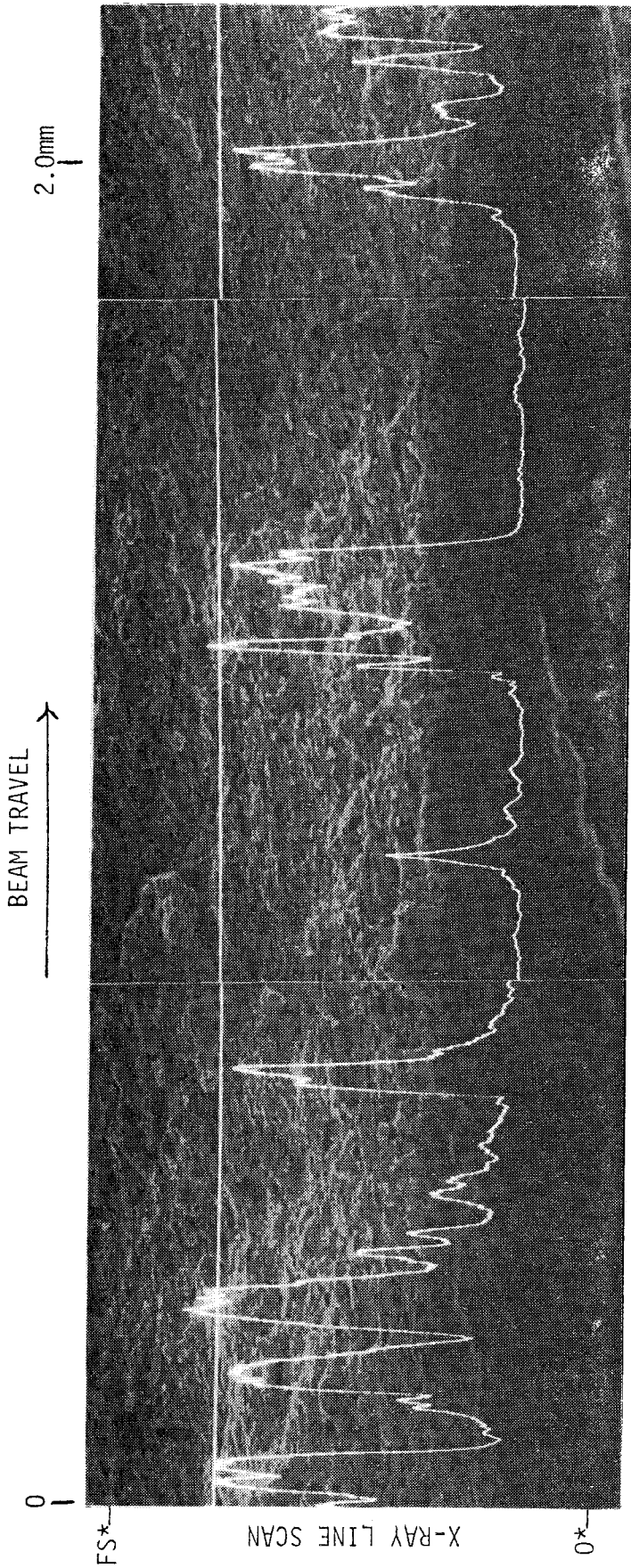
LINE — FULL SCALE SENSITIVITY: 0.5×10^3 cnts/sec.

SCAN SETTING: 7

MAP — SCAN SETTING: 11

SAMPLE K10

ELEMENT K



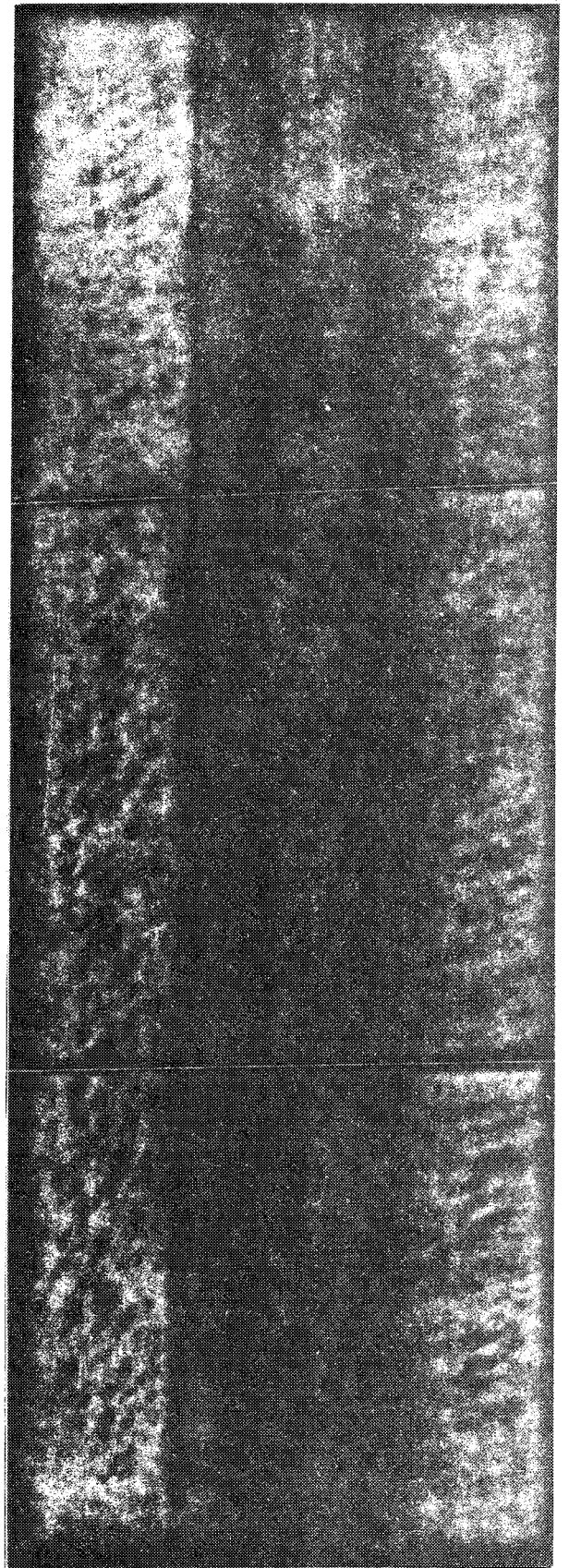
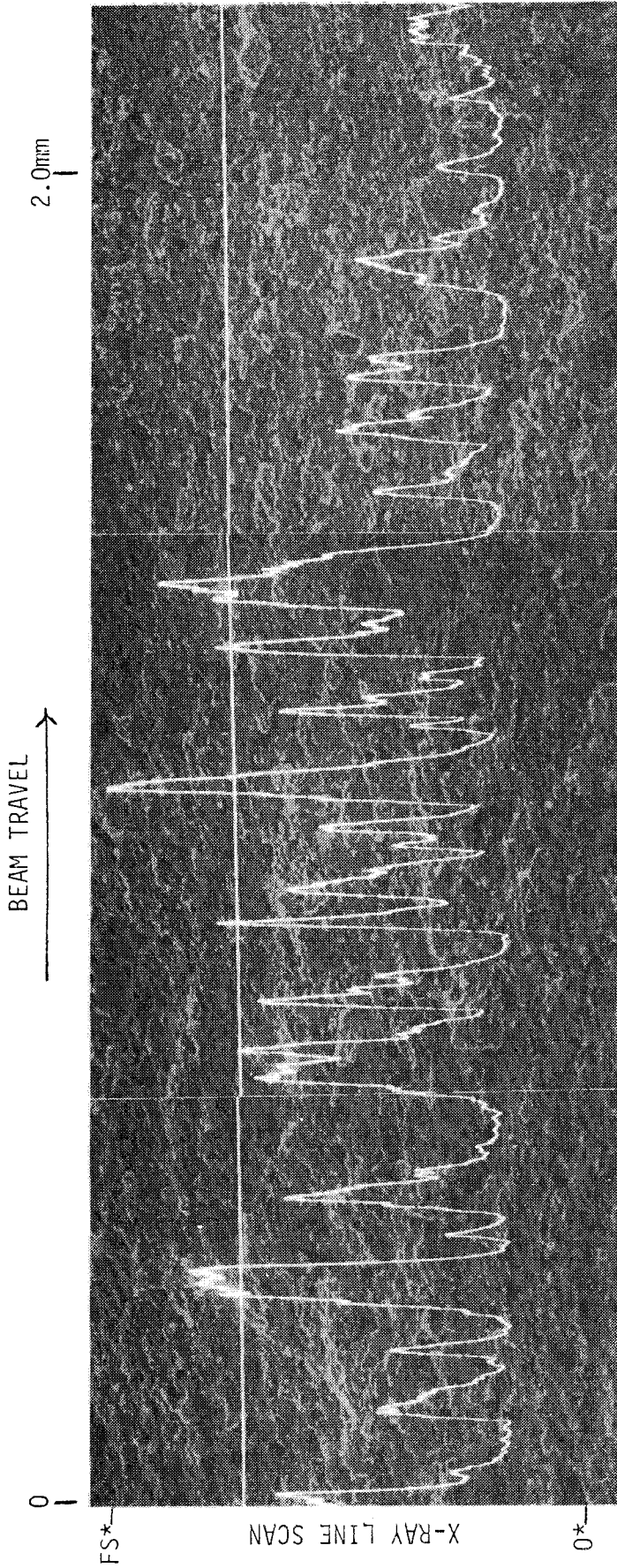
MACHINE SETTINGS

LINE - FULL SCALE SENSITIVITY: 0.5×10^3 cnts/sec.
SCAN SETTING: 7

MAP - SCAN SETTING: 11

SAMPLE K11

ELEMENT K



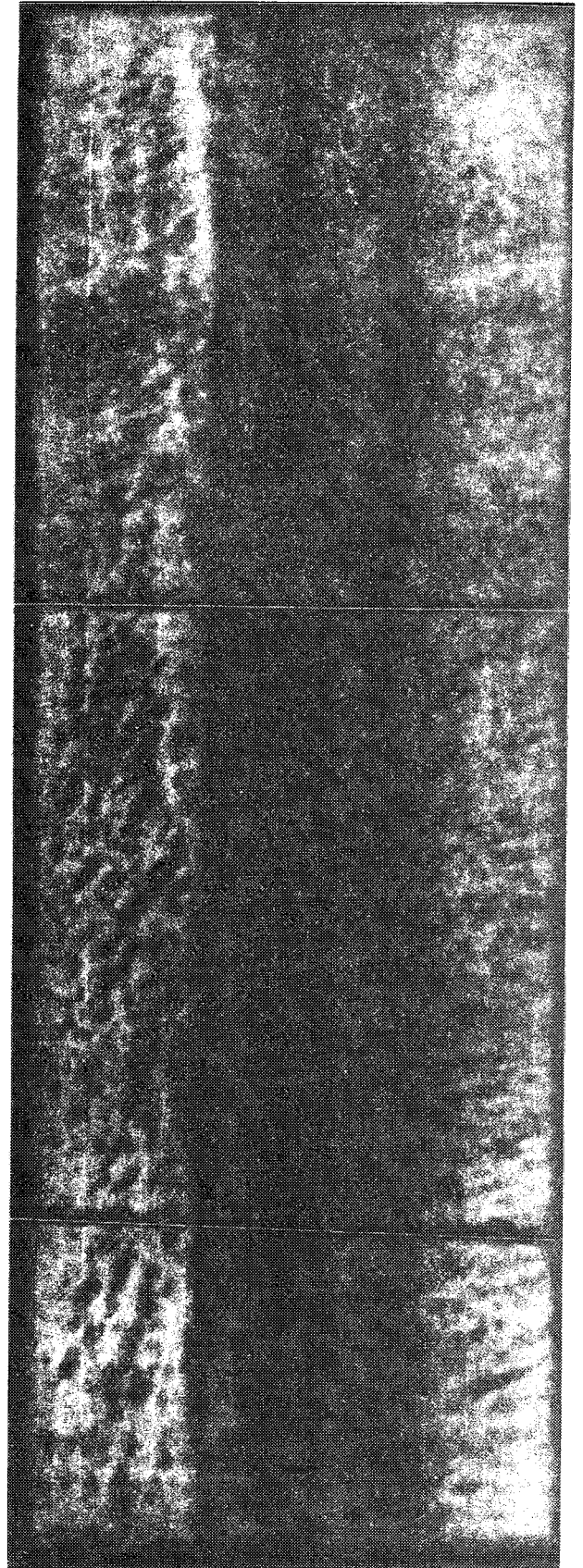
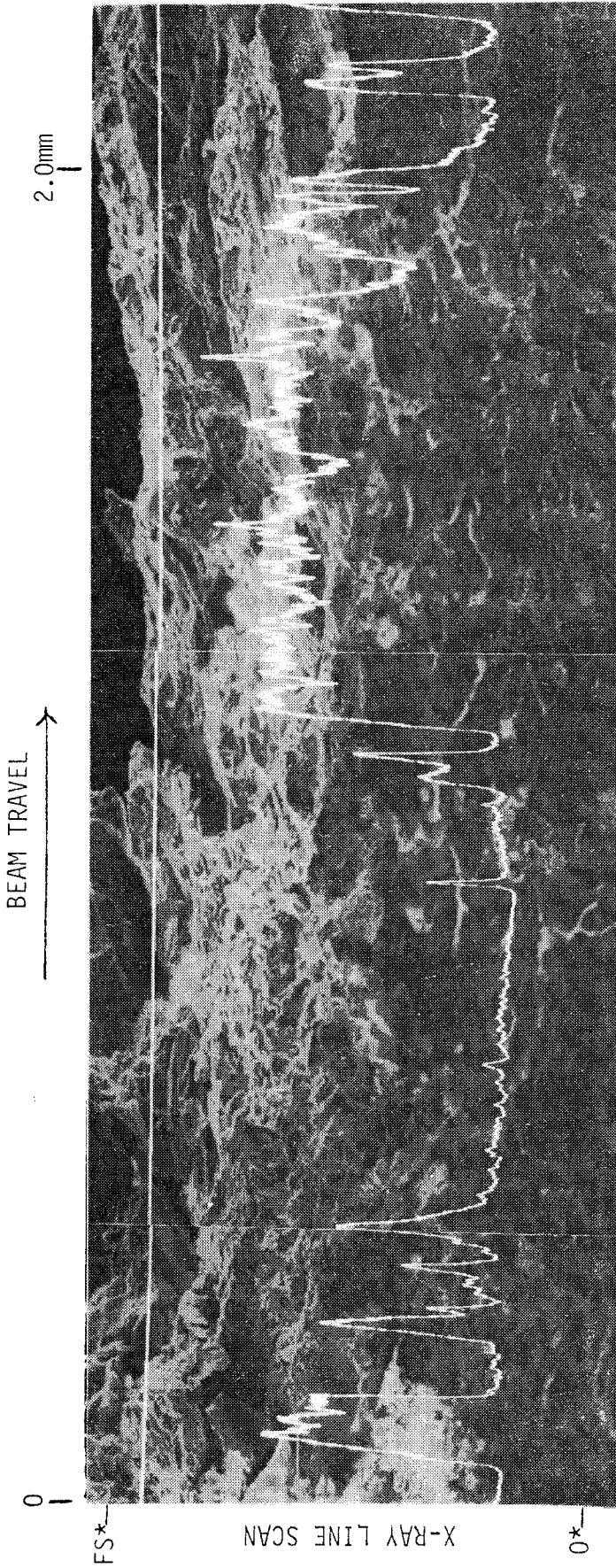
MACHINE SETTINGS

LINE - FULL SCALE SENSITIVITY: 0.5×10^3 cnts/sec.
SCAN SETTING: 7

MAP - SCAN SETTING: 11

SAMPLE K12

ELEMENT K



MACHINE SETTINGS

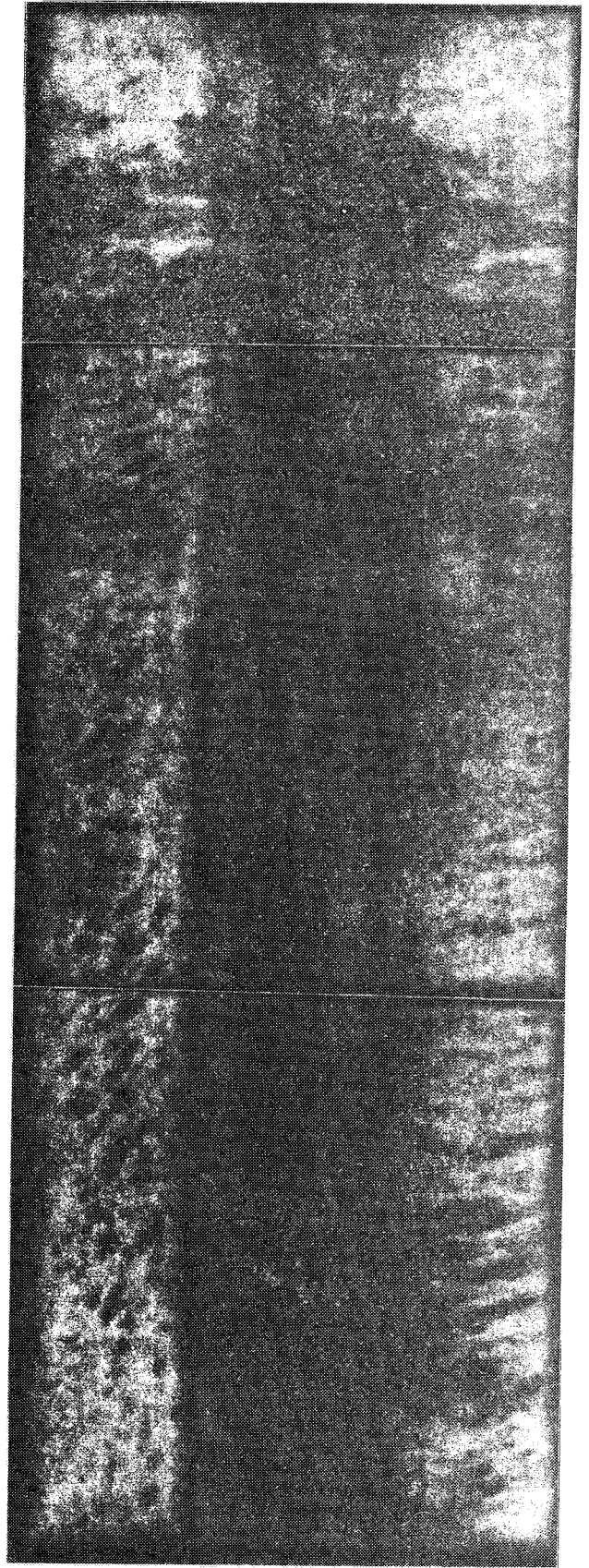
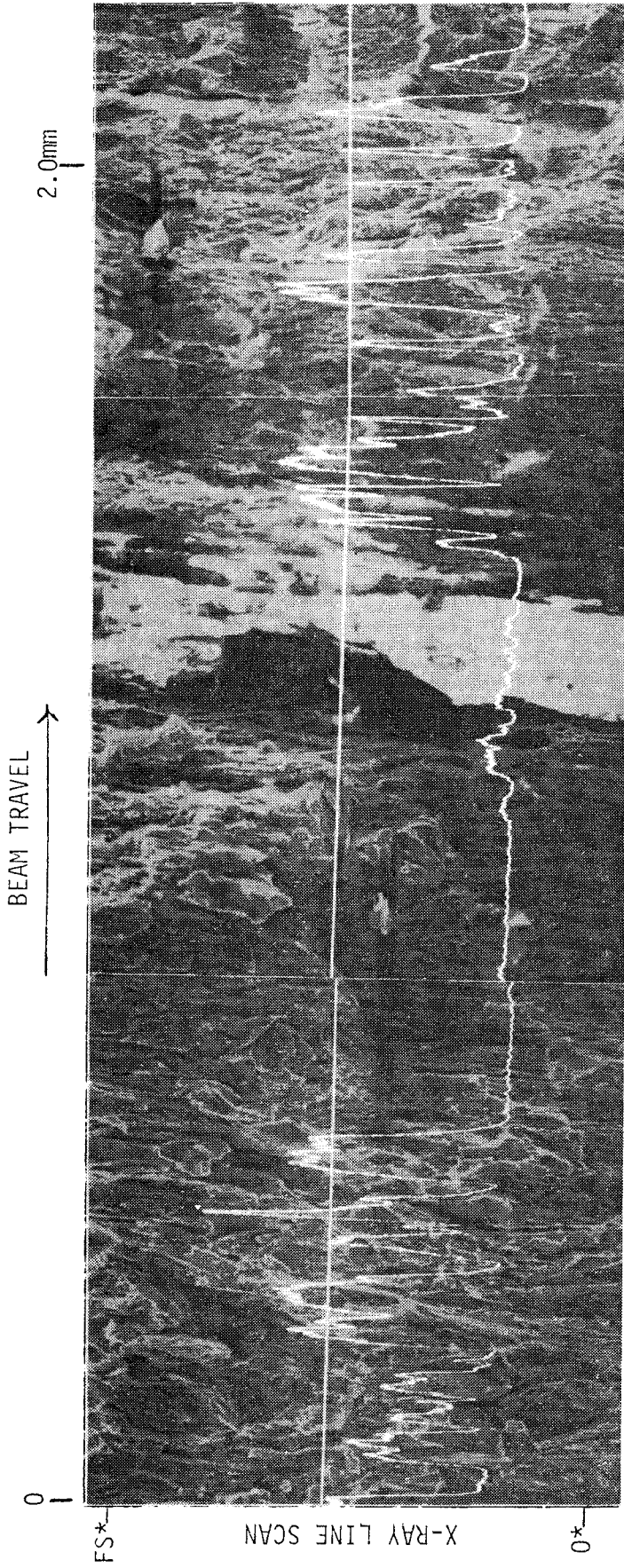
LINE — FULL SCALE SENSITIVITY: 1.0×10^3 cnts/sec.

SCAN SETTING: 7

MAP — SCAN SETTING: 11

SAMPLE K13

ELEMENT K



X-RAY MAP

MACHINE SETTINGS

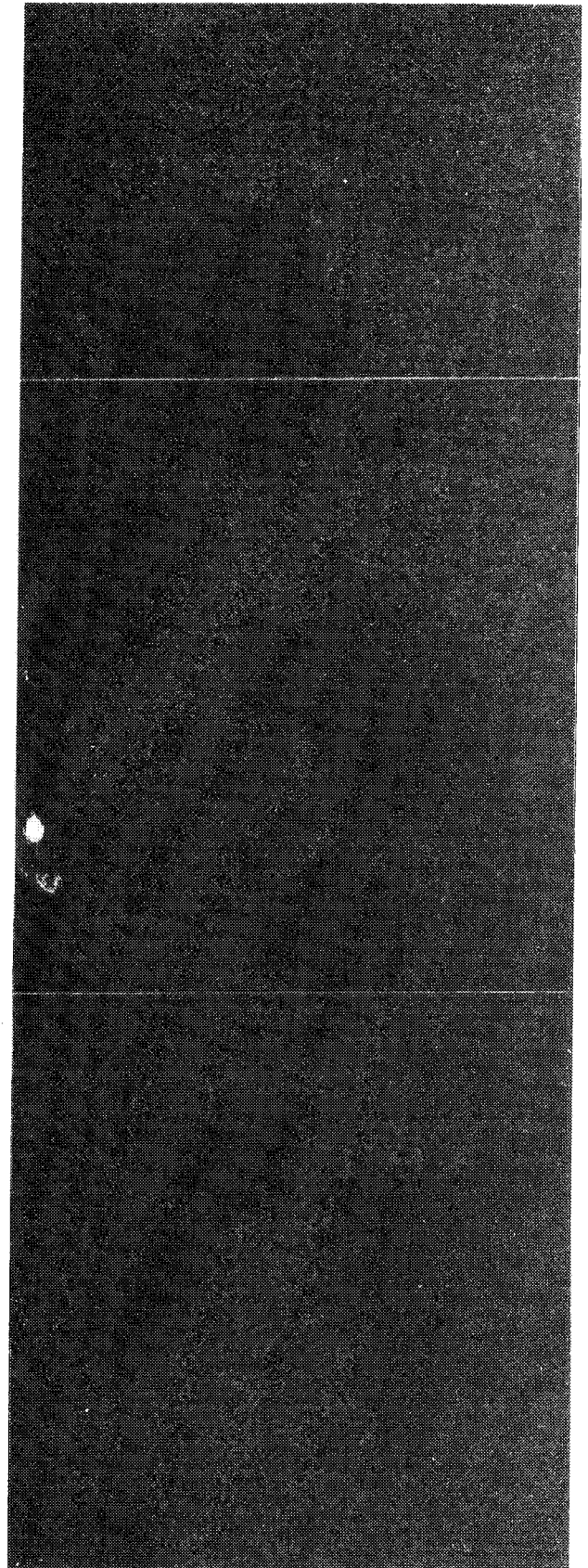
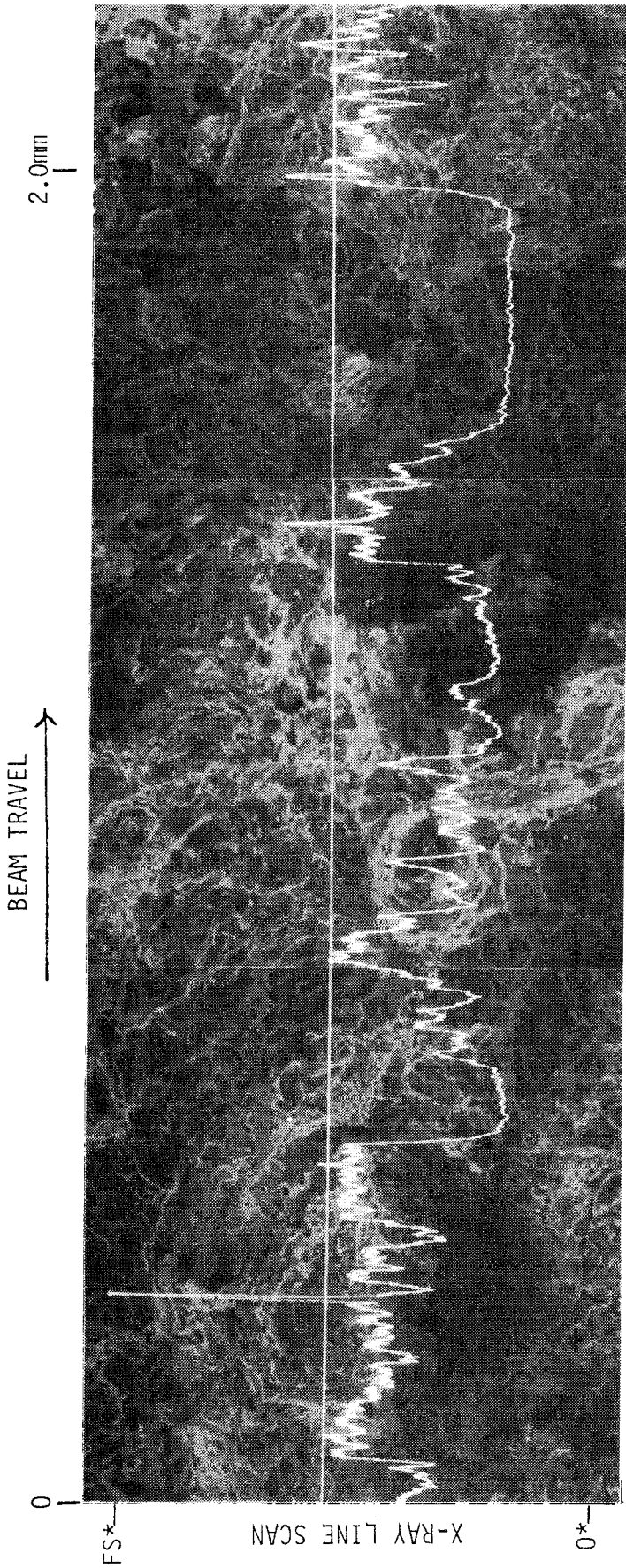
LINE - FULL SCALE SENSITIVITY: 1.0×10^3 cnts/sec.
SCAN SETTING: 7

MAP - SCAN SETTING: 11

APPENDIX 2
HÖGANÄS SMECTITES
ELEMENT ANALYSES (EMV)

SAMPLE YK1

ELEMENT Fe



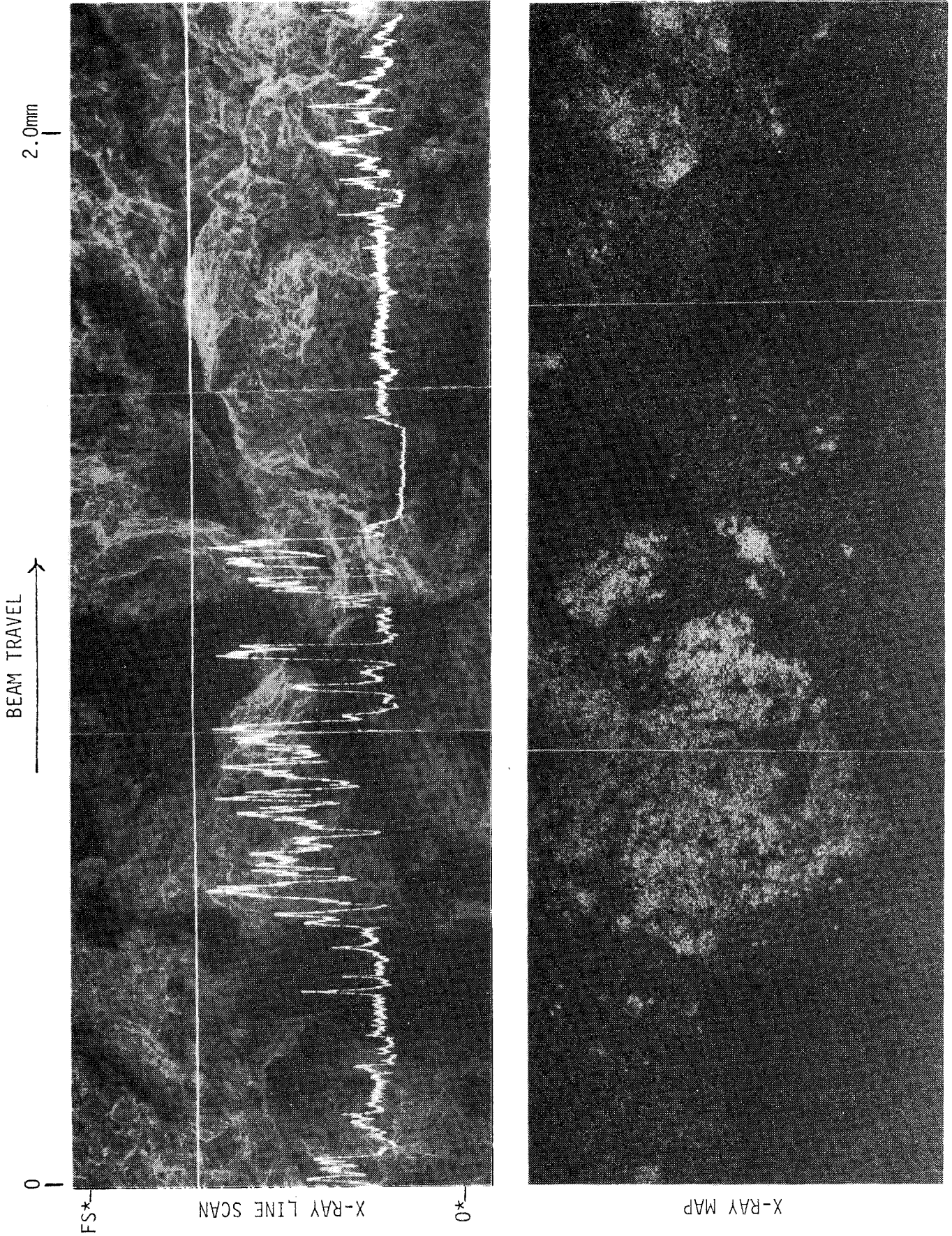
MACHINE SETTINGS

LINE - FULL SCALE SENSITIVITY: 1.0×10^3 cnts/sec.
SCAN SETTING: 7

MAP - SCAN SETTING: 11

SAMPLE YK2

ELEMENT Fe



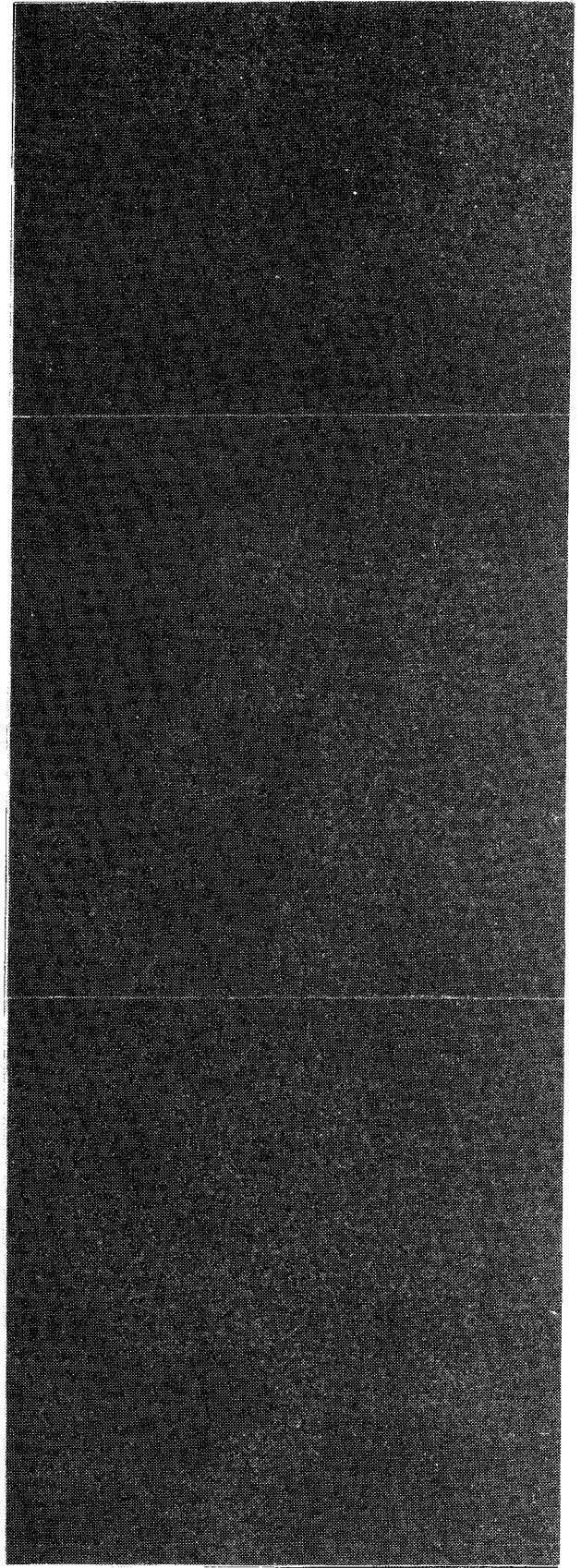
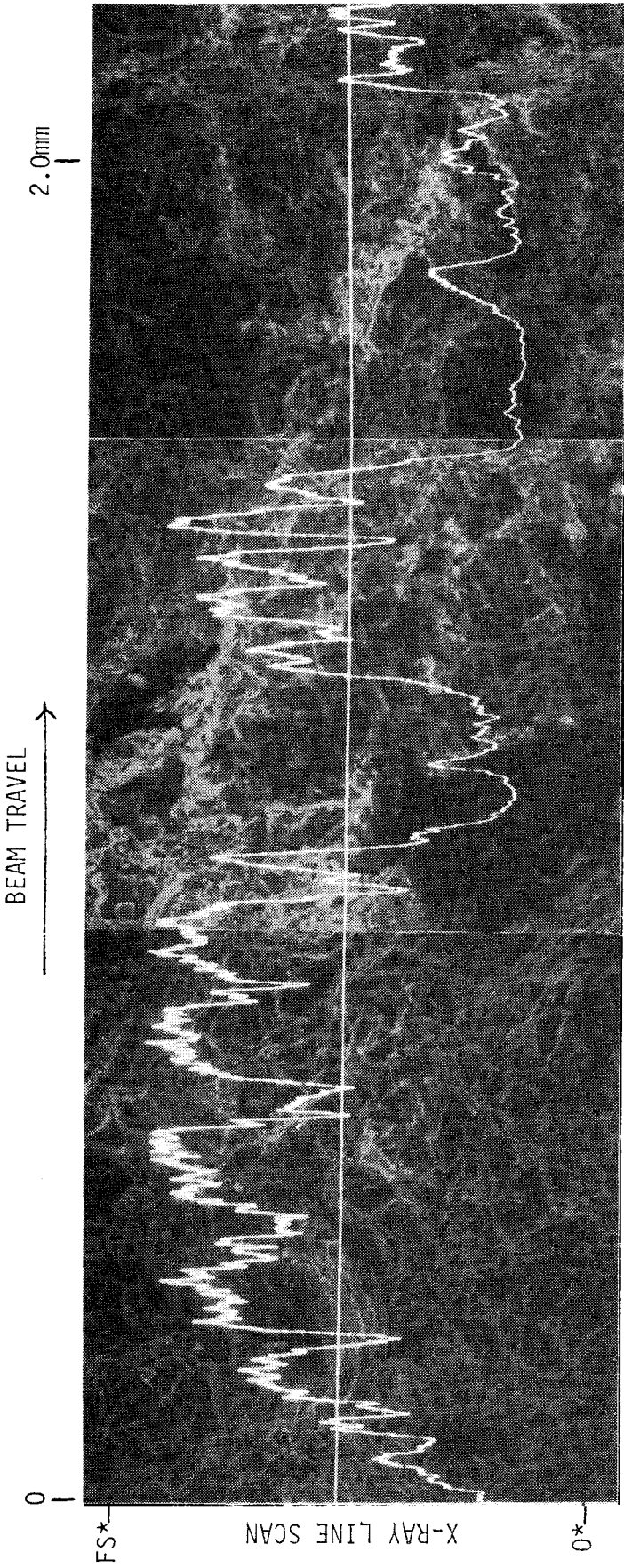
MACHINE SETTINGS

LINE - FULL SCALE SENSITIVITY: 0.5×10^4 cnts/sec.
SCAN SETTING: 7

MAP - SCAN SETTING: 11

SAMPLE RK3

ELEMENT Fe



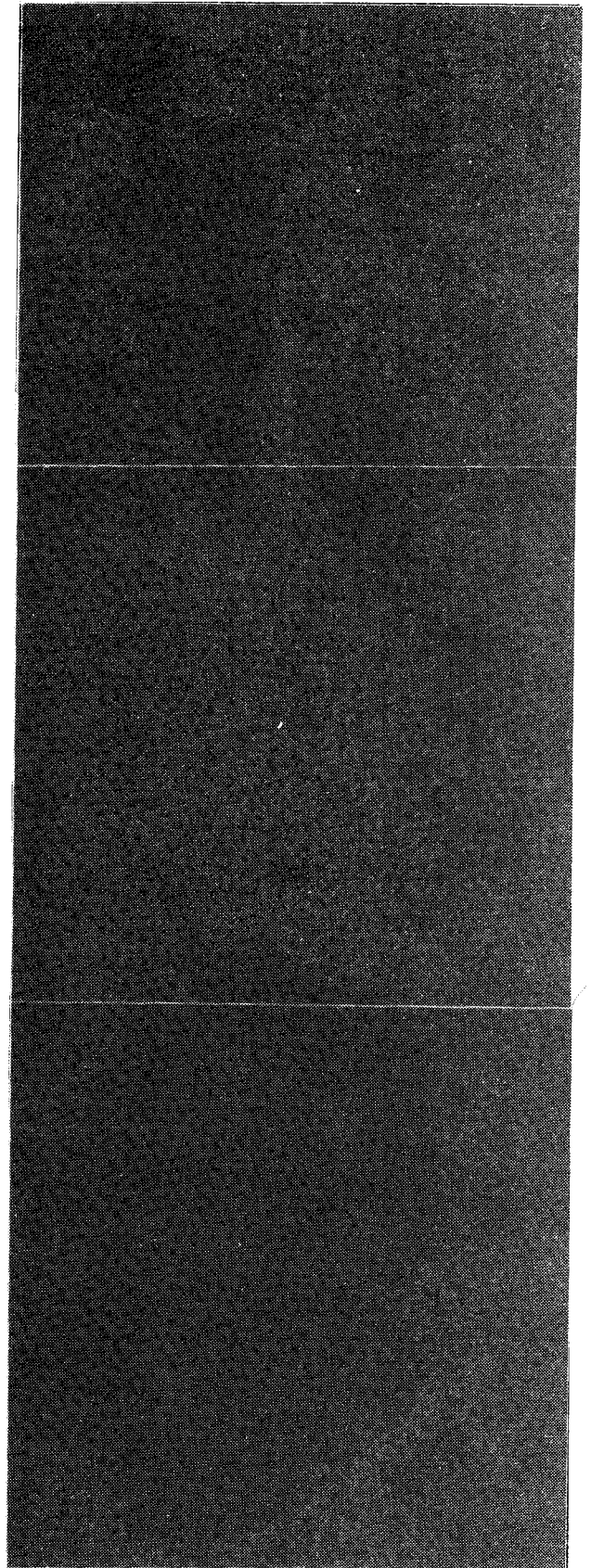
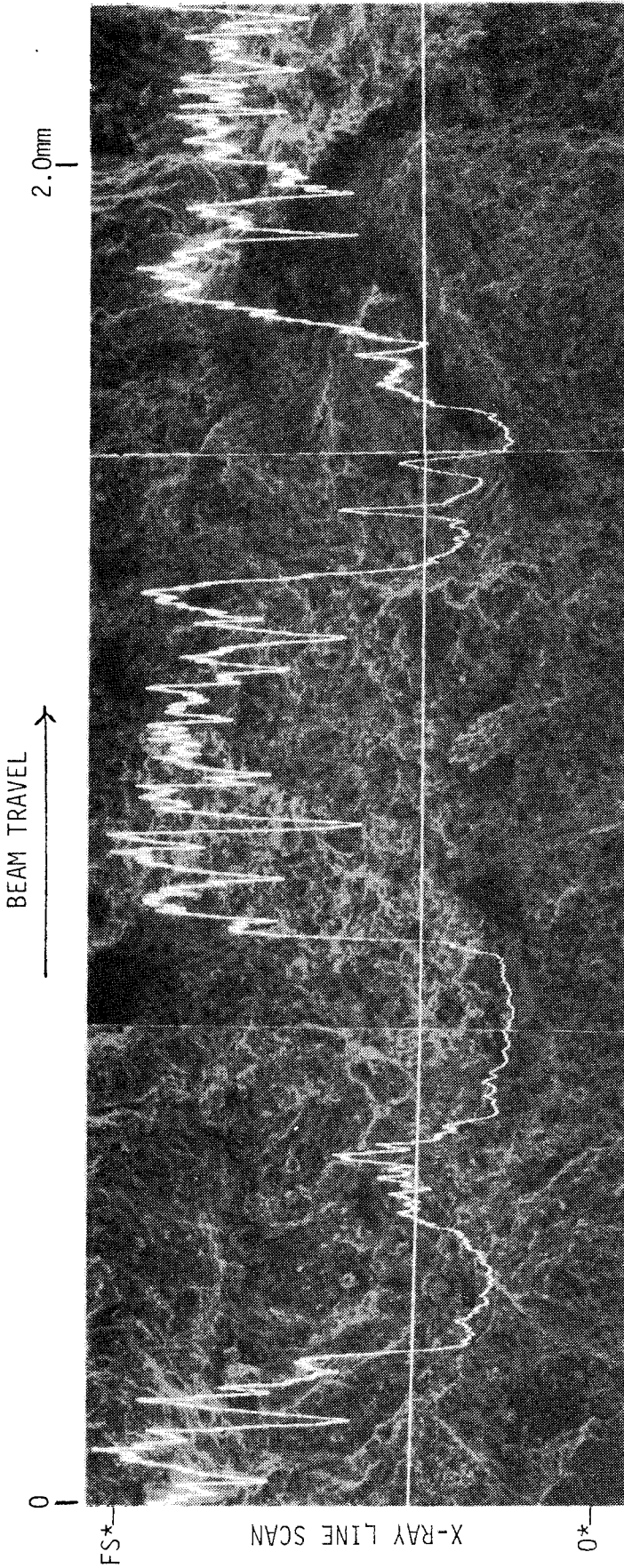
MACHINE SETTINGS

LINE - FULL SCALE SENSITIVITY: 0.5×10^3 cnts/sec.
 SCAN SETTING: 7

MAP - SCAN SETTING: 11

SAMPLE RK5

ELEMENT Fe



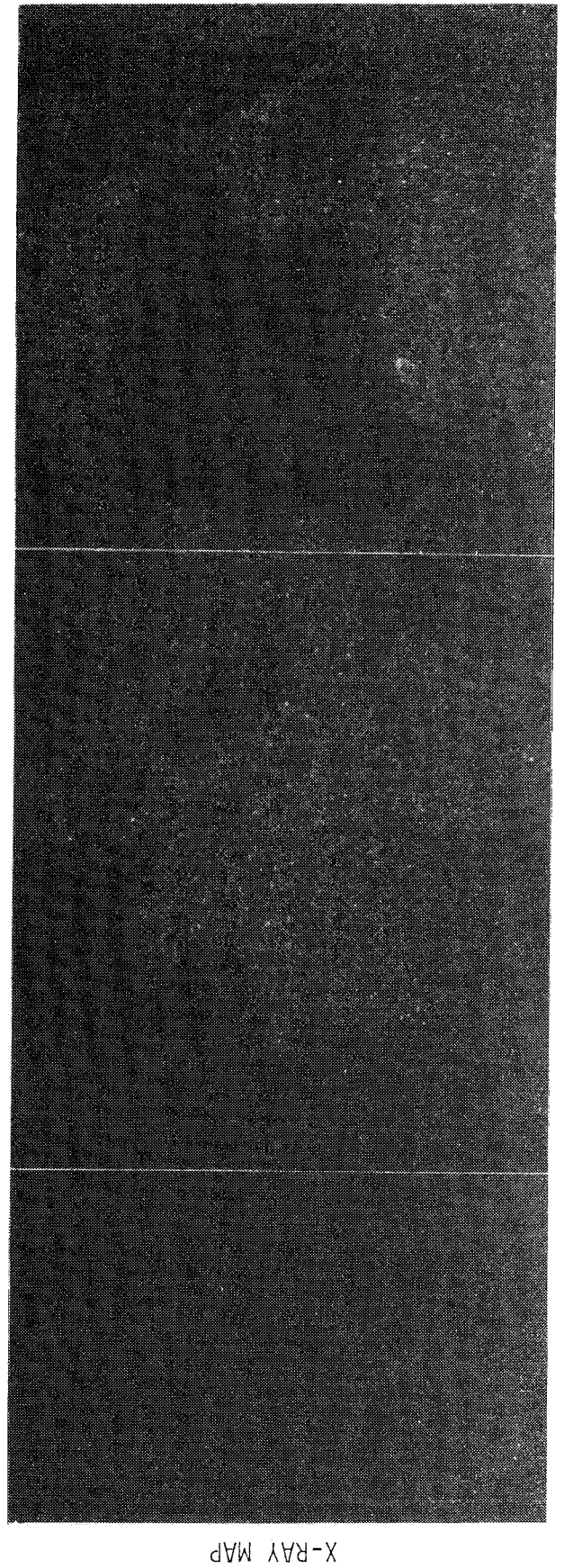
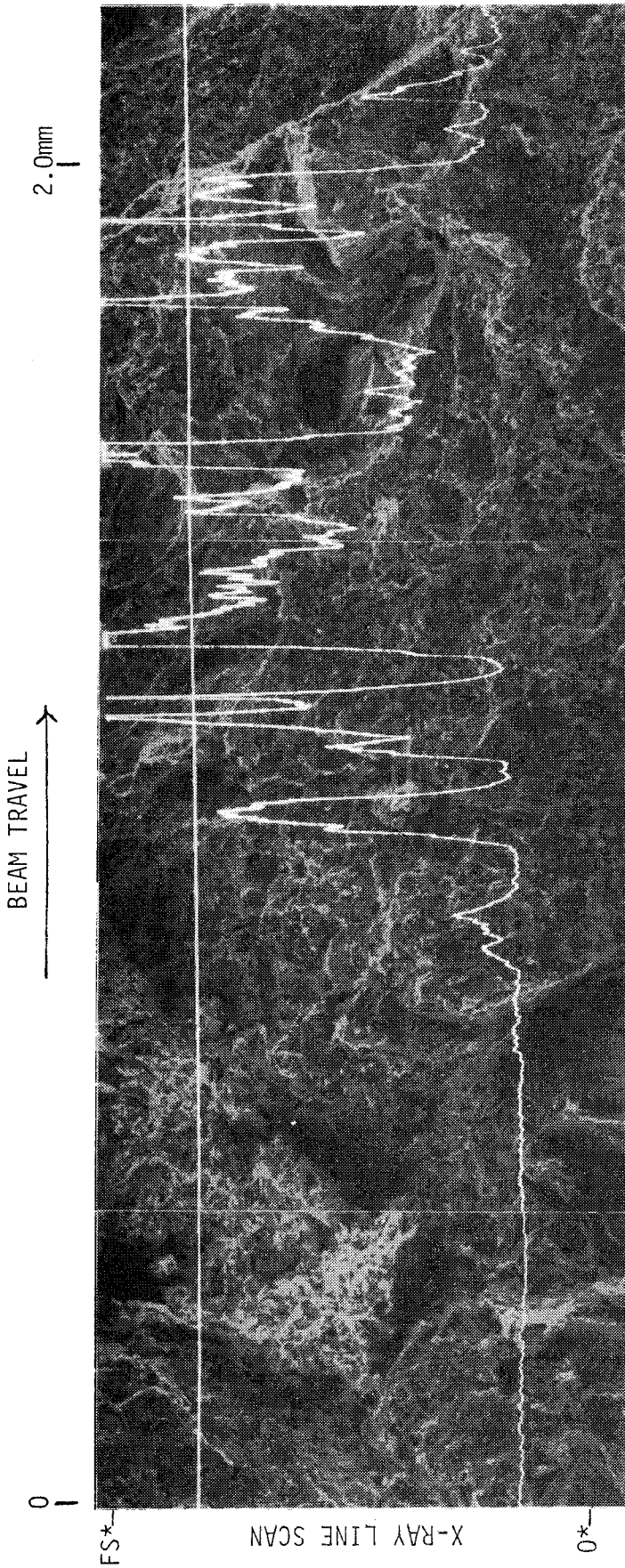
MACHINE SETTINGS

LINE — FULL SCALE SENSITIVITY: 0.5×10^3 cnts/sec.
SCAN SETTING: 7

MAP — SCAN SETTING: 11

SAMPLE R:K7

ELEMENT Fe



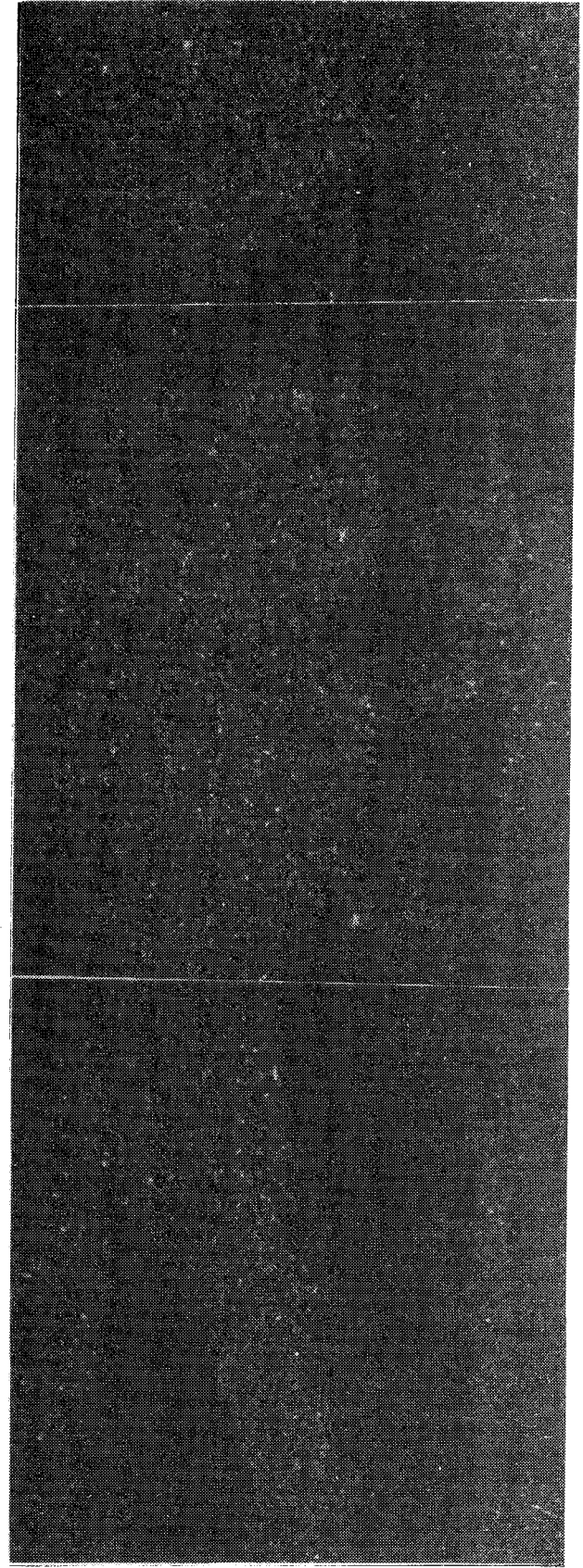
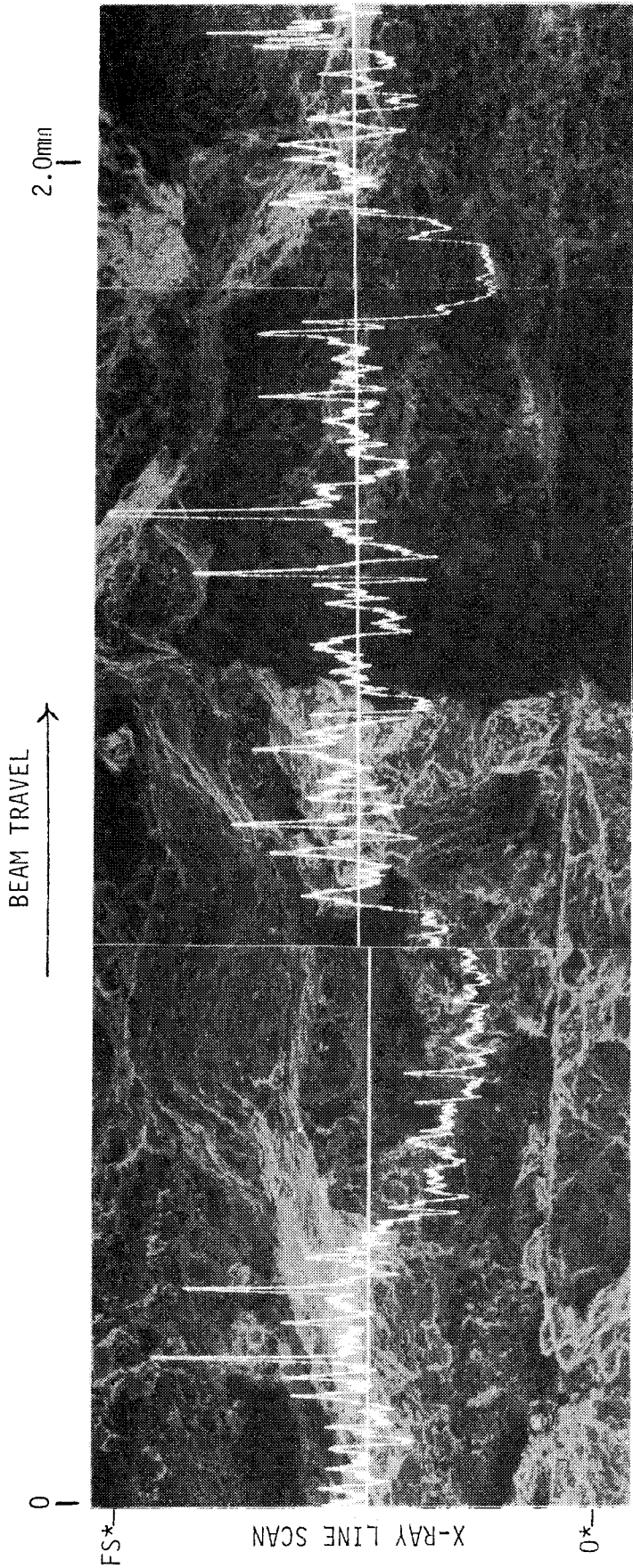
MACHINE SETTINGS

LINE -- FULL SCALE SENSITIVITY: 0.5×10^3 cnts/sec.
SCAN SETTING: 7

MAP -- SCAN SETTING: 11

SAMPLE RK9

ELEMENT Fe



X-RAY MAP

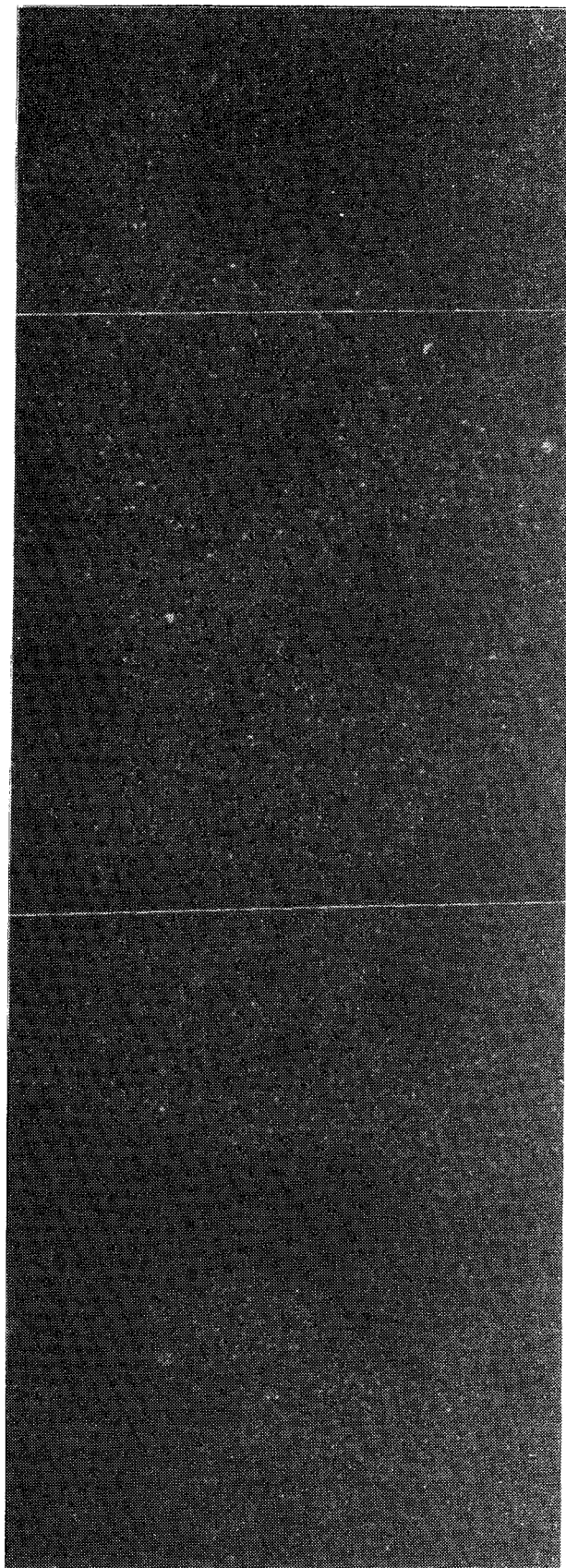
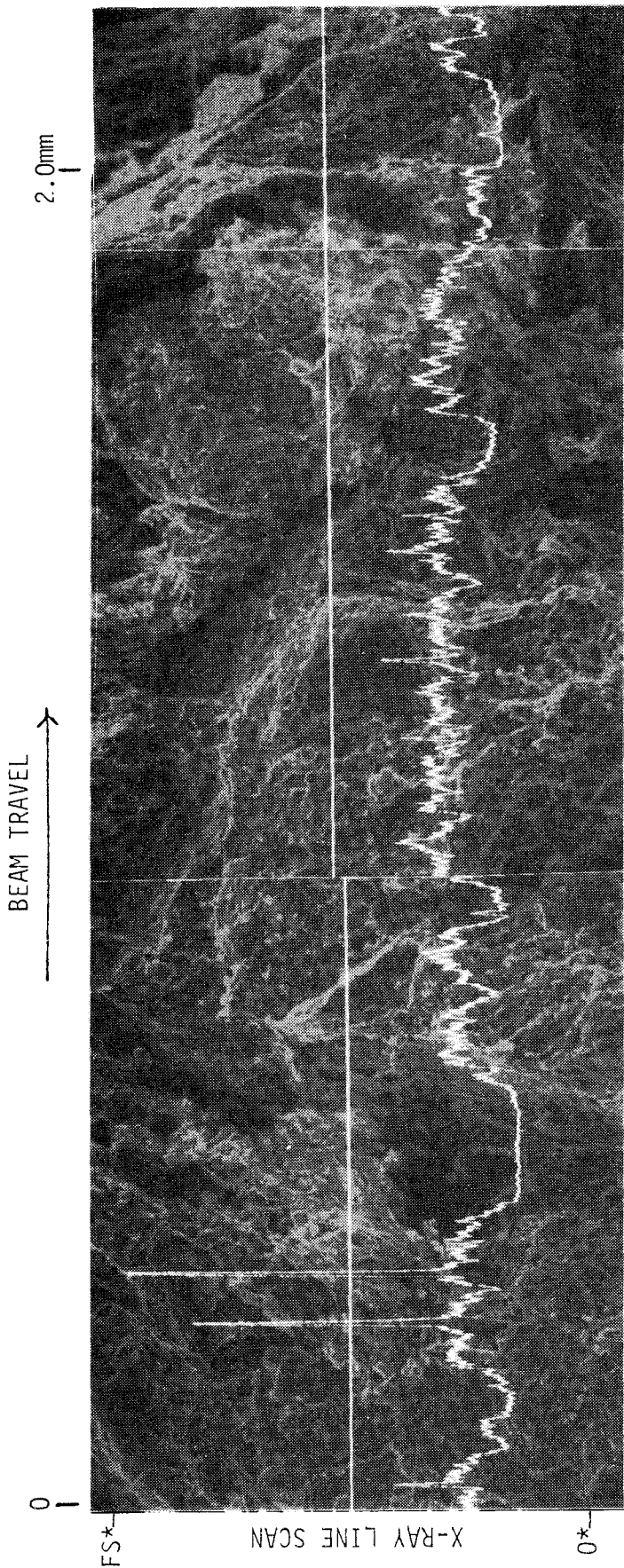
MACHINE SETTINGS

LINE — FULL SCALE SENSITIVITY: 1.0×10^3 cnts/sec.
SCAN SETTING: 7

MAP — SCAN SETTING: 11

SAMPLE RK11

ELEMENT Fe



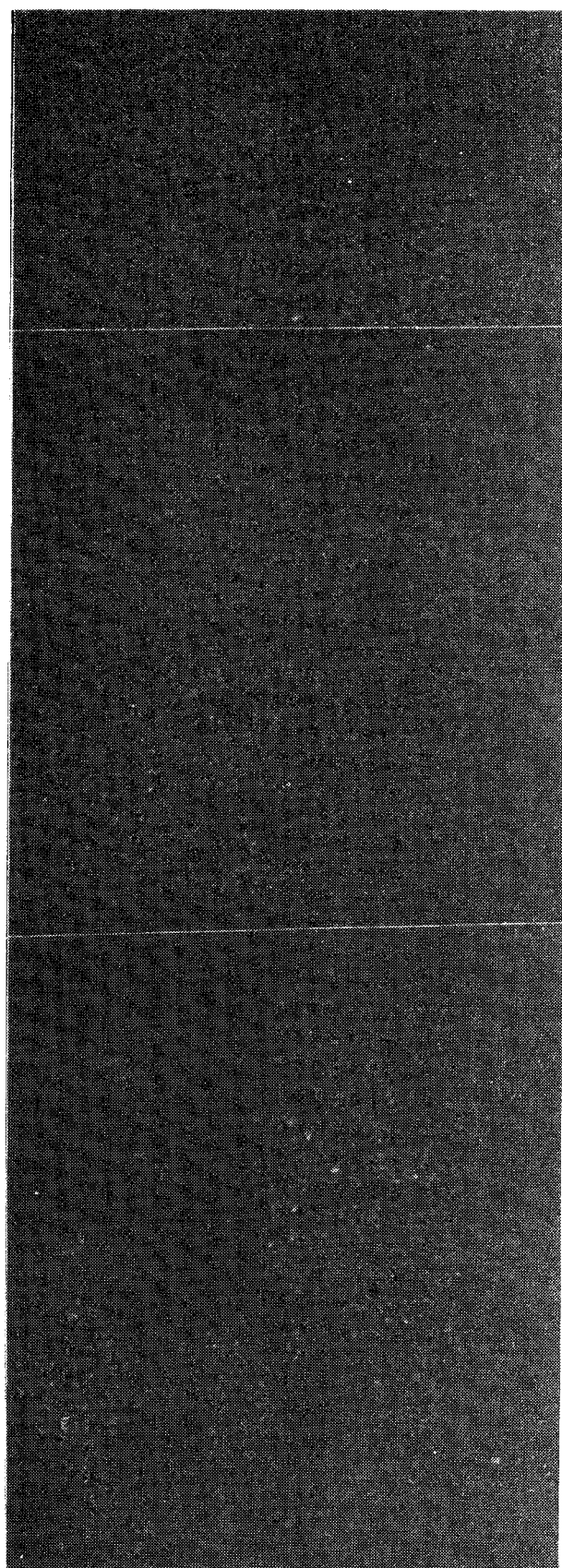
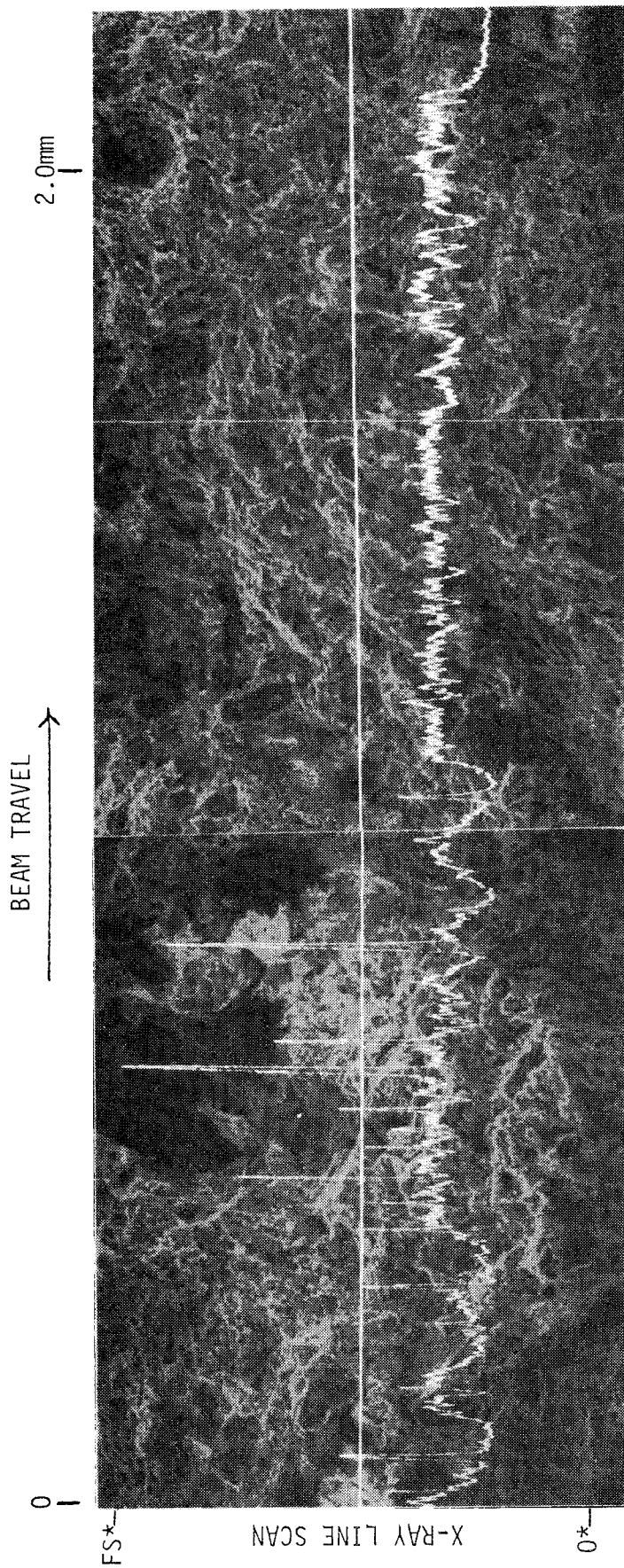
MACHINE SETTINGS

LINE - FULL SCALE SENSITIVITY: 2.5×10^3 cnts/sec.
 SCAN SETTING: 7

MAP - SCAN SETTING: 11

SAMPLE RK13

ELEMENT Fe



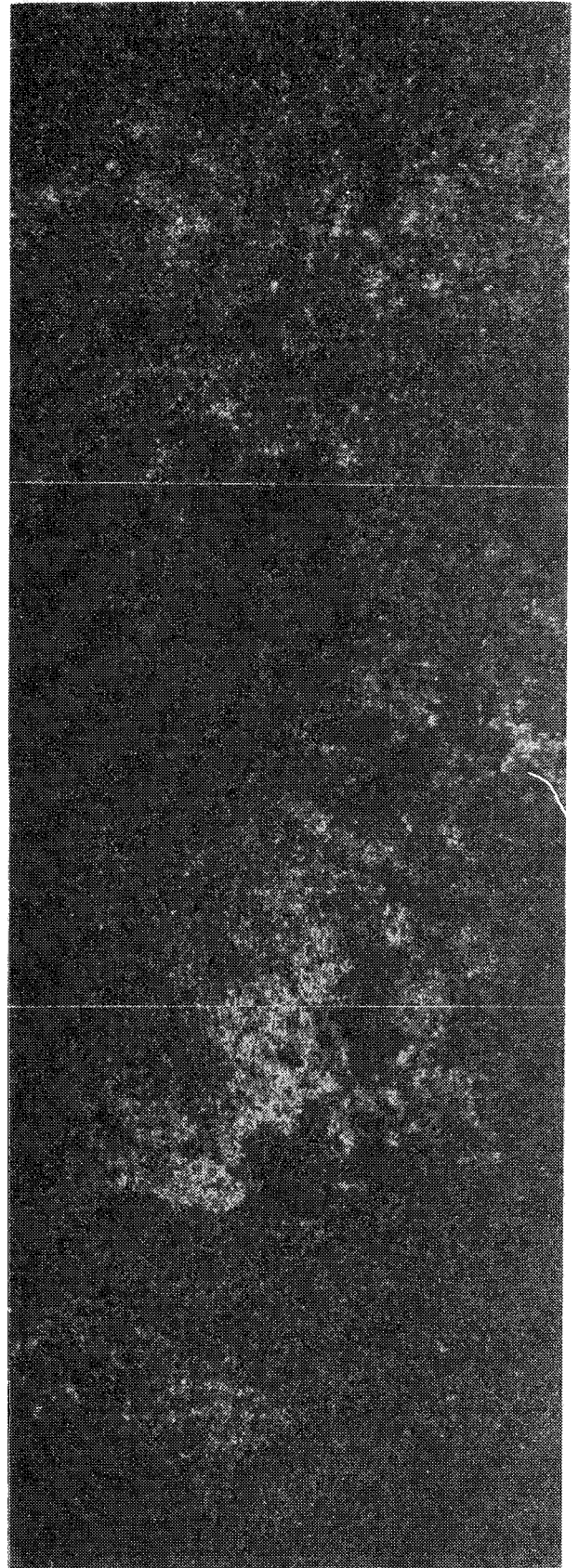
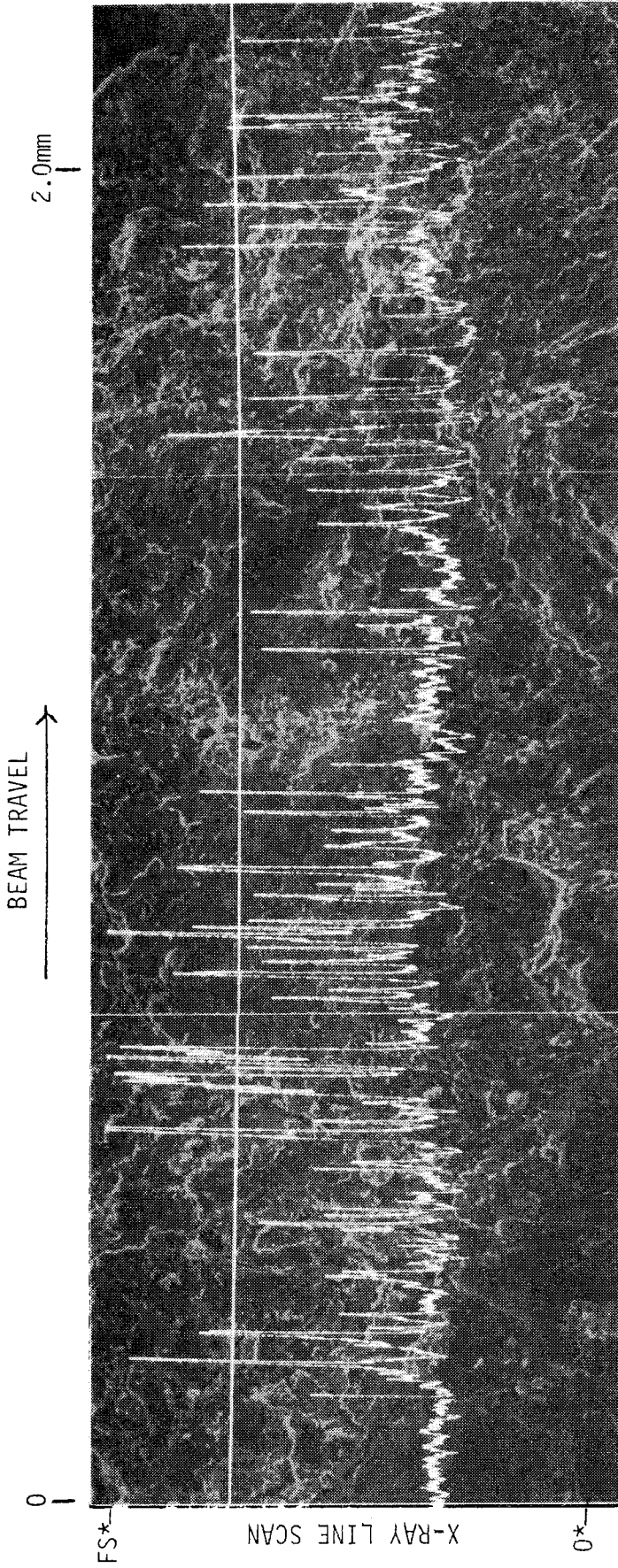
MACHINE SETTINGS

LINE - FULL SCALE SENSITIVITY: 2.5×10^3 cnts/sec.
SCAN SETTING: 7

MAP - SCAN SETTING: 11

SAMPLE RK15

ELEMENT Fe



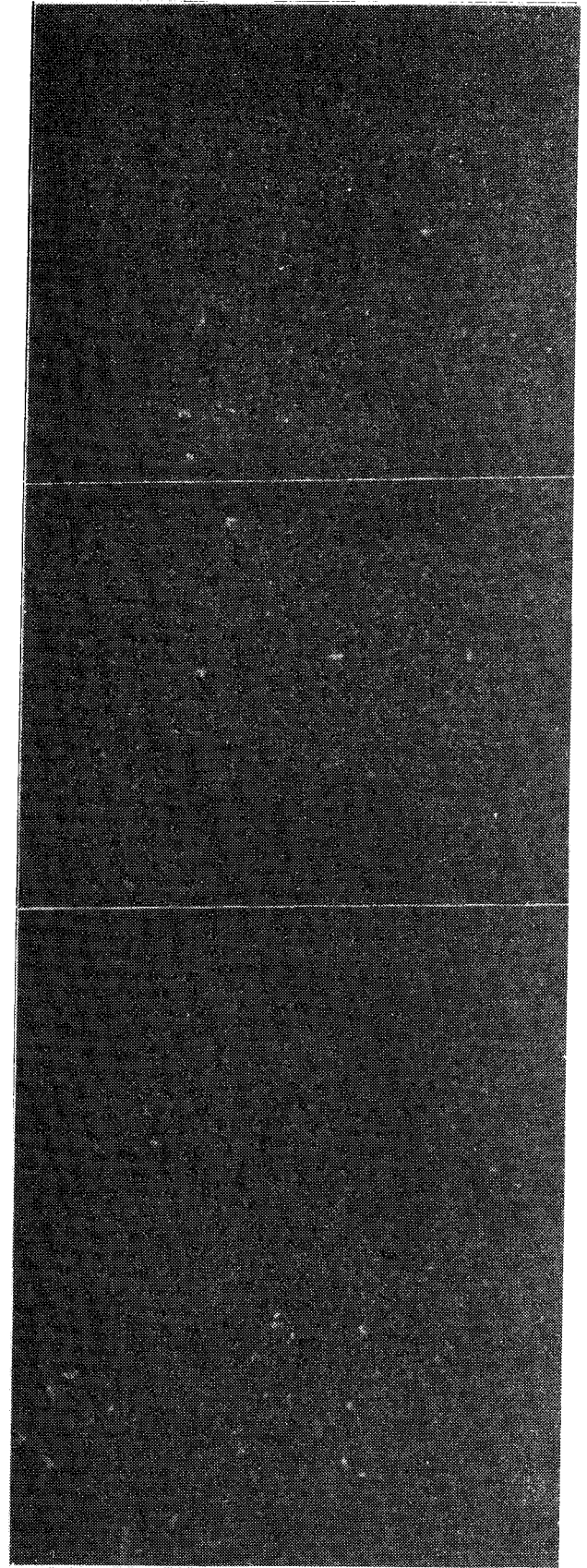
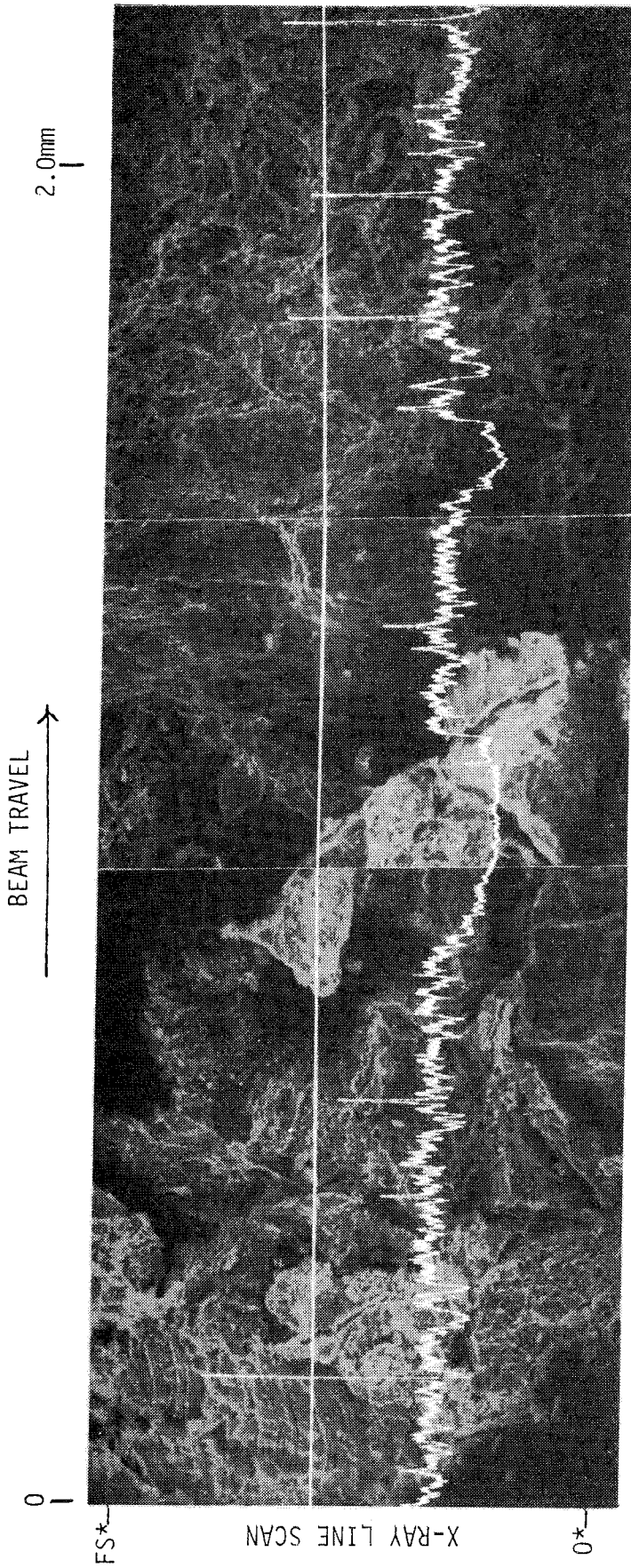
MACHINE SETTINGS

LINE - FULL SCALE SENSITIVITY: 2.5×10^3 cnts/sec.
SCAN SETTING: 7

MAP - SCAN SETTING: 11

SAMPLE RK17

ELEMENT Fe



MACHINE SETTINGS

LINE — FULL SCALE SENSITIVITY: 2.5×10^3 cnts/sec.
SCAN SETTING: 7

MAP — SCAN SETTING: 11

LIST OF KBS's TECHNICAL REPORTS

1977-78

TR 121 KBS Technical Reports 1 - 120.
Summaries. Stockholm, May 1979.

1979

TR 79-28 The KBS Annual Report 1979.
KBS Technical Reports 79-01--79-27.
Summaries. Stockholm, March 1980.

1980

TR 80-26 The KBS Annual Report 1980.
KBS Technical Reports 80-01--80-25.
Summaries. Stockholm, March 1981.

1981

TR 81-17 The KBS Annual Report 1981.
KBS Technical Reports 81-01--81-16
Summaries. Stockholm, April 1982.

1983

TR 83-01 Radionuclide transport in a single fissure
A laboratory study
Trygve E Eriksen
Department of Nuclear Chemistry
The Royal Institute of Technology
Stockholm, Sweden 1983-01-19

TR 83-02 The possible effects of alfa and beta radiolysis
on the matrix dissolution of spent nuclear fuel
I Grenthe
I Puigdomènech
J Bruno
Department of Inorganic Chemistry
Royal Institute of Technology
Stockholm, Sweden January 1983

- TR 83-03 Smectite alteration
Proceedings of a colloquium at State University of
New York at Buffalo, May 26-27, 1982
Compiled by Duwayne M Anderson
State University of New York at Buffalo
February 15, 1983
- TR 83-04 Stability of bentonite gels in crystalline rock -
Physical aspects
Roland Pusch
Division Soil Mechanics, University of Luleå
Luleå, Sweden, 1983-02-20
- TR 83-05 Studies of pitting corrosion on archeological
bronzes
Åke Bresle
Jozef Saers
Birgit Arrhenius
Archeological Research Laboratory
University of Stockholm
Stockholm, Sweden 1983-02-10
- TR 83-06 Investigation of the stress corrosion cracking of
pure copper
L A Benjamin
D Hardie
R N Parkins
University of Newcastle upon Tyne
Department of Metallurgy and Engineering Materials
Newcastle upon Tyne, Great Britain, April 1983
- TR 83-07 Sorption of radionuclides on geologic media -
A literature survey. I: Fission Products
K Andersson
B Allard
Department of Nuclear Chemistry
Chalmers University of Technology
Göteborg, Sweden 1983-01-31
- TR 83-08 Formation and properties of actinide colloids
U Olofsson
B Allard
M Bengtsson
B Torstenfelt
K Andersson
Department of Nuclear Chemistry
Chalmers University of Technology
Göteborg, Sweden 1983-01-30
- TR 83-09 Complexes of actinides with naturally occurring
organic substances - Literature survey
U Olofsson
B Allard
Department of Nuclear Chemistry
Chalmers University of Technology
Göteborg, Sweden 1983-02-15
- TR 83-10 Radiolysis in nature:
Evidence from the Oklo natural reactors
David B Curtis
Alexander J Gancarz
New Mexico, USA February 1983

- TR 83-11 Description of recipient areas related to final storage of unprocessed spent nuclear fuel
Björn Sundblad
Ulla Bergström
Studsvik Energiteknik AB
Nyköping, Sweden 1983-02-07
- TR 83-12 Calculation of activity content and related properties in PWR and BWR fuel using ORIGEN 2
Ove Edlund
Studsvik Energiteknik AB
Nyköping, Sweden 1983-03-07
- TR 83-13 Sorption and diffusion studies of Cs and I in concrete
K Andersson
B Torstenfelt
B Allard
Department of Nuclear Chemistry
Chalmers University of Technology
Göteborg, Sweden 1983-01-15
- TR 83-14 The complexation of Eu(III) by fulvic acid
J A Marinsky
State University of New York at Buffalo, Buffalo, NY.
1983-03-31
- TR 83-15 Diffusion measurements in crystalline rocks
Kristina Skagius
Ivars Neretnieks
Royal Institute of Technology
Stockholm, Sweden 1983-03-11
- TR 83-16 Stability of deep-sited smectite minerals in crystalline rock - chemical aspects
Roland Pusch
Division of Soil Mechanics, University of Luleå
1983-03-30